Signal Transducer and Activator of Transcription Protein 3 (STAT3): an Update on its Direct Inhibitors as Promising Anticancer Agents.

Arianna Gelain [1], Matteo Mori [1], Fiorella Meneghetti [1], Stefania Villa*[1]

[1] Dipartimento di Scienze Farmaceutiche, Università degli Studi di Milano, via L. Mangiagalli 25, 20133 Milano, Italy

* Corresponding author: Stefania Villa, Dipartimento di Scienze Farmaceutiche, Università degli Studi di Milano, via L. Mangiagalli 25, 20133 Milano, Italy Phone: +39-02-50319368. Fax: +39-02-50319359. E-mail: stefania.villa@unimi.it;

ABSTRACT

Background: Since Signal Transducer and Activator of Transcription 3 (STAT3) is a transcription factor which plays an important role in multiple aspects of cancer, including progression and migration, and it is constitutively activated in various human tumors, STAT3 inhibition has emerged as a validated strategy for the treatment of several cancers. The aim of this review is to provide an update, over the last decade, about the identification of new promising direct inhibitors targeting STAT3 domains, as potential anticancer agents.

Methods: A deep literature search focused on recently reported STAT3 direct inhibitors was undertaken. We considered the relevant developments, regarding the STAT3 domains, which have been identified as potential drug novel targets.

Results: In detail, 133 peer-reviewed papers and 7 patents were cited; the inhibitors that were taken into account targeted the DNA binding domain (gathered in natural compounds, small molecules, peptides and derivatives, aptamers and oligonucleotides), the SH2 binding domain (classified in natural, semi-synthetic and synthetic compounds) and specific residues, like cysteines (divided in natural, semi-synthetic, synthetic compounds and dual inhibitors) and tyrosine 705.

Conclusion: The huge number of direct STAT3 inhibitors recently identified demonstrates the interest of the medicinal chemistry research for this target, although it represents a challenging task since any derivative of this class is currently available for anticancer therapy. Notably, many studies on their mechanism of action evidenced that some of them act as dual inhibitors.

1. INTRODUCTION

STAT3 is a member of the signal transducer and activator of transcription family. In mammalian cells, the STAT family consists of seven members (STAT1, STAT2, STAT3, STAT4, STAT5a, STAT5b, and STAT6), having a rank of homology between 20 and 50 % [1].

STATs (79-113 kDa) are involved in the modulation of gene expression, playing a fundamental role in many biological events, such as embryonic development, innate and adaptive immunity, programmed cell death, organogenesis, and cell growth regulation. In particular, STAT3 and STAT5 control cell cycle progression and apoptosis, and therefore they are most often implicated in the progression of human cancers [2].

STAT3 exists in different isoforms, deriving from a single gene by alternative splicing; STAT3α is the long form, STAT3β, STAT3γ and STAT3δ are truncated congeners, each possessing different physiological function [3]. STAT3 shares a common structural organization with the other family members; its overall 3D architecture is characterized by highly conserved domains (Fig. (**1**)) [4]:

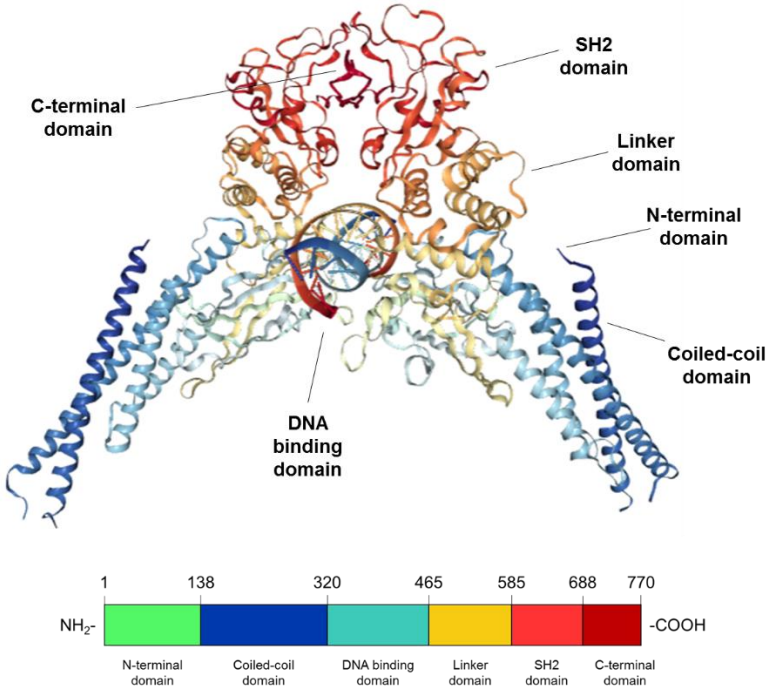

Fig. (1). Organization of STAT3 domains (PDB code 1BG1)

In particular:

- the *amino terminal domain* (NTD, residues 1-138) is essential for the dimer-dimer interactions, leading to in the formation of tetramers, which bind the DNA and then modulate the transcriptional activity [5] [6]
- the *coiled-coil domain* (CCD, residues 139-320) is constituted by four α-helices connected by short loops. This domain has a large hydrophilic surface involved in interactions with the transcription factors and other regulatory proteins; [7].
- the *DNA binding domain* (DBD, residues 321-465), a region with eight-stranded β-barrel, is involved in the formation STAT3-DNA complexes and in the control of nuclear translocation;
- the *linker domain* (LK, residues 466-585) is composed of a series of α-helices and allows the appropriate arrangement of the DBD and the Src homology 2 domains;
- the *Src homology 2 domain* (SH2, residues 586-688) is the most highly conserved domain (SH2, residues 586-688) and recruits phosphorylated STAT3 receptors to set up dimers from two activated monomers. [8].
- the *C-terminal Transcriptional Activation Domain* (TAD, residues 689-770) varies in its sequence and length among different homologues. It is involved in transcriptional activation of regulated genes and it includes the essential elements for STAT activation, in particular the conserved Tyr705, lying in a stretch of ordered residues belonging to the C terminus. This residue, upon phosphorylation, interacted with the SH2 domain of another monomer allowing the stabilization of the dimers (pTyr705), [9]. This process can be influenced by serine phosphorylation (Ser727).

STAT3 proteins are localized in the cytoplasm in inactive form. The binding of cell surface receptors by ligands, such as cytokines or growth factors, can activate the tyrosine phosphorylation cascade (Fig. (**3**)). Cytokine receptors must recruit Janus kinases (JAKs) to act as intermediaries for the activation. Inactive cytoplasmic monomers bind to receptors through the SH2 domain using phosphotyrosine (pTyr) residues as docking sites. Monomers are phosphorylated at their C-terminal tyrosine residue (Tyr705), by JAKs inducing the formation of ~~(~~homo- or heterodimer~~)~~, through reciprocal pTyr-SH2 interactions. The activated dimers translocate from the cytoplasm to the nucleus, where they bind specific DNA sequences and induce transcription. This process lead to the expression of genes~~,~~ controlling essential cellular functions. STAT3 activation is down-regulated by PIAS (protein inhibitor of STAT), SHP-1/2 (SH2 domain-containing phosphatase), SOCS (suppressor of cytokine signaling), and PTPRT (Receptor-type tyrosine-protein phosphatase T) [10] (Fig. (**3**)).

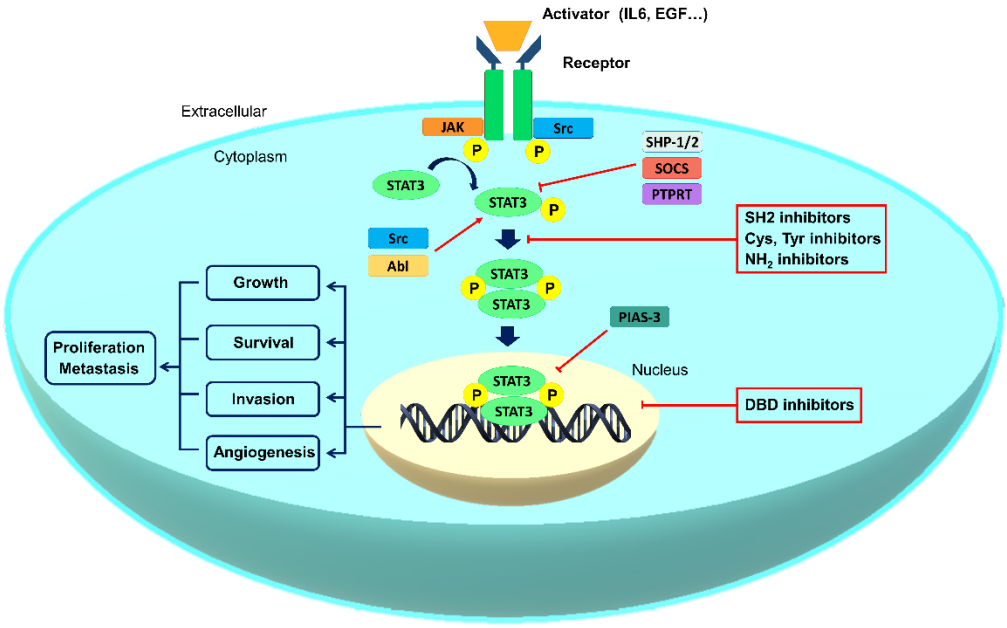

Fig. (2). A schematic representation of the STAT3 signaling pathway.

STAT3 has been demonstrated to play a crucial role in many cellular processes including oncogenesis, tumor growth and progression, also promoting angiogenesis and metastasis, and interfering with apoptosis and anti-tumor immune response. [11]

Although interesting evidences have highlighted the significant STAT3 activity involvment in human pathologies as cardiovascular disease, atherosclerosis, diabetes type 2, [12, 13, 14] liver, renal and pulmonary fibrosis [15 , 16, 17] its role in cancer is the primary topic. Indeed STAT3 is persistently activated in many types of human tumors, including more than half of breast and lung cancers, hepatocellular carcinomas, multiple myelomas and more than 95% of head and neck cancers [18] Noteworthy, the interruption of STAT3 activity in tumor cells leads to apoptosis with minimal effect on normal cells [19] Therefore STAT3 has been validated as a promising target and during the last years many compounds, belonging to various chemical classes have been identified as STAT3 inhibitors, blocking the activation pathway steps [20, 21, 22, 23, 24, 25] or directly interacting with STAT3 [20]. Since the indirect approach could lead to a low selectivity, this review focus on the direct inhibitors and their development over the last decade.

2. STAT3 DIRECT INHIBITION

Direct inhibitors can interact with STAT3 through the:

- N-terminal domain;
- DNA binding domain;
- SH2 domain;
- Cys and p-Tyr.

2.1.Interaction with the amino terminal domain (NTD)

As NTD is involved in several protein–protein interactions, e.g. in dimer formation, binding to promoter and assembly of transcriptional machinery, it can be considered an interesting target for the development of compounds inhibiting tumorigenesis. [26]

2.1.1 Peptides

A synthetic analogue of the second α-helix of STAT4 was able to specifically target NTD, thus determining the perturbation of its structure and a consequent cell death in multiple breast cancer cell lines. In order to enhance the cell membrane crossing, the peptide was fused with the C-terminus of penetratin (penetratin = RQIKIWFPNRR-Nle-KWKK-NH_2), the third helix of the homeodomain of the *Antennapedia* homeoprotein [27]. then the cell-permeable derivatives (STAT3-Hel2 = LDTRYLEQLHQLYS-penetratin (**1**), STAT3-Hel8 = RCLWEESKLLQTA-penetratin (**2**)) were found to directly and specifically bind to STAT3 but not STAT1 as determined by FRET analysis [[27]. The results of both the MTT and luciferase assays allowed the identification of the peptide STAT3-Hel2A-2 (**3**) (LDTRYLEQLHKLY) as the most potent (65±4% inhibition at 5μM conc. in MTT assay; 71±6% GAS−luciferase reporter activity at 10μm conc.). This inhibitor prevented the association of STAT3 with histone deacetylase and DNA methyltransferase.

Moreover, ST3-H2A2 (**4**) binds to NTD and activates expression of proapoptotic genes such as C/EBP-homologous protein (CHOP) to initiate apoptotic death in cancer cells [28].

2.2. Blocking the DNA binding domain (DBD)

Both STAT1 and STAT3 interact with very similar DNA binding sequences; gene targets are generally different, although they can sometimes overlap [29].

Nonetheless, there is a difference between STAT1 and STAT3 DBD sequences that may offer a possibility to design more selective STAT3 inhibitors. STAT1 DBD contains two Lys residues (Lys410 and Lys413) that can be acetylated and block STAT1 activity. STAT3, instead, has two Arg residues in the corresponding sites (Arg414 and Arg417) that cannot be acetylated. The replacement of these Arg residues with Glu residues (mimicking acetylated Lys in STAT1) at STAT3 weakens STAT3-dependent signaling, highlighting the important role that the Arg residues play in the binding of inhibitors to DBD [30].

Furthermore, STAT3 possesses a unique surface cysteine (Cys468) sited in the DBD. STAT1 equivalent residue is a serine. Alkylation of Cys468 blocks STAT3 DNA binding and induces apoptosis in human tumor cell lines characterized by high levels of p-STAT3 [31].

The inhibition of STAT3-DNA binding, and the subsequent impairment of the transcriptional activity, has been identified as a very effective strategy to block STAT3 signaling.

The available inhibitors can be classified according to their site of action (DBD or STAT3-DNA binding pathway) or based on their origin (natural or synthetic). The DBD consists of four DNA binding loops and linker regions and represents an alternative appealing target for the discovery of STAT3 direct inhibitors. Nevertheless, this approach is challenging due to the difficulties in the rational design of selective inhibitors since the STAT3-DNA binding interface is a diffuse surface area, including residues from many α-helices and β-sheets, and because its structure is highly conserved in other STATs. [32] To date, most of these direct inhibitors have not advanced in clinical studies despite their inhibitory effects on a variety of tumor cell lines and animal models, mainly because of their poor selectivity, unfavorable PK properties and serious side-effects. Although the targeting of the STAT3-DNA binding pathway is not properly a direct inhibition mechanism, we deemed it important to discuss it in this work, because it can be considered one of the most promising strategy for clinical applications. Moreover, we included SH2-targeted inhibitors, which have exhibited inhibitory activity against the DBD domain.

2.2.1 Natural compounds

Among natural compounds, carnosol (**5**) ((1,3,4,9,10,10a*S*-hexahydro-5,6-dihydroxy-1,1-dimethyl-7-isopropyl-2H-9*S*,4α*R*-(epoxymethano)phenanthren-12-one, Fig. (**3**)) emerged as potent DBD inhibitor.

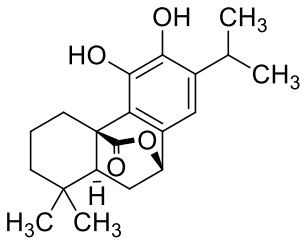

Carnosol (**5**)

Fig. (3). Structure of the natural compound (**5**) targeting DBD.

This molecule is an antioxidant diterpene, naturally present in *Rosmarinus Officinalis*, endowed with anti-inflammatory, analgesic, antimicrobial and anti-cancerous properties. [33, 34, 35, 36]

In HCT116 cells, (**5**) induced apoptosis in a time- and concentration-dependent manner by decreasing the activity of STAT3, through the inhibition of the phosphorylation mediated by Jak2 and Src kinases. Moreover, (**5)** reduced the constitutive STAT3-DNA-binding activity and the expression of STAT3-regulated genes, producing survivin, cyclin-D1, -D2, and –D3 [37].

Additionally, (**5**) decreased TNF-α and IL-1β levels in mice models *via* inhibition of STAT3 activation. As demonstrated by a pull-down assay, (**5**) had a significant STAT3 binding affinity (-7.7 kcal/mol); it effectively inhibited the phosphorylation of STAT3 and DNA binding activity in RAW 264.7 cells, transiently transfected with STAT3-Luc plasmid for luciferase activity measurement. In *in vitro* experiments showed that (**5**) induced the STAT3 and c-myc mediated programmed cell death *via* pro-apoptotic proteins such as Bax and p53. Computational docking experiments performed to identify the STAT3 binding site of (**5**), showed its binding within the DBD to His332, Ile467, Cys468, Met470, Pro471, Val563, Asp566, Asn567, Asp570, Lys574 and Lys642 residues. [33]

2.2.2 Semisynthetic compounds

The derivative of curcumin, **FLLL32** (**6**) ((2*E*,2′*E*)-1,1'-(cyclohexane-1,1-diyl)bis(3-(3,4-dimethoxyphenyl)prop-2-en-1-one, Fig. (**4**)), decreased the binding of STAT3 to the DNA: EMSA tests, performed in OSA cell lines, displayed a decreased STAT3-DNA binding after only 4 hours of treatment with (**6**) at 10 µm. It induced proteasome-mediated degradation of STAT3, resulting in a subsequent abolishment of VEGF, MMP2, and survivin production. It reduced canine and human osteosarcoma cells proliferation and decreased the levels of both total and pSTAT3. [38]

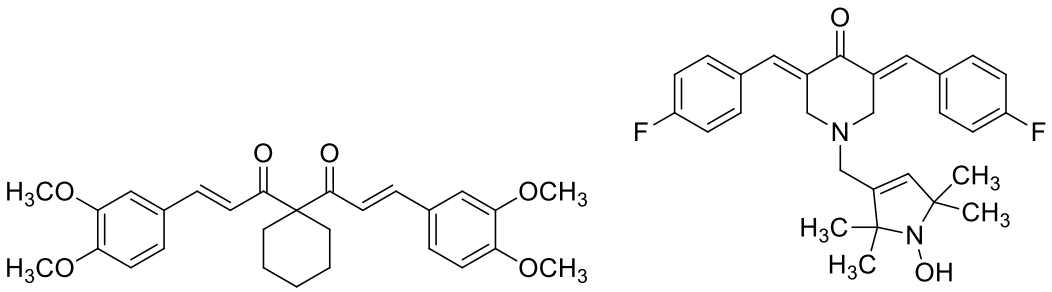

FLLL32 (**6**) HO-3867 (**7**)

Fig. (4). Structure of semi-synthetic derivatives targeting DBD.

The curcumin-based STAT3 inhibitor HO-3867 (**7**) ((3E,5E)-3,5-bis(4-fluorobenzylidene)-1-((1-hydroxy-2,2,5,5-tetramethyl-2,5-dihydro-1H-pyrrol-3-yl)methyl)piperidin-4-one, Fig. (**4**)) emerged as a direct binder of the DBD, as confirmed by ELISA assay, which confirmed the prediction of the docking experiments. [39] (**7**) exhibited minimal toxicity toward non-cancerous cells and tissues, but induced apoptosis in ovarian cancer cells. Pharmacologic analyses revealed greater bioabsorption and bioavailability of the cytotoxic metabolites in cancer cells compared with normal cells. *In vivo* tests assessed that (**7**) could block xenograft tumor growth without toxic side effects. [39]

2.2.3. Small molecules

Recently, the anthelmintic drug niclosamide (**8**) **(**(5-Chloro-N-(2-chloro-4-nitrophenyl)-2-hydroxybenzamide, Fig. (**5**)) demonstrated the ability to target the DBD, thus inhibiting STAT3 transcriptional activity [10]. It inhibited the STAT3-DNA binding with an IC_{50} value of 1.93 ± 0.70 μM, determined by means of a modified *in vitro* ELISA assay incorporating recombinant STAT3 [10].

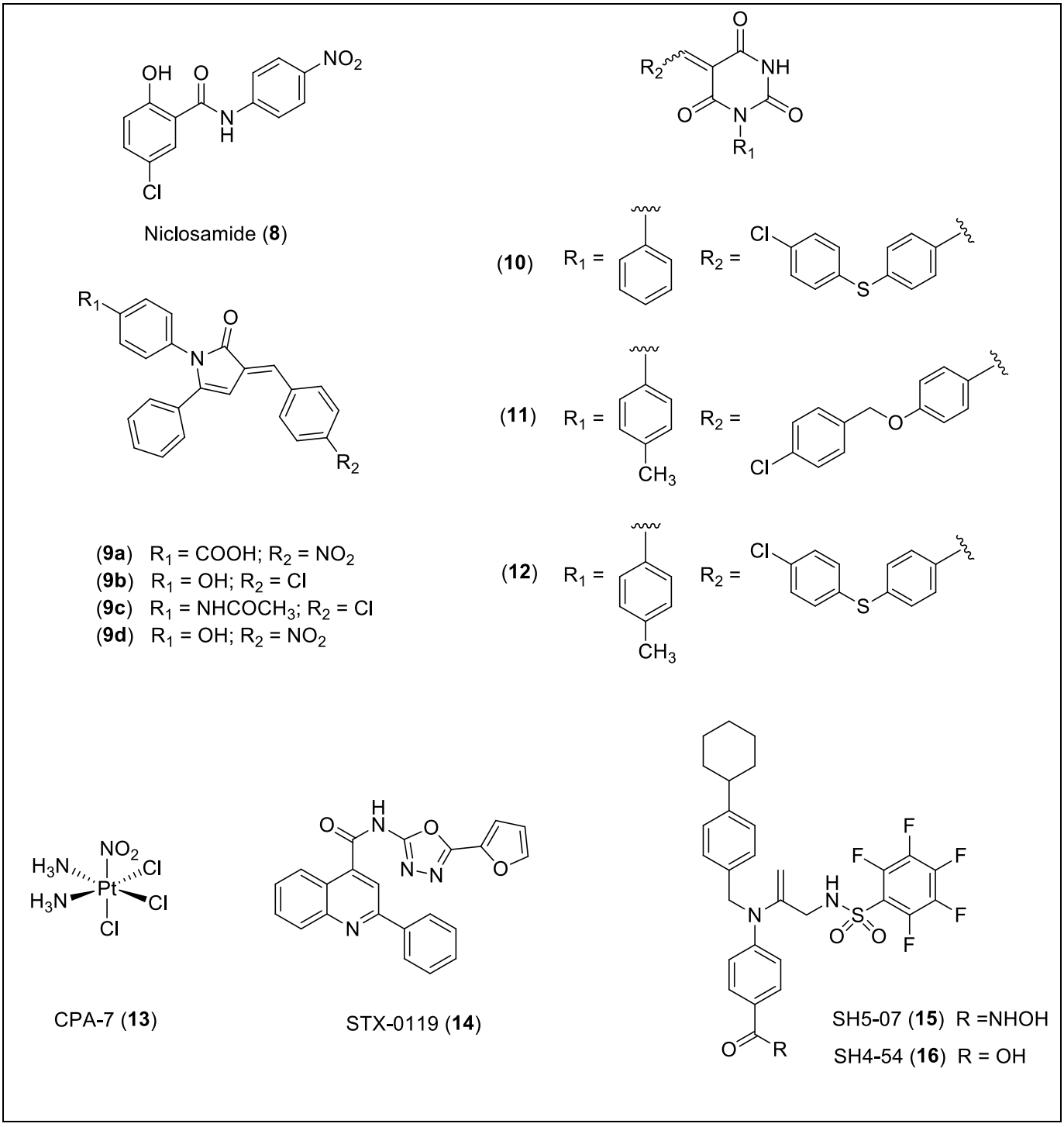

Fig. (**5**). Structure of small molecules (**8**)-(**16**) targeting DBD.

In addition, inhibitor (**8**) reduced cell viability of HeLa cells in a dose-dependent manner (EC_{50} of 1.09 ± 0.9μM), as assessed using a MTT assay [10]. Then, the dose-response curve of nuclear extracts from HeLa cells allowed the determination of an EC_{50} of 0.19 ± 0.001μM. The potent STAT3 inhibitory activity of (**8**) in cells indicated that this compound also targeted other members of the signaling cascades crosstalking with STAT3, having in this way a greater impact on STAT3-DNA binding [10]. Recently, other studies reported that (**8**) exhibited antiproliferative activity in head, neck, ovarian, breast, hematologic and colon cancer [40]. MTT-assay investigations in colon cancer cell lines evidenced the potent antiproliferative effects of (**8**) in SW620, HCT116 and HT29 cell lines, as shown by the IC_{50} values of 2.9, 0.4 and 8.1 μM, respectively. In HCT116 and SW620 cell lines, Western blot analyses showed that (**8**) (at 5 μM concentration) suppressed STAT3 phosphorylation in a time- and dose-dependent manner [40].

Using a virtual screening approach, a compound targeting the DBD, without interfering with STAT3 activation and phosphorylation, was disclosed (**9a**) ((4-[(3*E*)-3-[(4-nitrophenyl)-methylidene]-2-oxo-5-phenylpyrrol-1-yl] benzoic acid, Fig. (**5**)). It inhibited cancer cell proliferation with an IC_{50} of 3.2-5.4 μM in multiple cancer cell lines by impairing STAT3-dependent gene expression and inducing apoptosis [41]. In details, compound (**9a**) blocked the STAT3-dependent luciferase reporter expression in MDA-MB-231 cells with an IC_{50} of 13.8 ± 0.4 μM, suppressing cancer cell proliferation, migration, and invasion [41]. Electrophoretic mobility shift assay (EMSA) data evidenced for (**9a**) a selective inhibition of the DNA-binding activity of STAT3 over STAT1 (IC_{50} of ∼20 μM *vs* 300 μM). Molecular dynamics (MD) simulation indicated for (**9a**) a different docking pose in STAT1 with respect to STAT3, characterized by an unfavorable ΔG_{bind} due to physical hindrance from residue Pro326 and Thr327 [41]. The higher affinity of (**9a)** for STAT3 was confirmed by its less cytotoxic effect on non-cancer cells (IC_{50} range ∼10−12 μM) compared to cancer cell (IC_{50} range ∼3.2−5.4 μM). From further studies, performed to optimize the poor pharmacokinetic features of this molecule, emerged the improved lead (**9b**) (3-[(4-chlorophenyl)methylene]-1,3-dihydro-1-(4-hydroxyphenyl)-5-phenyl-2H-pyrrol-2-one, Fig. (**5**)) emerged. [42] A SAR analysis among the 69 analyzed analogs evidenced a relationship between the nature of the two side chains (R_1 and R_2) linked to the 5-phenyl-1H-pyrrol-2(3H)-ketone core and the inhibition of the STAT3-dependent luciferase expression on MDA-MB-231 cells (at 20 μM concentration) [41 42]. Compounds with R_1 = OH or COOH possessed high activity, whereas derivatives with the same function in *meta* position had low or null effects. Moreover, the molecule had higher activity when R_2 was a nitro, a chlorine or an amine group, while it became less active if R_2 was a methoxy group [42]. The direct and specific binding of these inhibitors to the DBD of these inhibitors was then validated. The most active ones (**9b**), (**9c**) ((*E*)-*N*-(4-(3-(4-chlorobenzylidene)-2-

oxo-5-phenyl-2,3-dihydro-1H-pyrrol-1-yl)phenyl)acetamide) and (**9d)** ((*E*)-1-(4-hydroxyphenyl)-3-(4-nitrobenzylidene)-5-phenyl-1H-pyrrol-2(3H)-one Fig. (**5**)) in the STAT3 luciferase assay (IC_{50} ~9-11) were submitted to EMSA test and they showed a selective inhibition of the DNA-binding activity of STAT3 *versus* STAT1, with (**9c**) the less effective among them. They did not affect the survival of STAT3-null hematopoietic progenitor cells, supporting the hypothesis that they are potentially specific to STAT3. These compounds induced apoptosis in breast and lung cancer cells with IC_{50S} ranging from 1.8 to 5.6 μM, while they displayed IC_{50S} from 4.0 to 12.0 μM for non-cancerous cells [42]. As (**9c**) was found to be highly cytotoxic on non-cancerous lung fibroblasts and (**9d**) was poorly soluble in oral formulations for *in vivo* studies, they were not further developed. Concerning compound (**9b**), multiple doses were efficaciously administered in mice, showing inhibition of tumor growth and metastasis with little cytotoxicity on non-cancerous cells (it was tolerated up to 200 mg/kg), thus it became the new lead compound among the inhibitors targeting DBD [42].

Novel pyrimidinetrione derivatives were identified as direct DBD inhibitors, with activity in the low micromolar range. These compounds bound at the STAT3-DNA binding interface, as proved by surface plasmon resonance (SPR) data [43].

Among the compounds tested in the EMSA assay, two hits (**10**) (5-(4-((4-chlorophenyl)thio)benzylidene)-1-phenylpyrimidine-2,4,6(1H,3H,5H)-trione) and (**11**) (5-(4-((4-chlorobenzyl)oxy)benzylidene)-1-(*p*-tolyl)pyrimidine-2,4,6(1H,3H,5H)-trione) exhibited a dose-dependent inhibition of STAT3-DNA binding with IC_{50} values of 2.5 μM and 3.8 μM, respectively and demonstrated a selective activity on STAT3 over STAT1. Both compounds reduced the cell viability of the human pancreatic cancer cell line Panc-1, harboring constitutively active STAT3.
3D-QSAR calculations indicated that the substituent at R_2 is critical for STAT3 inhibitory activity. Accordingly, compounds endowed with the most highest inhibitory activity had a 4-((4-chlorophenyl) thio)phenyl substituent at R_2 and a bulky group at R_1, Fig. (**5**). Docking studies of this class of derivatives on the DBD showed a good correlation between binding energy and the biological activity, whereas this correlation is absent in the results of the docking experiments on the SH2 domain. The best poses suggested that hydrophobic or sterically bulky groups at R_1 could block the DNA binding to STAT3. Following this indication, new derivatives bearing sterically hindered functions on R_1 were synthesized in order to improve the competitive inhibition of DNA binding to STAT3. SPR assay revealed that compound (**12**) (5-(4-((4-chlorophenyl)thio)benzylidene)-1-(*p*-tolyl)pyrimidine-2,4,6(1H,3H,5H)-trione) had the best K_D (10.7 μM), without disrupting the pTyr peptide binding to STAT3.

The metal complex **CPA-7** (**13**) ((trichloronitritodiammineplatinum(IV), Fig. (**5**)) interfered *in vitro* with the binding of STAT3 to DNA in mouse fibroblast cells and in breast, prostate, melanoma and colon tumor cells. It interacts with the DBD, but whether this platinum derivative directly binds to the DNA-binding domain to exert its function is still unclear. (**13**) also induced tumor regression in a murine colon cancer model; however, it was active in murine glioma models, but further developments are still needed to improve its ability to penetrate the BBE [44].

STX-0119 (**14**) (*N*-(5-(Furan-2-yl)-1,3,4-oxadiazol-2-yl)-2-phenylquinoline-4-carboxamide (Fig. (**5**)) has a mixed mechanism of action, being able to bind both the SH2 and the DNA binding domains. This molecule suppressed the expression of various STAT3-regulated proteins, including c-myc, cyclin D1, and Bcl-xL and the growth of many cancer cell lines. Recent results demonstrated that (**14**) abrogated the growth of glioblastoma multiforme stem-like cells (GBM-SC), inhibiting the target gene expression of STAT3 [45].

SH5-07 (**15**) (4-((4-cyclohexylbenzyl)(3-(perfluorophenylsulfonamido)prop-1-en-2-yl)amino)-*N*-hydroxybenzamide) and SH4-54 (**16**) (4-((4-cyclohexylbenzyl)(3-(perfluorophenylsulfonamido)prop-1-en-2-yl)amino)benzoic acid), Fig. (**5**), are potent inhibitors of tumor models harboring persistently active STAT3, including glioma, breast, prostate, and lung cancer models. The inhibition of STAT3 signaling by (**15**) and (**16**) produced antitumor effects, *in vitro*, associated with decreased Bcl-2, Bcl-xL, Cyclin D1, c-Myc, Mcl-1, and survivin expression, and antitumor responses in human glioma and breast cancer models *in vivo*. Among the mechanisms involving STAT3 inhibition, NMR data identified a putative binding to the DBD. An EMSA analysis showed that the SH2 domain is the main target, but a DBD interaction also contributed to the overall effect against STAT3 [46].

2.2.4 Peptides and derivatives

An interesting approach to directly block STAT3-DNA binding includes the employment of peptides and peptide-like biopolymers. Despite their proved efficacy, they suffer from metabolic instability and poor cell permeability during *in vivo* tests, limiting their clinical development [47].

Recently, a new class of peptidomimetics, specifically targeting STAT3–DNA interaction, was developed: the "γ-AApeptides", Fig. (**6**) [48]. They are oligomers of *N*-acylated-*N*-aminoethyl amino acids, bearing the same number of side chains of a peptide of the same length. As their side chains can be chosen from an infinite set of acylating agents, it is possible to generate a high number of chemically different libraries. Moreover, they are highly resistant to proteolytic degradation. [48, 49].

One-bead-one-compound Aγ-AApeptide combinatorial library (OBOC) was submitted to biological tests evidencing a lack of binding to the STAT3–SH2 domain, while in nuclear extracts the disruption of the DNA–STAT3 binding was detected. In this respect, sequences (**17**), (**18**) and (**19**) at 100 μM concentrations, (Fig. (**6**)) showed IC_{50} values in the range of 10-30 μM, with the most potent γ-AApeptide (**17**) a maximum inhibition (90%) of DNA–STAT3 binding at 30 μM. Even though their dimensions are fairly large, they all retained an inhibitory activity against STAT3–DNA binding in whole MDA-MB-468 cells, and decreased the levels of survivin and cyclin D1 [48].

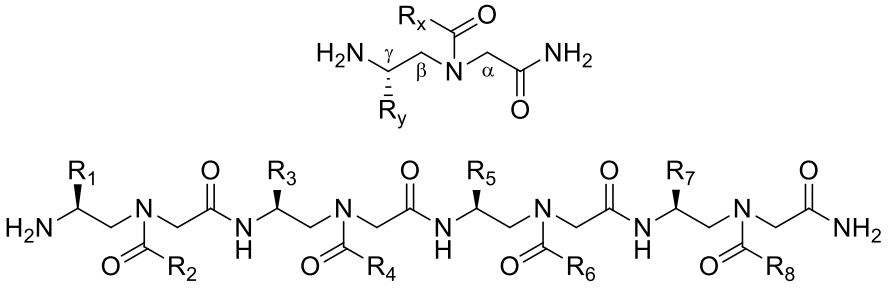

(17) $R_1 = CH_2CH_2COOH$; $R_2 = CH_2CH(CH_3)_2$; $R_3 = CH_2Ph$; $R_4 = CH_2CH_2COOH$; $R_5 = CH_2CH(CH_3)_2$; $R_6 = CH_2CH_2Ph$; $R_7 = CH_2CH_2COOH$; $R_8 = CH_2CH(CH_3)_2$

(18) $R_1 = CH_2CH(CH_3)_2$; $R_2 = CH_2CH_2Ph$; $R_3 = CH_2CH(CH_3)_2$; $R_4 = CH_2CH(CH_3)_2$; $R_5 = CH_2CH(CH_3)_2$; $R_6 = CH_2CH(CH_3)_2$; $R_7 = CH_2CH_2COOH$; $R_8 = CH_2CH_2Ph$

(19) $R_1 = CH_2CH(CH_3)_2$; $R_2 = CH_2CH_2Ph$; $R_3 = CH_2CH(CH_3)_2$; $R_4 = CH_2CH(CH_3)_2$; $R_5 = CH_2CH(CH_3)_2$; $R_6 = CH_2CH_2Ph$; $R_7 = CH_2CH_2COOH$; $R_8 = CH_2CH(CH_3)_2$

Fig. (6). The general structure of Aγ-AApeptide OBOC library and chemical structures of (**17**), (**18**) and (**19**)

The most active sequences were identified from the γ-AApeptide OBOC library. Modeling studies showed that the most negatively charged sequence in the identified γ-AApeptides interacted better with the STAT3-DNA binding domain, through charge-charge interactions and hydrophobic interactions [48].

2.2.5 Aptamers

Further efforts for developing new molecules that non-covalently bind to the DBD for disorder the STAT3–DNA interactions were also directed to the design and synthesis of cell permeable peptide aptamers. These latter are appealing drug candidates as they can discern between normal and cancerous cells, exerting their toxic effects specifically on malignant cells; moreover, they have a long half-life and can be produced without displaying immunogenicity and by means of a feasible synthesis. Nowadays, aptamers can also be delivered using nanoparticles, in order to improve their cell-permeation [50 51].

DBD-1 (**20**) (PLTAVFWLIYVLAKALVTVC), inhibited *in vitro* STAT3 transcriptional activity with high potency without affecting the phosphorylation. Although *in vivo* assays showed only a weak interaction between (**20**) and STAT3 DBD, TUNEL (terminal deoxynucleotidyl transferase-mediated nick end labeling) experiments performed on murine B16 melanoma cells transfected with the peptide aptamer (**20**) showed a significant reduction of the transcriptional activity of STAT3 and a decrease of the cell viability; (**20**) also induced apoptosis in about 50% of the cells but it suffered of intracellular instability [52].

2.2.6 Oligonucleotide decoys as specific DBD inhibitors (DNA-binding modifiers)

The strategy of competitively blocking STAT3-DNA binding with synthetic double-stranded oligonucleotides (ODNs) was initially employed for assessing the STAT3-dependent gene regulation in *in vitro* assays. ODNs can compete with endogenous *cis*-elements of STAT3, thus altering the subsequent gene expression and tumor cell growth [53]. These STAT3 decoys (decoy = bait) closely resemble STAT3 DNA binding sites; therefore, STAT3 dimers interact with them, precluding in this way their nuclear localization and DNA binding (Fig. (**7**)) [54].

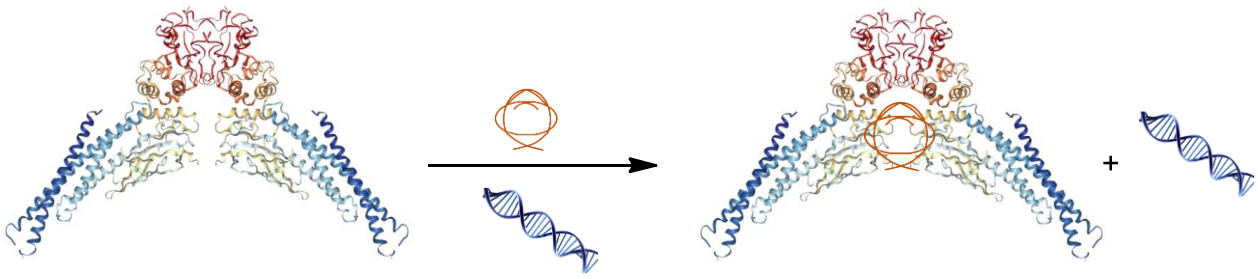

Fig. (7). ODNs (red) mechanism of action.

Hairpin oligodeoxynucleotide decoy (hpdODN), Fig. (**8**), characterized by a modified consensus sequence containing two STAT3-binding sites selectively targeting STAT3, was able to discriminate DNA sequences differing between STAT3 and STAT1 [55].

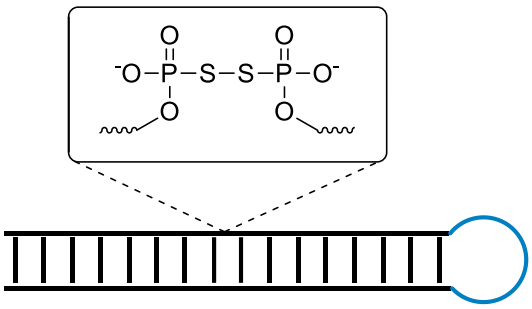

Fig. (8). Hairpin decoy (hpdODN)

The investigated decoys were RHN$(CH_2)_6$-CATTTCCCGTAAATCGAAGATTTACGGGAAATG-$(CH_2)_3$NHR, derived from the serum-inducible element of the human c-fos promoter, and RHN$(CH_2)_6$-CATTTGCCACAATCGAAGATTGTGGCAAATG-$(CH_2)_3$NHR, where R was either H, a fluorescein isothiocyanate moiety (FITC) or biotin [56]. hpdODN specifically interacted with STAT3 dimers, trapping them into the cytoplasm and thus blocking their nuclear transfer, with a consequent decrease of cyclin D1 expression. STAT3 cytoplasmic trapping by hpdODN resulted from the interaction of the decoy with the DBD domain of an activated STAT3 dimer, thus preventing its interaction with karyopherin, necessary for its transfer into the nucleus. hpdODN inhibited STAT3 only in STAT3-dependent cancer cells [55]. Notably, hpdODN B (**21**) (having three different base pairs with respect to the correct STAT3 consensus sequence (T instead of dC 1003, dC in place of dG in 1011 and dG replacing dC in 1017), was effective at inducing the death of SW480 colon carcinoma cells (which depend on STAT3 overexpression for survival), without acting on STAT1. The capability of (**21**) to distinguish between STAT1 and STAT3 was proved by evaluating its ability to kill cells without interfering with IFNγ-induced cell death and to inhibit STAT3 targets, including cyclin D1; moreover, it was unable to inhibit IRF1 expression and IFNγ-induced STAT1 phosphorylation and nuclear translocation; finally, and it did not interact with STAT1 in pull-down assays. This privileged interaction with STAT3 depends on the ODN sequence changes (i.e. T at 1003 did not lead to STAT1 binding) and on the hairpin DNA shape deviations responsible of the modified protein/DNA interactions; however, the precise mechanism is still a matter of debate [55].

The STAT3 decoy composed of a 15-bp duplex oligonucleotide (5′-CATTTCCCGTTAATC-3′) (**22**), having phosphorothioate modifications of the three 5′ and 3′ nucleotides, displayed selective binding to STAT3, inhibiting the proliferation and survival of head and neck squamous cell carcinoma (HNSCC) cells *in vitro* and limiting the growth of HNSCC xenograft tumors *in vivo* [57] This STAT3 decoy also showed antitumor activity in lung, breast, skin, and brain preclinical models, without exerting toxic effects [57]. Nevertheless, the oligonucleotides modified with terminal phosphorothioate moieties retained a susceptibility to endonuclease activity [57] limiting their

antitumor activity when injected intravenously. Therefore, to evaluate the anticancer effects of this STAT3 decoy in patients with HNSCCs, their cyclic versions, characterized by a hexaethylene glycol spacer linking the oligonucleotide strands at both ends, were synthesized ((**23**) Fig. (**9**)) in order to confer resistance to serum nucleases and thermal stability, both important for an effective systemic administration.

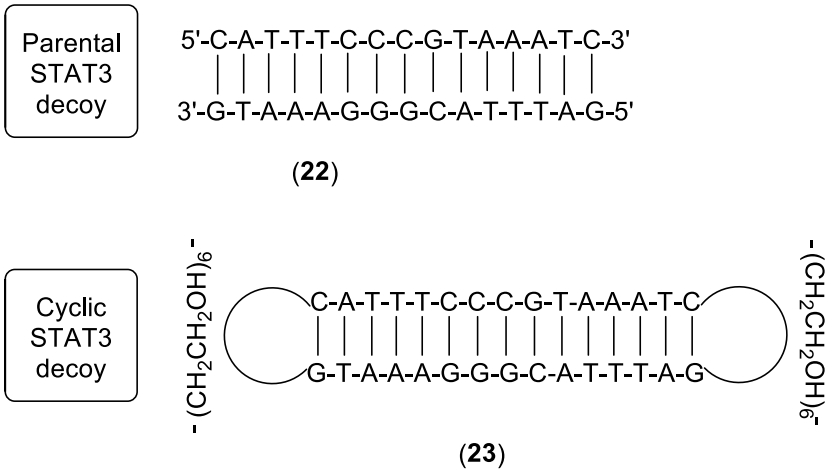

Fig. (9). The parental STAT3 decoy (**22**) and the completely circularized cyclic STAT3 decoy (**23**)

For the parent decoy (**22**) and the cyclic derivative (**23**), K_D constants of $1.22x10^{-7}$ and $2.53x10^{-7}$, respectively, were calculated by fitting of SPR data. These values indicated a comparable strength of interaction between the STAT3 decoy and the pSTAT3 protein. Additionally, in three HNSCC cancer cell lines they showed EC_{50} values in the low nanomolar range (7.2-36.2 nmol/L). The immunoblotting technique showed that thecyclic STAT3 decoy (**23**) downregulated the expression of Bcl-XL and cyclin D1. The systemic delivery of the cyclic STAT3 decoy suppressed HNSCC xenograft tumor growth and decreased the expression of STAT3-targeted genes in the tumors ($P < 0.0001$) with a reduction in cyclin D1/β-actin ratio ($P = 0.0015$) and Bcl-XL/β-actin ratio ($P = 0.0021$), without alteration of the expression of total or phosphorylated STAT3 in the tumors. The safety of this successful first-in-human study of a single dose intratumoral injection of the decoy in patients with HNSCC was assessed by a Phase 0 clinical trial (ClinicalTrialsgov identifier: NCT00696176), concluded few years ago [57].

Preliminary results were reported regarding new decoys linked to cytosine guanine dinucleotide (CpG), designed and synthesized with the aim of improving the cell-selective, *in vivo* STAT3 targeting. The synthetic Toll-like Receptor 9 ligand CpG allowed to its dODN conjugates to selectively enter TLR9+ immune cells. The chemically modified CpGSTAT3 inhibitors (**24**) were not modified by serum nucleases, so they could be administered intravenously. After the uptake, CpG-

STAT3dODNs (**24**) was extruded from endosomes and bound STAT3 in the cytoplasm, inhibiting its downstream gene expression [58]. The cellular targets for CpG-STAT3dODNs (**24**) included non-malignant, tumor-associated myeloid cells, such as polymorphonuclear MDSCs, as well as cancer cells in acute myeloid leukemia, B cell lymphoma and certain solid tumors [59].

Very recently, cyclic STAT3 decoy CS3D (**25**) showed anti-tumor effects in NSCLC cells and emerged as an effective anticancer agent. *In vitro* MTS assays (**25**) showed 50% inhibition of cell proliferation. Additionally, it lowered the expression of c-Myc, Bcl-xL and IL6 STAT3-regulated genes. In 201T and H1975 NSCLC cells mouse xenograft models, (**25**) reduced the tumor growth by 96.5% ($P<0.007$) in 201T and 81.7% in H1975 cell lines, respectively. Moreover, Western blot analysis evidenced a 70% decrease of c-Myc protein level in response to (**25**) [60].

2.3. Binding the SH2 domain

STAT3 activation is possible through to the phosphorylation of Tyr705, an amino acid residue located in the SH2 domain, which drives SH2 mediated homodimerization or heterodimerization with other members of STAT family [61] STAT3 dimerization occurs by the interaction of the SH2 domain on a STAT3 molecule with a loop section located from Ala702 to Phe716 on the other STAT3 monomer. This interaction is allowed by p-Tyr705 on a monomer, which binds to a cavity in the SH2 domain of the other protein [62]. The blockage of SH2 domain prevents STAT3 dimerization, antagonizing its biological effects and representing a possible treatment for cancerous diseases that depend on the overexpression of p-STAT3.

In detail, STAT3 SH2 domain contains three binding "hot spots": pTyr705-binding pocket (with polar residues), Leu706 subsite (the most dynamic and hardest to target) and a hydrophobic side pocket, which is unique to STAT3 and may consent the design of STAT3-specific inhibitors [63].

Moreover one of the main issues in the development of new inhibitors is that STAT3 and STAT1 SH2 domains share high sequence and structure similarity, making difficult to obtain selectivity towards STAT3. Since STAT1 is vital for inflammation, immune response, differentiation, cell apoptosis and its role may be neutral or negative in cancer development, it is important, but also challenging, to develop anti-cancer drugs that do not suppress STAT1 activity [64]. Recently, a theory to explain the selectivity of some compounds toward STAT3 (“selectivity by distraction”) has been hypothesized [64]. Since almost all STAT1 inhibitors are considered bound with higher probability to DNA-binding and the coil−coil domains of STAT1 in comparison to STAT3, it is statistical probable that fewer molecules will bind to the SH2 domain of STAT1 in comparison to

STAT3 because they are “distracted” by other domains of STAT1. This distribution could lead to higher effective probability of binding to the SH2 domain of STAT3 although no significant differences in the structures of the SH2 domains of STAT1 and STAT3 are observed.

To understand the protein-ligand interactions, the mechanisms associated with the binding and the dynamic changes in the protein, structural mass spectrometry based studies have been crucial, demonstrating that the binding of inhibitors to SH2 domain caused structural changes in the protein. [61].

During the last years, STAT3 dimerization inhibitors, based on the pharmacophore structure of Salicylic Acid several derivatives have been developed [20, 65, 66]. Analyzing the protein distortions consequent to their interaction with STAT3 by investigation of site-specific changes in deuterium uptake allowed the mapping of the inhibitors binding site in the SH2 domain. The inhibitors binding induced important local decreases in dynamics and solvent exclusion from the molecule binding site and increase in rigidity of the inhibitor-complexed SH2 domain. Moreover, hotspots of allosteric perturbation were found outside of the SH2 domain after their binding, highlighted by increased deuterium uptake, in DNA binding and nuclear localization regions of STAT3 [61].

Furthermore recently it has been for the first time evidenced the allosteric communications between the SH2 and the linker domain (LD) of STAT3 connected to the activation and the construction of a transcriptional active complex for a STAT transcription factor [67].

Allosteric communication among different domain in STAT3 protein was confirmed also by an assay, involving mutant I568F of HIES (hyper-immunoglobulin E syndrome) that, even though located in the linker domain, provoked chemical shift perturbations in SH2, DBD and coiled-coiled domain, lowering SH2 ability to bind p-Tyr containing peptide because of allosteric effect, reducing STAT3 signaling [67].

Moreover it has been established, through mutants located all over the protein, that inter-domain allosteric interaction can control and modify STAT3 function [67].

Considering the SH2 domain inhibitors, they can be divided in natural, semi-synthetic, and synthetic compounds, including metal complexes and patented derivatives.

2.3.1 Natural compounds

Danshen plant contains two major tanshinones derivatives: cryptotanshinone (**26**) and tanshinone IIA (**27**) (Fig.(**10**)). Compound (**26**) (Fig.(**10**)) is an interesting quinoid diterpene purified from the root of *Salvia miltiorrhiza* Bunge (Danshen plant) [62, 68].

It has been widely used both in traditional oriental medicine and in clinic to treat several disorders, such as circulatory, liver, coronary and renal diseases, cardiac fibrosis, arthritis and acute lung injury [62, 68]. Although tanshinone IIA (**27**) was described as a pro-apoptotic agent on human hepatocellular carcinoma cells [69, 70], human promyelocytic leukemic cells [62], human colon adenocarcinoma cells [71] and human erythroleukemic cells, it is better-known for its anti-inflammatory properties [62, 72]. In HCT-116 colon cancer cells, cryptotanshinone inhibited STAT3 activity in a dose-dependent way (IC_{50} = 4.6 μM) [73], while tanshinone IIA showed no inhibitory activity. Cryptotanshinone was later tested on DU145 prostate cancer cell line, displaying substantial growth inhibitory effect [62]. Computational modeling was employed to discover whether cryptotanshinone, which is co-localized in the cytoplasm with STAT3, can effectively bind the SH2 domain. These studies revealed that (**26**) binds at the exact site of interaction of p-Tyr in the SH2 domain, and that it forms hydrogen bonds with Arg609 and Ile634. Cryptotanshinone showed inhibitory activity only towards p-Tyr in STAT3, but not in STAT1 and STAT5 within 30 minutes, suggesting a selective inhibition of STAT3–Tyr phosphorylation.

Further investigations revealed that the major activity of cryptotanshinone was not due to any upstream interfering, because the only upstream effect of this compound is the inhibition of JAK2 phosphorylation, occurring 4 hours after the treatment; conversely, STAT3 was inhibited within 30 minutes, highlighting that STAT3 inhibition does not depend on the interference with upstream kinases. Such results have great importance, proving that cryptotanshinone can be a very selective STAT3 inhibitor without general cytotoxic effects [62].

Scoparone (**28**) is extracted from *Artemisia capillaris,* a Chinese herb named Yin Chin, (Fig. (**10**)). This natural coumarin derivative blocks the transcriptional activity of STAT3; *in silico* docking studies suggest that it might directly bind the SH2 domain of STAT3 to exert at least part of its activity. Scoparone (**28**) is known to have multiple effects, including anti-inflammatory, anti-oxidant and anti-coagulant activities. It is able to avoid the phosphorylation and the nuclear accumulation of STAT3, thus impairing its transcriptional activity, resulting in the inhibition of the proliferation of hepatoma, cervical and colon cancer cell lines.

Treatment of DU145 cells with this molecule evidenced a significant inhibition of the proliferation, with an IC_{50} = 41.3 μM, meaning that Scoparone represents a valid candidate for the treatment of cancers with overexpressed STAT3 [74].

Further studies showed that another natural compound, the polyisoprenylated benzophenone Garcinol (**29**) (Fig. (**10**)) binds to the SH2 domain of STAT3, suppressing its dimerization *in vitro* and inhibiting both constitutive and IL-6-mediated STAT3 activation in HCC (Hepatocellular carcinoma) cells. Garcinol (**29**) is isolated from the dried rind of the fruit *Garcinia indica*. Since it is an acetyltransferase inhibitor, it also inhibits STAT3 acetylation, impairing its DNA binding ability. As a consequence of the inhibition of STAT3 activation, garcinol suppresses the expression of many different genes involved in survival, proliferation and angiogenesis. A computational docking analysis revealed multiple interactions of garcinol with the amino acids of the SH2 domain namely Ser614, Gly617, Glu638 and Thr641, confirming the experimental data showing that garcinol could block STAT3 dimerization in a dose-dependent manner *in vitr*o, also suggesting a direct inhibitory mechanism [75]. Finally, garcinol suppressed the growth of HCC in xenograft mice models, substantiating its potential use as an anti-cancer therapeutic agent. [75].

Another interesting natural compound is EGCG **(30)** (epigallocatechin-3-gallate), one of the major components of green tea (Fig. (**10**)). Recent SPR binding assay experiments showed that it is able to directly compete with p-Tyr peptide for the interaction with the SH2 domain (IC_{50} = 10-30 μM). Molecular docking studies confirmed that EGCG interacts with Arg-609 in STAT3 SH2 domain (Fig. (**10**)) [76]. Moreover, EGCG suppressed cell proliferation *in vitro*, inducing apoptosis and lowering the levels of p-STAT3, thus inhibiting the expression of multiple genes involved in cancer cell proliferation.

One of the most recently discovered natural compound that interacts with the SH2 domain of STAT3 is Crispene E **(31)** (Fig. (**10**)), a clerodane-type diterpene from *Tinospora crispa*, a Malaysian woody climber, traditionally used against hypertension, diabetes mellitus, malaria and diarrhea. A Fluorescence Polarization assay evidenced that (**31**) impedes STAT3 binding to the p-Tyr peptide pYLPQTV-NH (IC_{50} = 10.27 μM). Furthermore, MTT cell viability assay performed against MDA-MB-231 breast (STAT3-dependent) and A4 (STAT3 null) cancer cell lines, displaying an IC_{50} = 5.35 μM and IC_{50} >100 μM respectively, provided evidence of a STAT3-specific inhibition, with a citotoxyc effect.

Further confirmation of its selectivity towards STAT3 with respect to STAT1 was obtained by Western Blot analysis on MDA-MB-231 at 5μM concentration. Moreover, other investigations evidenced that Crispene E does not interact with IL-6 directly. Molecular docking calculations

performed on (**31**) suggest that it might be capable to interact with the SH2 and DNA binding domains of STAT3, though with a different affinity. [77]

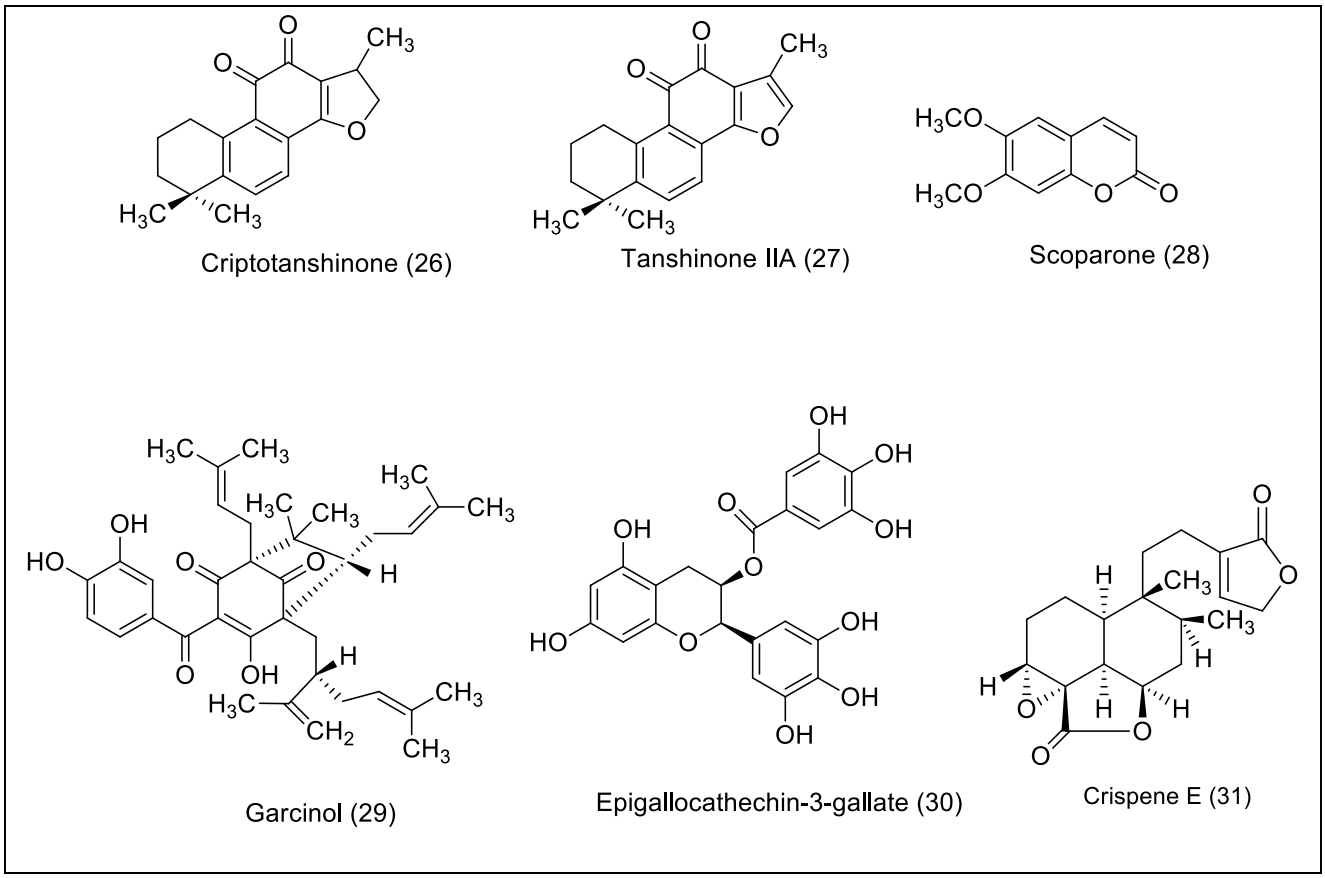

Fig. (10). Natural compounds structures targeting SH2 domain.

2.3.2 Semi-synthetic compounds

The diketone analogs of curcumin (**32**), FLLL32 (**6**) and its more soluble derivative FLLL62 (**33**) (Fig. (**12**)), bind STAT3 more selectively than the parent compound. The replacement of two hydrogen atoms on the central carbon of curcumin (**32**) with a spiro-cyclohexyl or with a spiro-tetrahydropyranyl ring improves the interaction of (**6**) and (**33**) with the Src homology-2 (SH2) domain of STAT3. This strategy confers a better stability to these derivatives with respect to curcumin (**32**), preventing the enolization of the two keto groups in the linker region [38].

In SK-RC-54, a human RCC cell line, FLLL32 (**6**) and FLLL62 (**33**) showed an absolute IC_{50} of 5.8 μM and 4.6 μM respectively [38]. Docking studies proved that both compounds bind to the STAT3

SH2 domain at the p-Tyr705 binding site identically, with a slight difference occurring at Leu706. Moreover, the interaction of the two ketones of (**6**) and (**33**) with Lys591 and Arg609 respectively, and with a hydrophobic side pocket block the homodimerization of p-STAT3. [78]

FLLL32 (**6**) was found to be more potent than other STAT3 inhibitors (e.g. Stattic, S3I-201) and curcumin (Fig. (**11**)) in colorectal, glioblastoma, multiple myeloma, rhabdomyosarcoma, and liver cancer cell lines, promoting apoptosis in multiple human cancer cell lines and inducing downregulation of STAT3 phosphorylation and DNA binding [38].

In human hepatocellular cancer cells, FLLL32 (**6**) also demonstrated to inhibit IL-6-induced phosphorylation of STAT3, displaying improved efficacy against STAT3 functional activity in tumor cells compared to curcumin and other STAT3 inhibitors [38].

Heterocyclic modification at the keto-enol moiety of curcumin (**32**) generated an important pharmacophore, which is able to modulate various biological pathways, acting as an antioxidant, anti-Alzheimer, anti-androgenic and cytotoxicity scaffold, and improving the pharmacokinetic profile [79].

The *in vitro* cytotoxicity of the synthesized curcumin analogues (**34**)-(**41**) ((Fig. (**11**)) was evaluated by MTT assay against head and neck cancer cell lines CAL27 and UM-SCC-74A, showing that all the compounds except for compound (**37**) are considerably active. To define the molecular mechanisms, a detailed study was performed [79].

Compounds (**34**) and (**37**) displayed a good activity against pSTAT3 phosphorylation in CAL27 cell line and compound (**40**) appeared to be active on pFAK and pAKT pathways. Moreover, compounds (**35**), (**36)**, (**38**) and (**39**) exhibited a potent cytotoxicity against CAL27 and UM-SCC-74A, but did not show any activity on pSTAT3, pFAK, PERK1/2 and pAKT signaling pathways.

The molecular docking of compound (**34**) into the STAT3 SH2 domain was performed. The predicted binding mode showed the formation of a hydrogen bond formation between a methoxy substituent of the compound and Arg609 and an interaction between Lys 591 and a phenyl ring [79].

In order to identify new STAT3 inhibitors, an *in silico* screening by molecular docking techniques was applied to a database of over 90 000 natural products and natural product-like compounds. The virtual screening provided 14 hit compounds, from which compound (**42**) ((Fig. (**11**)) emerged as a top candidate. Its molecular docking analysis on STAT3 SH2 was performed in order to better understand its binding mode. Its carboxylate group forms hydrogen bonds with Ser611 and Glu612, while the other moiety of the molecule binds Arg609. The benzofuran and isopropyl ester groups, instead, do not significantly interact with the protein [80].

In order to investigate the selectivity of compound (**42**) for STAT3, docking studies were also performed on STAT1 and STAT5. Very surprisingly, the binding mode of compound (**42**) with STAT1 and STAT5 is a lot different with respect to STAT3: it forms hydrogen-bond interactions with Glu612 and Lys591 of STAT1 *via* its carboxylate group, but does not bind any residue of STAT5 SH2 domain. Therefore, compound (**42**) shows unfavorable binding scores with STAT1 (–14.24) and STAT5 (–15.1). To further investigate its activity, docking analysis of the corresponding acid, which could be obtained from the cleavage of the isopropyl ester group by intracellular enzymes, has been performed showing a less favorable binding score [80].

In a co-immunoprecipitation assay, HEK293T cells were treated with compound (**42**) in a 6-well plate for 6 h. The results suggest that it inhibits STAT3-STAT3 dimerization in a dose-dependent way. The selectivity of (**42**) for STAT3 over STAT1, was also tested, highlighting that it selectively interferes with STAT3 dimerization, having no significant effect on STAT1 dimerization [80].

To investigate its cytotoxicity, LO2, HepG2, RAW264.7, and Caco2 cell lines were exposed to compound (**42**) (1–100 μM) for 72 h; then an MTT assay evaluated cellular proliferation. Compound (**42**) was found to be relatively non-toxic towards the normal liver LO2 cell line (IC_{50} >100 μM) and exhibited dose-dependent inhibition of cell proliferation in neoplastic HepG2, RAW264.7 and Caco2 cell lines (IC_{50} = ~ 30 μM).

Moreover, a dose-dependent reduction in STAT3-DNA binding activity was detected in its presence. Under the same conditions, compound (**42**) showed an IC_{50} = ~ 15 μM, comparable to the IC_{50} of S3I-201 (IC_{50} = ~10 μM). Such results identify this compound as a specific STAT3 inhibitor exhibiting a selective cytotoxicity on cancer cells over normal cells. [80].

From recent researches, shikonin (**43**) (Fig. (**11**)), the major active component of the Chinese herbal medicine *Lithospermum erythrorhizon*, was identified as an inhibitor of the STAT3 pathway [81]. It displayed impressive pharmacological activity on STAT3 in breast cancer models, like MCF-7 (IC_{50} = 4.57 ± 0.69), BT-474 (IC_{50} = 5.74 ± 0.66), SKBR-3 (IC_{50} = 3.75 ± 0.52), MDA-MB-436 (IC_{50} = 3.28 ± 0.41), MDA-MB-231 (IC_{50} = 2.88 ± 0.25) and MDA-MB-468 (IC_{50} = 3.61 ± 0.34) [82].

Many synthetic STAT3 inhibitors, like plumbagin and LLL-12, share the same backbone with (**42**), suggesting a scaffold predisposition for targeting STAT3 [83, 84]. Therefore (**43**) structure might be a good starting point to synthesize new drugs with an improved profile against STAT3 [82].

Virtual simulations were employed to define the binding mode of (**43**). Therefore, maintaining the key intermolecular interactions, the backbone of (**43**) was modified, leading to a small library of (**43**) derivatives with higher binding affinity [82].

Among these derivatives, the hit compound PMM-158 (**44**) ((Fig. (**11**)) shares a similar binding mode with the original scaffold of (**43**), while the substituent group adds favorable interactions with STAT3. It was tested in six kinds of breast cancer cells: MCF-7 (IC_{50} = 12.1 ± 0.42), BT-474 (IC_{50} = 15.6 ± 1.03), SKBR-3 11.5 ± 0.74), MDA-MB-436 (IC_{50} = 10.1 ± 0.92), MDA-MB-231 (IC_{50} = 9.17 ± 0.99) and MDA-MB-468 (IC_{50} = 10.6 ± 0.65). This compound was structurally modified in order to better understand the structure-activity relationships. Molecular dynamics studies were performed on (**43**), (**44**) and PMM-172 (**45**) ((Fig. (**11**)) resulting in good values for both systems and ligands that are quite stable in the equilibrium state [82].

The identified compounds were synthetized, and they showed lower toxicity against the non-tumorigenic MCF-10A cells than (**43**), during *in vitro* tests. Moreover, these compounds displayed potent anti-proliferative activity against a HER2-over-expressing cell line and, among them, (**45**) showed a better anti-proliferative activity (IC_{50} = 1.98 ± 0.49 μM) against MDA-MB-231 cell line, compared to (**43**) (IC_{50} = 3.28 ± 0.41 μM) and Stattic (IC_{50} = 3.76 ± 0.50 μM). Furthermore, (**45**) induced apoptosis in a dose- and time- dependent way, even more effectively than Stattic, elevating the expression of cleaved PARP and cleaved caspase-3, which are hallmarks of cell apoptosis [82].

Interestingly, the level of the phosphorylated STAT3 was not affected by (**45**) in non-cancer MCF-10A cells; the expression levels of STAT1, STAT5 and their phosphorylated forms in MDA-MB-231 cells were analyzed to evaluate the selectivity of (**45**). Since no evident changes were observed in STAT1 and STAT5 phosphorylation levels, the conclusion may safely be that (**45**) predominantly suppresses STAT3 activation in STAT3-dependent breast cancer cells [82].

During the treatment of MDA-MB-231 cells with (**45**), the expression levels of STAT3 in the nucleus was reduced, as well as the levels of representative downstream proteins like Bcl-2, Bcl-XL, survivin and cyclin D1 [82].

In summary, these results suggest that this class of natural product derivatives might be extremely helpful for the future development of potent direct STAT3 inhibitors [82].

STA 21 is a molecule able to bind to the SH2 domain of STAT3 and block the dimerization of STAT3, forming hydrogen bonds near Arg 595, Arg 609 and Ile634. As the benzo[a]anthracene-1,7,12-trione moiety of STA 21 makes it hard to design analogs for SAR studies, STA 21 was simplified by retaining the anthracene moiety and the functional groups, which are critical for STAT3 SH2 domain binding; therefore, it was converted into an anthraquinone to generate compound (**46**) ((Fig. (**12**)) [85].

Molecular docking studies revealed that compound (**46**) retains the main interactions of STA 21 with the SH2 domain [82].It has a similar anti-proliferative activity compared to STA 21 towards DU145, PC3, and LNCaP with IC_{50} values of 16.2, 13.4, and 34.1 μM, respectively. Such activity is directly proportional to the level of constitutively active STAT3 expression. Compound (**46**) exhibited a weak anti-proliferative activity only towards MCF-7 cells (IC_{50} = 84 μM), like STA 21 [85].

Other analogs highlighted the importance of the H-bonding interaction in SH2 surface. Among them, compound (**47**) ((Fig. (**12**)), bearing a hydroxyl group in position 8 on the anthracene moiety, could not form a hydrogen bond with Ile634 in the SH2 domain. Nevertheless, molecular docking suggests that the 8-OH group of compound (**47**) is bound to Glu594, located in the SH2 domain, justifying its anti-proliferative activities, which makes it a lead for the design of more potent and selective STAT3 inhibitors [85].

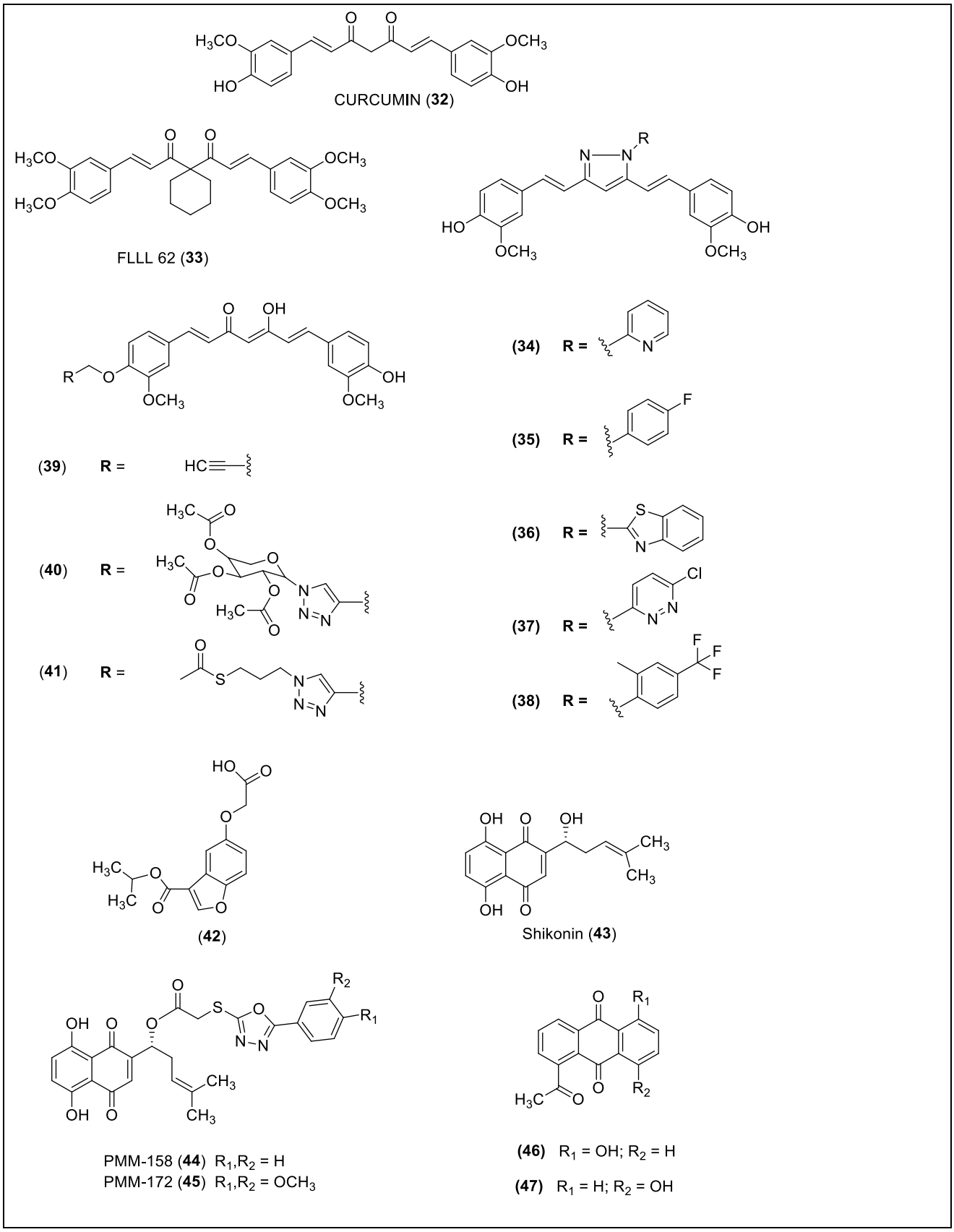

Fig. (11). Structure of semi-synthetic compounds (**32**)-(**47**) targeting SH2 domain

2.3.3. Synthetic compounds

2.3.3.1. Peptidomimetics

Among the synthetic derivatives, peptidomimetics have been investigated to obtain STAT3 SH2 domain inhibitors. In particular, a set of 12 peptidomimetic compounds mimicking the pTyr-Xaa-Yaa-Gln recognition motif have been designed and tested. Fluorescence polarization evaluated their binding affinities, obtaining for them IC_{50} values that range from 39 nM (strong binder) to over 100.000 nM (weak binder). A computational modeling strategy was employed to study the structures of the peptidomimetic-SH2 domain complexes. Considering the flexibility of the SH2 domain, the variations of the bound conformations and the estimated binding affinities (crucial to differentiate strong from weak binders), 1000 conformations for each peptidomimetic complexing the SH2 domain were obtained.

Three strong binders, compound (**48**) (IC_{50} = 190 nM) (Fig. (**12**)), compound (**49**) (IC_{50} = 83 nM) (Fig. (**12**)) and compound (**50**) (IC_{50} = 68 nM) (Fig. (**12**)), showed three different, stable binding modes: the bent, the extended, and the wedged mode respectively. The bent and the extended binding modes were already known from previous modeling studies, whereas the wedged mode was a new discovery. In this mode, the peptidomimetic (compound 50) binds to the SH2 domain with the negatively charged phosphate group of the pTyr situated inside a positively charged pocket, forcing the C-terminal benzyl group to wedge in a cavity made by two loops of the SH2 domain containing the residues 623–629 and 656–668 respectively. Hydrogen bond interactions can be found in this pocket and between the peptidomimetic and the residues on the two loops [86].

Despite the overall success of the modeling strategy, there are some exceptions: for instance, considering (**51**) (Fig. (**12**)), a relatively strong binder (IC_{50} = 105 nM), its estimated binding affinities are comparable to those of weak binders: however this anomaly could be due to an inaccurate starting conformation of the peptidomimetic, leading to inaccurate estimation of binding affinity [86].

Although the computational docking of large ligands such as peptidomimetics is extremely challenging, the abovementioned strategy and the subsequent data analysis revealed crucial aspects of the peptidomimetic binding to the SH2 domain of STAT3. Moreover, a novel binding mode resulting in stable binding interactions was discovered. These results could be useful to improve the design of compounds targeting the identified sub-binding pockets [86].

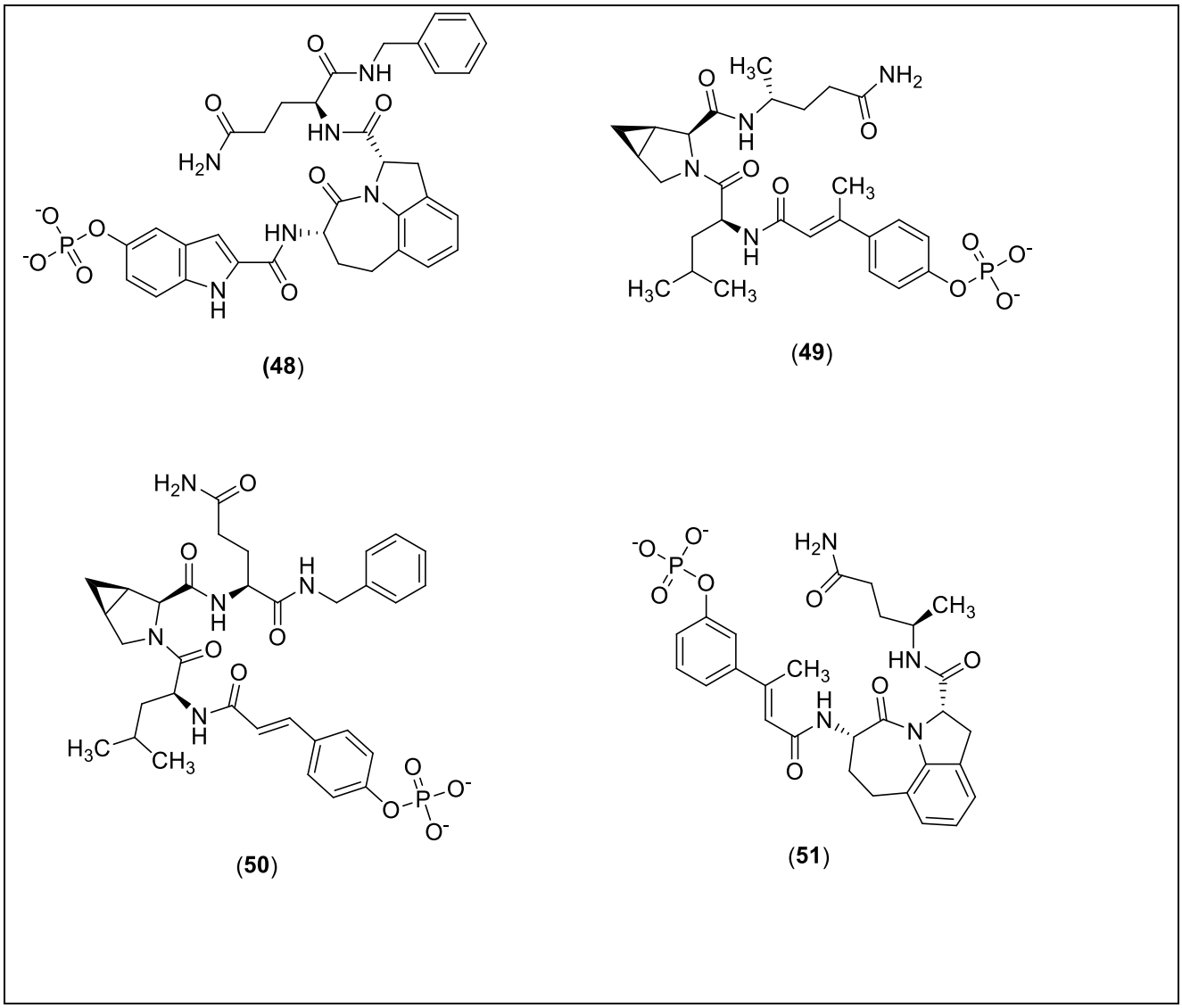

Fig. (12). Structure of peptidomimetics STAT3 inhibitors targeting SH2 domain

2.3.3.2 Non-peptidic compounds

In the last decade, many attempts have been made in order to synthesize new non-peptidic compounds characterized by a good ADME profile.

However, before exploring the newest options for STAT3 direct inhibition, it is important to mention the first non-peptidic small molecule that was demonstrated to inhibit the function of STAT3 binding in the SH2 domain regardless of STAT3 phosphorylation state *in vitro*. Stattic (**52**) (Fig. (**13**)) (acronym for STAT3 inhibitory compound), or 6-nitro-benzo[b]thiophene-1,1-dioxide) [20], was identified through a screening on a chemical librarie of 17.298 substances, among the 144 compounds inhibiting the binding of a fluorescein-labeled p-Tyr containing peptide to the STAT3 SH2 domain by more than 60%. Stattic (**52**) is able to prevent IL-6-induced STAT3 nuclear translocation and DNA

binding of p-STAT3 in a temperature-dependent manner, exhibiting high potency at 37°C (IC_{50} = 5.1 ± 0.8 μM) and selectivity over STAT1 [87].

This compound has no relevant effect on the binding of other p-Tyr-peptides to SH2 domains of different proteins (like Lck kinase), nor in the dimerization of other dimeric transcription factors (like c-Myc/Max and Jun/Jun). Further specificity evaluations were performed to check the behavior of (**52**) towards STAT1 and STAT5b, resulting in a lower inhibition of the SH2 domains of STAT1 (78% homology with STAT3) and STAT5b (59% homology with STAT3) [86]. SAR of (**52**) and two modified molecules at 37°C highlighted the importance of the nitro group, since its substitution with an NH_2-group or with a hydrogen led to a loss of activity in the fluorescence polarization assay. Similarly, a decrease in the activity was observed when the double bond of the vinyl sulfone moiety was saturated [86]. Electrophoretic mobility shift assays (EMSA) performed at 37° C using nuclear extracts containing p-STAT3 and p-STAT1, demonstrated the inhibition of DNA binding of STAT3 homodimers by Stattic at a concentration of 10 μM, whereas the binding of STAT1 homodimers was not significantly inhibited at concentrations up to 200 μM. In conclusion, Stattic selectively inhibits activation, dimerization, and nuclear translocation of STAT3, inducing apoptosis in STAT3-dependent cancer cell lines [86].

By a virtual screening, compound STX-0119 (**14**) (Fig. (**5**)) was discovered [88, 89, 90] It selectively binds to STAT3 SH2 domain and could lead to the generation of a new class of inhibitors of STAT3 dimerization. Many analogs were synthesized, but they exhibited a lower activity: for instance, whereas (**14**) presents 99% inhibition at 100 μM, the truncated derivative STX-0872, lacking the 2-Ph group, is inactive in the performed reporter gene assay (no inhibition at 100 μM)] [88].

A fluorescence resonance energy transfer (FRET) confirmed the ability of (**14**) to inhibit STAT3 dimerization in cells and Western blotting analysis evidenced a concentration-dependent reduction of the levels of STAT3 target proteins like c-myc, cyclin D1, and survivin. Notably, STX-0119 has no effects on the level of total STAT3 or p-STAT3, suggesting a direct interaction with the protein and excluding an interference with upstream regulators. Moreover, no inhibition was observed on other STAT family members [88]. A docking model of (**14**) bound to the STAT3-SH2 domain suggested that the Ph ring accommodates into the hydrophobic fissure nearby the p-Tyr binding pocket, justifying the lack of activity of its analogues, which bear a smaller substituent such as a hydrogen atom at this position. The amidic carbonyl group of Ser636 forms a hydrogen bond with the amidic-NH and a hydrophobic interaction is observed between the furan ring and the indole moiety of Trp623 [88].

More recently, carbazole derivatives have been considered, because they exhibit many different biological profiles, among which antiproliferative effects on SVR murine endothelial cells and cytotoxic activity against human solid cancer cells. These effects suggest that the carbazole scaffold is a privileged structure, able to bind different classes of macromolecules with high affinity and modifiable with different chemical substitutions; therefore, it has been proposed as a lead compound for STAT3 direct inhibition [91]. Starting from a 1,4-dimethyl-carbazole structure, further modifications were investigated to find out the minimum structural elements for the target binding ; new substituents were introduced to increase the affinity for the macromolecule, although to the detriment of bioavailability [91]. p-Tyr plays a pivotal role in STAT3 recognition during the homodimerization process, in which one monomer recognizes the Pro-Tyr/p-Tyr- Leu-Lys-Thr-Lys sequence of the other; for the screening of potentially interacting compounds, the protein region accommodating this sequence and, especially, the one interacting with p-Tyr, were considered. Through molecular docking, a 3D model of the STAT3-(**53**) complex (Fig. (**13**)) was obtained. The latter was utilized as a scaffold to design compounds **(54)-(62)** (Fig. (**13**)), whose substitution was hypothesized by looking at the 3D model itself. Since Tyr705/p-Tyr705 is accommodated in a small cavity, interacting with the side chains of Lys591, Arg609, Ser611, Glu612 and Ser613, compounds (**54**)-(**57**) were designed with a H-bond acceptor on C6, to mimic the pivotal interactions responsible for protein dimerization [91]. To further evaluate changes in interaction, different groups and substituents were inserted, like a hydroxyl group, a methoxy, an ethyl ester group, a chlorine, and a sulfonamide function. It was also noticed that the position 3 of the carbazole is close to Arg595 side chain, therefore compounds (**59)** and (**60**) were substituted at C3 with a nitro group. Leu706 NH group from the Pro-Tyr/p-Tyr- Leu-Lys-Thr-Lys sequence forms an H-bond with the backbone C=O of Ser636, but it has also van der Waals interactions with side chain of Trp623 and Val637. Therefore, compounds (**54)**-(**60**) mimic the H-bond of Leu706, while compounds (**61**)-(**62**) could increase the contacts with STAT3 through van der Waals interactions by the introduction of an alkyl group on the nitrogen, weakening the hydrogen bond. All the newly designed compounds (**54**)-(**62**) docked well into STAT3 binding site. These small molecules represent the first example of u-STAT3 modulation by a substitued 1,4-dimethyl-carbazole scaffold. Even though compounds (**54**)-(**62**) showed only a modest efficacy, the aim of the study was to simplify the carbazole scaffold in order to develop more potent and druggable STAT3 inhibitors [91].

The aminotetrazole ring is another important moiety present in STAT3 direct inhibitors. A structure-based screening was used to select non-peptide compounds that mimic the p-Tyr peptide, leading to the identification of compound (**63**) (Fig. (**13**)) as the most promising candidate. SAR were performed on compound (**63**), in which every radical (R_1, R_2, R_3) was replaced with different chemical groups

and afterwards each obtained analog was tested for activity, and selectivity towards STAT3 over STAT1. The results showed that electron donating and hydrophilic groups in R_1 reduce the activity on STAT3, while small electron withdrawing groups maintain or increase activity and selectivity against STAT1 [92]. Among those, compound (**64**) (Fig. (**13**)), bearing a nitro group at *para* position, led to an increased selectivity and efficacy towards STAT3, whereas the introduction of additional nitro groups did not enhance the inhibitory activity. Moreover, the methoxy group in R_2 is fundamental, being neither removable nor replaceable. The pivotal role of the secondary amine in the aminotetrazole moiety was highlighted by the reduced activity of the methylene derivative and the bioisoster in which the tetrazole was replaced by a carboxylic acid. Non-ionizable aldehyde and cyanamide derivatives with a planar structure displayed the same level of inhibition as the tetrazole analogs, suggesting that the planar structure of the hydrophilic site of the inhibitor is pivotal in STAT3 binding. A negative charge on the tetrazole moiety is essential for the selectivity, as evidenced by compound (**64**), which is the only compound showing low activity on STAT1[92]. Furthermore, inhibitors containing a tetrazole group display stronger binding energies than those lacking this group, suggesting its importance in the binding of the molecules to the interface of SH2 domain of STAT3. A similar binding ability on STAT3 monomers is shown by every compound containing a planar hydrophilic part and the presence of the aminotetrazole group prevents interaction with STAT1. Western blot analysis confirmed that (**64**) is able to bind STAT3 and prevent its translocation into the nucleus, having antiproliferative effects in B9 myeloma cell line and MDA-MB-231 breast cancer cell lines, and in the luciferase assay, it exhibits a significant activity (IC_{50} = 25.7 ± 2.6 μM) [92].

A series of 2-carbonylbenzo[b]thiophene 1,1-dioxide derivatives (CBT) were initially developed to block STAT3 phosphorylation; however, by incorporating flexible groups to the benzo[b]thiophene 1,1-dioxide (BTP) core structure, more potent compounds were discovered. [93]. The benzo[b]thiophene 1,1-dioxide was considered as the leading scaffold. Previous studies demonstrated the ability of this moiety to bind to the fissure of STAT3 SH2 domain, which contains the polar pTyr705 site, the contiguous hydrophobic side pocket, and the Leu706 site. Molecular docking analysis showed that an aromatic/aliphatic moiety at position 2, bound through different linkers (like amide, carbonyl, and ester), strengthens the interaction between BTP and the protein, improving potency and selectivity. Therefore, a series of 2-carbonylbenzo[b]thiophene 1,1-dioxide derivatives (CBT) was synthesized and their inhibitory activity tested [93]. Among the synthesized analogs, compound (**65**) (Fig. (**13**)) displayed a better activity towards MDA-MB-231 (IC_{50} = 0.70 ± 0.34 μM), MDA-MB-435S (IC_{50} = 0.79 ± 0.09 μM), MCF-7 (IC_{50} = 0.91 ± 0.07 μM), DU145 (IC_{50} = 1.03 ± 0.29 μM), PANC-1 (IC_{50} = 2.81 ± 0.46 μM) and A549 (IC_{50} = 1.70 ± 0.29 μM) cell lines. Therefore, the mechanism of its inhibition in a STAT3-dependent dual luciferase reporter assay in HeLa cells

(expressing high levels of p-STAT3) was studied. This compound exhibits a concentration-dependent activity and at 4 μM the luciferase activity is decreased by 48%, which is a remarkable result. Western blot analysis revealed that Tyr705 phosphorylation is inhibited in a dose-dependent manner, whereas the total level of STAT3 is not affected. Moreover, compound (**65**) displayed high inhibitory effect on STAT3 phosphorylation, without showing a significant inhibition on the phosphorylation of other kinases involved in the STAT3 signaling pathway [93].

Through a recent molecular docking study, a new compound, which binds directly to STAT3 SH2 domain has been identified: benzyloxyphenilmethylaminophenol (**66**) (Fig. (**13**)). In order to perform Structure Activity Relations studies and discover more potent inhibitors, analogues of (**66**) were produced and tested, firstly to optimize the A, B rings, and then the linker. The inhibitory activity of the new derivatives towards STAT3 was evaluated using a luciferase reporter method. The hydroxyl group at C4 in ring A is crucial for the activity. Considering the B ring, the removal of chlorine at C5 in compound (**66**) (derivative (**67**), Fig. (**13**)) improved the luciferase activity (IC_{50} = 26.68 μM and IC_{50} = 7.71 μM for compounds (**66**) and (**67**), respectively). Moreover, the substitution with a fluorine atom in C5 of ring B (compound (**68**), Fig. (**13**)) is favorable while hindered substituents in C5 abolish the inhibiting activity, highlighting the importance of the dimension of substituents at C5 of ring B [94]. The activity is lost also when the position of chlorine in ring B changes from C5 to C4 and C6, whereas moving it from C5 to C3 increases luciferase activity (compound (**69**), Fig. (**13**)) (IC_{50} = 1.38 μM). The presence of the electron-withdrawing nitro group in ring B (compound (**70**), Fig. (**13**)) confers similar activity to compound (**66**) (IC_{50} = 24.09 μM), while electron-donating groups decrease or cancel the activity. Moreover, after the treatment with derivatives (**67**) and (**69**), the expression of total STAT3 did not change, whereas p-Tyr decreased in a dose-dependent manner. Both showed no effect on upstream kinases, such as Src, which can also activate STAT3, excluding an indirect mode of action [94]. Molecular docking revealed that (**67**) and (**69**) bind to a unique site of STAT3 SH2 domain, and not in the p-Tyr705 binding site: ring A inserts into an hydrophobic fissure provided by Tyr640 and Ile653. Ring A contains a hydroxyl group, which forms a H-bond with Cys712, which is a key interaction, because changing the hydroxyl group leads to a decrease in the activity, which is completely abolished when the group is removed. The NH group between ring A and ring B forms a H-bond with Gln644. Rings B and C bind the target protein like a clip; therefore, a flexible linker is pivotal, as demonstrated by the fact that conformational restricted compounds do not bind to the target and therefore have no activity [94].

Lately, a series of 4-carbonyl-2,6-dibenzylidenecyclohexanone derivatives were synthesized and tested as antiproliferative agents. Compound (**71**) (Fig. (**13**)) showed a potent antiproliferative activity in a range of cancer cell lines and demonstrated to effectively inhibit Tyr705 phosphorylation in STAT3 protein, exhibiting also low toxicity against normal human cells. SAR study, evidenced that all derivatives containing electron-withdrawing substituent ((**71**) included) exhibited greater potency compared to compounds bearing the electron-donating substituents (OMe, OH, H) [95]. Among all the synthetized analogs, the IC_{50} value of compound (**71**) is lower towards three cancer cells lines (IC_{50} values of ~ 0.6 , ~2 and ~1.7 μM *versus* MDA-MB-231, A549 and DU145 respectively) than against normal human liver cell line HL-7702 (IC_{50} = ~ 3.6 μM). This result highlights its high cytotoxic effects on cancerous cells and the great selectivity against cancer cells *versus* normal cells. Molecular docking studies showed that compound (**71**) can inhibit STAT3 by simultaneously occupying three sub-pockets in the SH2 domain, composing the p-Tyr705 and Leu706 sites and a side pocket. In particular, the amino group of the diethylamino moiety forms a salt bridge interaction with the carboxylic group of Glu594, while the carbonyl oxygen accepts a H-bond from the amino group of the backbone in Ser636. The alkyl group of diethylamino moiety has hydrophobic interactions with the residues Ile634, Ile597 and Glu594. The fluorobenzene ring occupying pTyr705 site interacts with amino group of Lys591. These observations suggest that compound (**71**) could be further developed as lead compound for the discovery of potent STAT3 SH2 direct inhibitors [95].

Another small molecule, which is orally bioavailable for the treatment of cancer is BP-1-102 **(72**) (Fig. (**13**)). This compound is able to bind to the three solvent-accessible subpockets of the STAT3-STAT3 dimerization interface (SH2), forming H-bonds in the third subpocket and additional interactions with a charged Lys side chain through the pentafluorobenzene. Compound (**72**) has consistent *in vivo* efficacy and antitumor effect, disrupting STAT3 binding to p-Tyr containing peptide in the SH2 domain with an IC_{50} = 4.1 μM, as determined by FP assay [20, 66].

Recently, two new compounds were identified as promising scaffolds for the development of potent and selective STAT3 inhibitors: the hydroxamic acid, SH5-07 (**15**) (Fig. (**5**)), and the benzoic acid, SH4-54 (**16**) (Fig. (**5**)), analogues of BP-1- 102 (**72**). The blockage of STAT3 signaling by SH5-07 and SH4-54 is associated with decreased Bcl-2, Bcl-xL, Cyclin D1, c-Myc, Mcl-1 and survivin expression, and antitumor responses in human glioma and breast cancer models at concentrations of 1 to 8 μmol/L, as evidenced by STAT3-dependent luciferase reporter assay. Nuclear Magnetic Resonance analysis showed interactions between these molecules and the SH2 domain of STAT3 (but also with the DBD) [96]. An EMSA analysis demonstrated that both (**15**) and (**16**) inhibit STAT3 in a dose-dependent manner (IC_{50} = 3.9 ± 0.6 μM and IC_{50} = 4.7 ± 0.5 μM, respectively), exhibiting improved potency values with respect to (**72**), (IC_{50} = 6.8 μM). Further studies demonstrated that the

compounds preferentially inhibit STAT3-STAT3 activity, with lower effects on STAT1-STAT3, STAT1-STAT1 or STAT5-STAT5 and none of them displayed appreciable effects against STAT1 or STAT5 activity. NMR studies demonstrated that these compounds interact specifically with STAT3. The binding of the compounds produces a selective changes in Ile597, Ile386 and Ile439 and Leu411. The modification of Ile signals shows that the compounds bind to both the STAT3 SH2 and DBD domains. Residues Leu411, Ile386, and Ile439 form a hydrophobic pocket, which has a pivotal role in compound binding. EMSA analysis indicated that the SH2 domain represents the primary target site for the compounds, whereas the DBD interaction only moderately contributes to the overall compound effect against STAT3 [96]. Considering their responsiveness in tumor models characterized by persistently active STAT3 (including glioma, breast, prostate, and lung cancer) in comparison with other noteworthy agents (like (**72**), (**15**) and (**16**)), they possess stronger activity and therefore represent potential candidates for future development of potent STAT3 inhibitors to be used in clinic, particularly for human glioma and breast cancers, where they induce antitumor response *in vitro* and *in vivo* [46].

Subsequently, a set of STAT3 SH2 domain binders was considered to construct a pharmacophore model in order to identify the common features required for the binding of STAT3 inhibitors to the SH2 domain. The best pharmacophore model contains one hydrophobic unit, three hydrogen bond acceptors and one aromatic ring unit. This model was used to screen a database of 78 compounds and the four highest-scoring compounds and a negative control were tested. Among them, compound (**73**) (Fig. (**13**)) was the most potent derivative, satisfying all the features of the pharmacophore model [46]. A molecular docking analysis of compound (**73**) with STAT1 and STAT5 demonstrated that this compound is able to bind to both of them with unfavorable binding scores. A STAT3 DNA-binding assay was performed to examine the effect of the hit compound on DNA-binding activity, treating nuclear extracts from EGF-stimulated cells with the new compound and S3I-201 (**74**) (a known STAT3 inhibitor, Fig. (**14**)) [20]. An ELISA test was performed and the results showed that (**73**) has a great ability to inhibit STAT3 DNA-binding activity *in vitro* and that the reduction of such activity is dose-dependent. The activity of compound (**73**) is comparable to that of the known STAT3 inhibitor (**74**) (IC_{50} = ~10 μM for both) and it is able to inhibit STAT3 DNA-binding activity [46]. To study the effects of (**73**) on STAT3-dependent transcription, HeLa cells were used in a luciferase reporter assay and treated with different concentrations of compound (**73**) or (**74**) for 6 h. Afterwards, they were stimulated with EGF for 30 min. The treatment of cells with compound (**73**) led to a reduction in luciferase activity, indicating that the latter could inhibit STAT3 transcriptional activity (IC_{50}= ~ 10μM), much better than (**74**) (IC_{50} = ~ 30 μM). A fluorescence polarization assay was performed in order to investigate whether (**73**) could target the SH2 domain of STAT3 *in vitro*. The results show

that it displaces the fluorescent pTyr peptide from STAT3 and decreases the fluorescence polarization signal of the system, which means that it is indeed able to inhibit the binding of the p-Tyr peptide to STAT3 in a dose-dependent manner (IC_{50} = 10 μM) [46]. Compound (**73**) inhibits STAT3 phosphorylation in a dose-dependent manner and it has no significant effect on the expression of total STAT3 in cells. Considered together, these results suggest two potential mechanisms of action: compound (**73**) might directly bind to the SH2 domain and block reciprocal pTyr–SH2 interactions, or may inhibit Tyr705 phosphorylation, indirectly repressing STAT3 dimerization. Therefore, compound (**73**) represents a promising scaffold to be modified to obtain new direct STAT3 inhibitors [46].

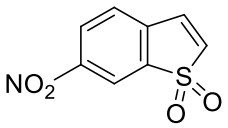

Stattic (**52**)

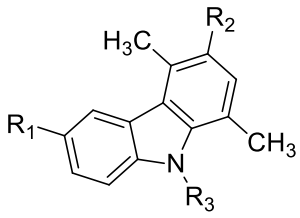

(**53**) - (**62**)

(**53**)	R_1 = H;	R_2 = H;	R_3 = H;
(**54**)	R_1 = OH;	R_2 = H;	R_3 = H;
(**55**)	R_1 = OMe;	R_2 = H;	R_3 = H;
(**56**)	R_1 = COOEt;	R_2 = H;	R_3 = H
(**57**)	R_1 = Cl;	R_2 = H;	R_3 = H;
(**58**)	R_1 = SO_2NH_2;	R_2 = H;	R_3 = H;
(**59**)	R_1 = OMe;	R_2 = NO_2;	R_3 = H;
(**60**)	R_1 = COOEt;	R_2 = NO_2;	R_3 = H;
(**61**)	R_1 = OMe;	R_2 = H;	R_3 = Me;
(**62**)	R_1 = OMe;	R_2 = H;	R_3 = Et.

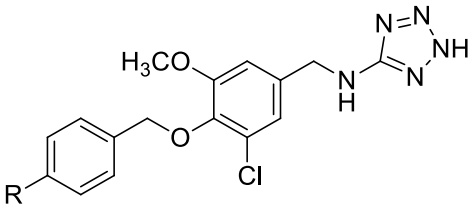

(**63**) R = CH_3
(**64**) R = NO_2

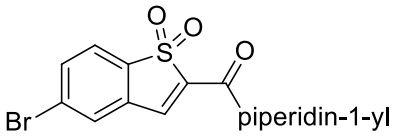

(**65**)

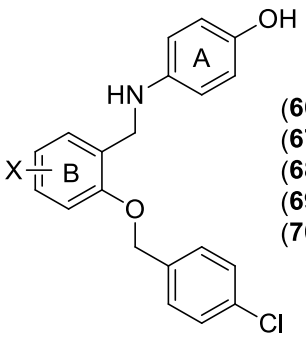

(**66**) X = 5-Cl
(**67**) X = H;
(**68**) X = 5-F;
(**69**) X = 3-Cl;
(**70**) X = 5-NO_2

(**66**)-(**70**)

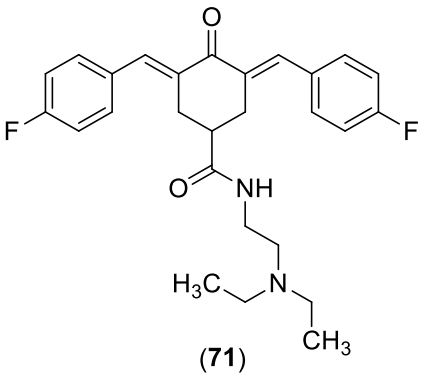

(**71**)

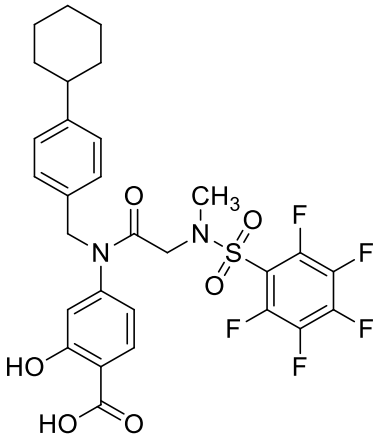

BP-1-102 (**72**)

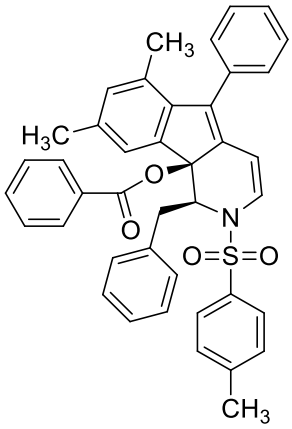

(**73**)

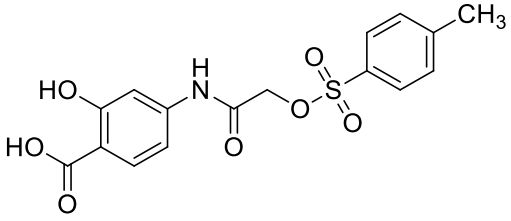

S3I-201 (**74**)

Fig. (13). Structures of synthetic SH2 domain inhibitors (to be continued).

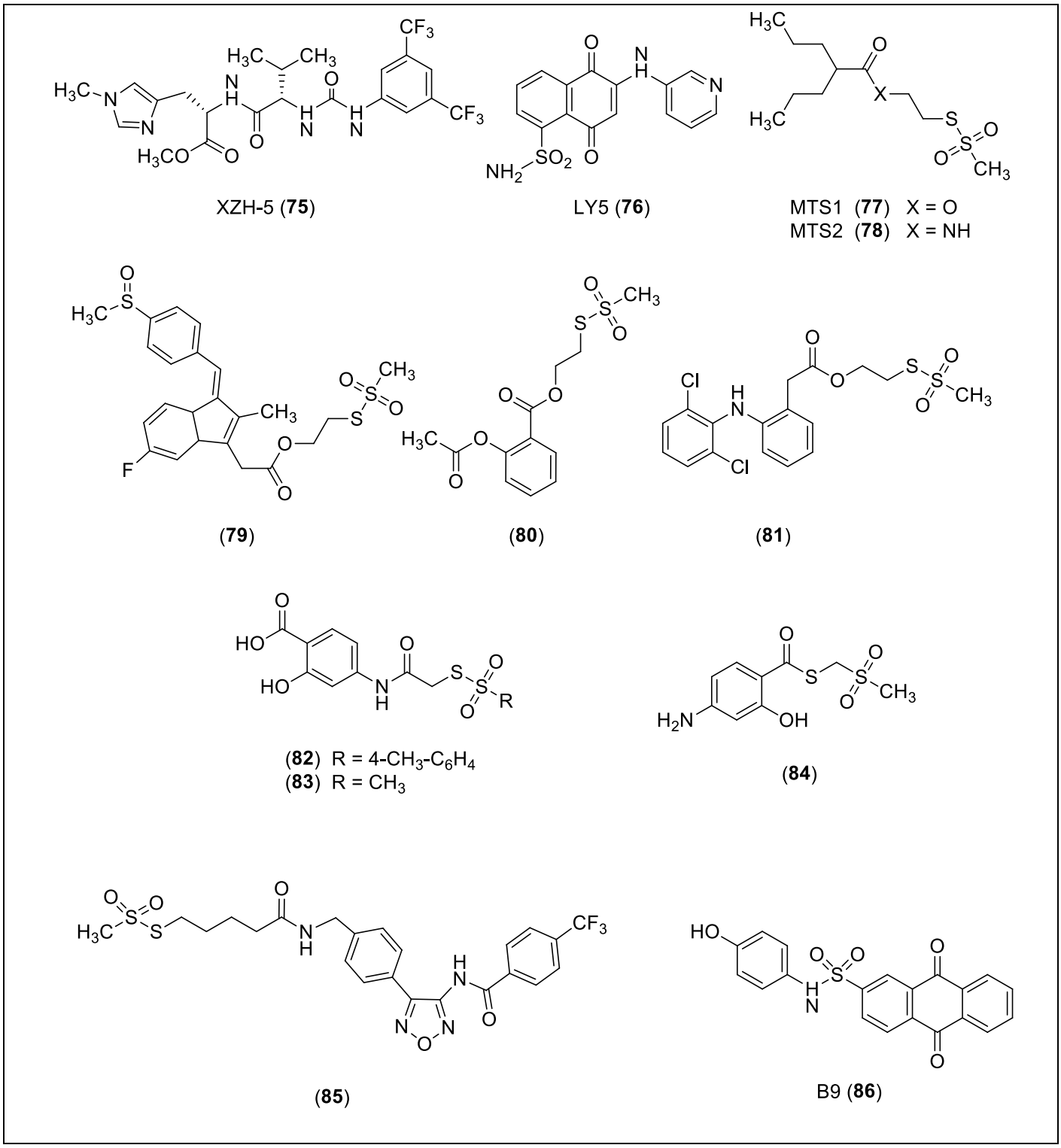

Fig. (13). Structures of synthetic SH2 domain inhibitors.

Another small molecule that was reported to inhibit STAT3 binding to the SH2 domain is XZH-5 (**75**) (Fig. (**13**)). This compound exhibits antitumor activity in human hepatocellular carcinoma cells, rhabdomyosarcoma cells, breast and pancreatic cancer cells. The target of (**75**) and its analogs is the p-Tyr705 binding pocket and the nearby hydrophobic side pocket. A carboxylate portion derived from histidine mimics the phosphate of p-Tyr, whereas the trifluoromethyl-benzene moiety forms hydrophobic interactions with the side pocket. Urea and peptidyl linkers provide the right distance between the two binding sites, forming H-bonds along the space separating the two sites. (**75**) is very flexible; therefore, a large number of structural modifications can be made and studied in order to enquire the SAR characteristics [97]. Derivative (**75**) represents a modifiable scaffold, already possessing antitumor activity. In analyzing the structure, it has been found that both the trifluoromethyl groups were found to be necessary, probably because they influence the lipophilicity and the pKa of the phenyl ring. As for the histidine moiety, derivatives were synthetized removing the imidazole substituent at R_2, but they showed poor activity compared to the lead compound, providing evidence that the imidazole ring is a pivotal part of the molecule. Considering the central valine portion of (**75**), eight different analogs have been synthesized using different amino acids, in order to obtain different groups at R_3. The results showed that when R_3 substituent is a methyl group, the IC_{50} value increases from 24.7 μM to 50-100 μM against PANC-1 cell line; an aromatic phenyl group at R_3 also increases inhibitory activity. R_1 and R_2 groups contribute to hydrophobicity, allowing the inhibitor to maintain a position overlapping p-Tyr705 binding site with R_3 and R_1 bound in SH2 domain pockets [97].

By an *in silico* fragment-based drug design (site directed FBDD), with the aim of identifying fragments targeting the SH2 domain, a new non-peptide small molecule, LY5 (**76**) (Fig. (**13**)), was selected. Computational docking studies showed that it has a highly favorable docking energy towards STAT3 SH2 domain. LY5 was designed as a novel STAT3 scaffold with high potency and selectivity. Further studies confirmed that LY5 significantly inhibits STAT3 phosphorylation at low drug concentrations in medulloblastoma cells overexpressing STAT3 and lowers the levels of downstream genes in treated tumor cells. LY5 is cell-permeable and blocks STAT3 activation binding with high affinity to STAT3 SH2 domain, as confirmed by the fluorescence polarization assay (IC_{50}= 0.5 – 1.4 μM) [98, 99]. Moreover, (**76**) induces apoptosis and provokes a dramatic VEGF, MMP-9 and angiopoietin decrease *in vitro.* Compound (**76**) is also able to decrease STAT3 phosphorylation, IL-6-dependent STAT3 nuclear translocation, prevent cell migration and suppress angiogenesis [99]. However, very recently, *in vivo* studies did not confirm that the anticancer activity of (**76**) is mediated by STAT3 inhibition [100].

In the past years, (**74**) was recognized as a selective STAT3-SH2 domain inhibitor, able to block STAT3 homodimerization (Fig. (**13**)). It demonstrated the ability to inhibit breast and hepatocellular cancer cells proliferation in mice, although its electrophilic tosylate group renders it very susceptible to alkylate other substrates. Therefore, several derivatives of (**74**) were designed and synthesized [101]. Considering that literature has provided evidences about the ability of S-methyl methanethiosulfonates (SMMTS), isolated from cauliflower, to inhibit colon tumor incidence in rats, recently [102], two methanethiosulfonate (MTS) derivatives of valproic acid (MTS 1 (**77**) and MTS 2 (**78**)) (Fig. (**13**)) were synthesized and studied, exhibiting interesting anticancer properties. In particular, (**77**) demonstrated to have antiproliferative activity on several different tumor cell lines *in vitro* at micromolar concentration, and to inhibit PC3 growth in subcutaneous xenografts *in vivo*. To evaluate the ability of (**77**) and (**78**) to interact with STAT3 SH2 domain, they were tested by an AlphaScreen-based assay. Both (**77**) and (**78**) displayed a potent blockage of phosphopeptide binding to STAT3 SH2 domain; therefore, to better understand thiosulfonate behavior towards STAT3, further investigations involving other thiosulfonate compound hybrids and parent drugs were performed [101]. Since COX inhibitors could be extremely useful in cancer treatment, NSAIDs-thiosulfonate hybrids (**79**), (**80**), and (**81**) (Fig. (**13**)) (which derive from sulindac, acetyl salicylic acid (ASA), and diclofenac, respectively) were also considered, with the aim of finding a new compound, in which the COX-inhibitor moiety and the anticancer-thiosulfonate portion could act separately but in a synergistic way against cancer development [101]. Several known NSAIDs possess anticancer activities: in detail, ASA induces apoptosis *via* downregulation of IL-6 dependent STAT3 activation and sulindac exerts an important time-dependent cell growth-inhibitory effect on oral squamous cell carcinoma. These effects are related to the interaction of NSAIDs with different and upstream signaling pathways (not to a direct interaction with the SH2 domain of STAT3); therefore, the linkage of a NSAID drug with a direct STAT3 inhibitor, such as a thiosulfonate derivative, could represent a valid strategy to obtain a more powerful STAT3 inhibitor. To investigate whether the modification of (**74**) structure by the substitution of the oxygen with a sulfur atom (compound (**82**), Fig. (**13**)) or through the replacement of the tosylate group with the methanethiosulfonate (compound (**83**), Fig. (**13**)) could modify the ability of (**74**) to interact with STAT3 and its potency as antiproliferative agent, an AlphaScreen-based assay was performed [101].

The thiosulfonate-NSAID hybrids (**77**)–(**81**), the (**74**) analogs (**82**) and (**84**) (Fig. (**13**)) and their parent compounds were tested to check their ability to directly bind the SH2 domain of STAT3. The results suggest that all thiosulfonate hybrids can strongly and selectively bind STAT3-SH2 domain, whereas parent drugs are completely unable to do this at the highest concentration tested (30 μM). Therefore, acetylsalicylic acid and sulindac anticancer activities are strictly related to an indirect

mechanism. High hydrophilicity or small size molecules exhibit low activity, whereas bulky and lipophilic molecules result to be more successful [101]. Although the thiosulfonate-drug hybrids display interesting STAT3 inhibition *in vitro*, only three compounds (**77**), (**79**), and (**80**)) (Fig. (**13**)) present a good antiproliferative activity on HCT-116 cell line. Compounds (**78**) and (**81**), instead, are inefficacious at concentration up to 100–200 μM. The low cytotoxicity found in the tested compounds might be related to their physicochemical properties, like poor solubility and chemical stability in the culture medium (time-related hydrolysis), cell permeation, and enzymatic hydrolysis inside cells; therefore, these aspects should be better explored in future studies, alongside with the cytotoxicity against other cancer cell lines [101]. Compound (**82**) displays better interaction with STAT3 SH2 domain, compared with S3I-201 by AlphaScreen test (58.4% *versus* 7.2% target inhibition at 30 μM), but it does not exhibit any cytotoxic effect up to 200 μM. [101].

Other compounds obtained by merging from methathiosulfonates (MTSs) and dithiolethiones (DTTs) moieties with 1,2,5-oxadiazole derivatives were synthesized and tested as SH2 domain inhibitors by an AlphaScreen-based assay [102]. The most interesting and selective derivative, belonging to MTSs, derivative (**85**) (Fig. (**13**)), potently interacts with STAT3 SH2 domain (IC_{50}= 0.7 ± 0.04 μM), exhibiting a significant antiproliferative activity against HCT-116 cell line (IC_{50}= 84.5 ± 9.8 μM).

A structure-based virtual screening of 45 small compounds by fluorescence polarization evidenced that compound B9 (**86**) (Fig. (**13**)) can inhibit the interaction of a fluorescein-labeled-p-Tyr-containing peptide to STAT3, binding the SH2 domain [42, 103]. To confirm growth inhibition in cell lines overexpressing p-STAT3, (**86**) was tested in MDA-MB-468 (IC_{50} = 5.1 μM), DU145 (IC_{50} = 63.77 μM) and MDA-MB-231 (IC_{50} = 13.8 μM) breast cancer cell lines, displaying a significant reduction of viability and growth. In contrast, the same parameters in MCF-7 cells, which do not harbor aberrant STAT3 activity, were not altered by (**86**) treatment (IC_{50} = 133.7 μM). Such findings demonstrate that (**86**) selectivity towards breast cells depends on constitutively activated STAT3. In addition, the activity of (**86**) on STAT3 mutants (K591A, K591A/S611G, R595G, and I634S/Q635G) was tested detecting the K_d values. Compared to wildtype the Kd values of mutants, K591A (K_d=3.84 μM), K591A/S611G (K_d= 4.8 μM), and R595G (K_d= 6.534 μM) are nearly equivalent to that of wildtype; while K_d of I634S/Q635G is different. This demonstrates that the direct interaction of (**86**) with STAT3, K591A, K591A/S611G and R595G do not affect the binding affinity, whereas I634S/Q635G decreases it, due to a loss of a hydrogen bonds between I634, Q635 and (**86**) [42]. Moreover, (**86**) exhibits dose-dependent inhibition of STAT3 luciferase reporter activity (IC_{50}= 12.5 μM). Further evaluation of STATs levels have evidenced that (**86**) has no effect on STAT3 levels, but, besides p-STAT3, it also suppresses the phosphorylation of STAT1 and STAT5, lacking of desired selectivity on p-STAT3 [42].

C188-9 (**87**) is a high-affinity STAT3 inhibitor (*K*d ~5 nM), which prevents ligand-induced STAT3 phosphorylation targeting the phosphotyrosine (pTyr) peptide binding site within the SH2 domain. It can be orally administered and inhibits the growth of radioresistant head-and-neck cancer xenografts. C188-9 is currently being evaluated in a phase I study involving patients with advanced-stage solid tumors (Fig. (**14**)). Johnson_et_al-2018-Nature_Reviews_Clinical_Oncology Ref nuovo

Another small molecule interfering with the STAT3 signaling pathway is OPB-31121 (**88**) (structure undisclosed) This compound exhibits potent anticancer activity *in vitro* and in tumor xenografts [104, 105, 106] and is currently investigated in clinical trials [104].

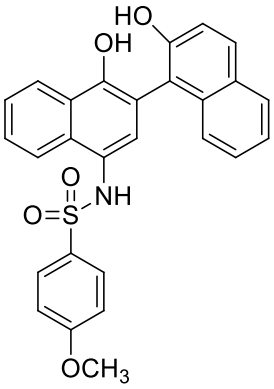

C188-9 (**87**)

Fig. (14). Structure of C188-9 (**87**)

OPB-31121 (**88**) has a unique mode of interaction with the STAT3 SH2 domain, which is not shared by any of the other tested STAT3 inhibitors. *In silico* studies [104, 105, 106] compared (**88**) with several STAT3 inhibitors, such as STA-21 [20], S3I-201 (**74**) and Cryptotanshinone (**26**) , known to bind the STAT3 SH2 domain. Molecular dynamics simulation recorded relevant drug/protein affinities of (**88**), which was docked into the SH2 domain; the same analysis was performed for all the other considered STAT3inhibitors. The IC_{50} value found for (**88**) was in the low nanomolar range (IC_{50}= ~18 nM), much lower than the values estimated for the other STAT3 inhibitors, which ranged from 1.4 to 27.2 μM [104]. The residues mostly involved in the binding of (**88**), gathered in two regions inside of the SH2 domain, were: a) region 1 including residues from Gln635 to Glu638; b) region 2 incorporating residues from Thr714 to Thr717. In addition, four other residues (Trp623, Lys626, Ile659 and Val667) were involved in stabilizing interactions with (**88**) [104]. The interaction area identified for (**88**) is undoubtedly distinct from those of all the other STAT3 inhibitors, demonstrating the existence of a first pocket, occupied by (**88**) and a second pocket, which was common to all the other inhibitors considered. Therefore, (**88**) exhibits the ability to bind with extraordinarily high affinity to

STAT3, interacting with a separate pocket in the SH2 domain. This means that the compound possesses different residue specificity compared to other STAT3 inhibitors, confirming the *in silico* prediction of the presence, in the SH2 domain of STAT3, of independent, non-overlapping binding pockets for (**88**) and other STAT3 inhibitors. STAT3-SH2 crystal structure reveals the presence of one hydrophilic and two hydrophobic sub-pockets; most STAT3 inhibitors (cryptotanshinone, STA-21 and S3I-201 included) bind to the hydrophilic site, which encompasses the side chains of Lys591, Arg609, Ser611 and Ser613 residues, or to the partly hydrophobic region formed by Lys592, Arg595, Ile597 and Ile634. On the contrary, (**88**) binds to a separate region that includes the third, hydrophobic sub-pocket and it interacts with more residues in the SH2 domain with respect to the other compounds. This contributes to the higher affinity of (**88**) for STAT3, as further confirmed by the extremely favorable comparison of each IC_{50} value. The substitution of Ser636 or Val637 with alanine residues influences the positioning of (**88**) in its binding pocket and greatly reduces the binding affinity, resulting in a dramatic increase in the IC_{50} values (from 18 nM to IC_{50} = 5 μM for Ser636 and to IC_{50} = 1.1 μM for Val637). The higher affinity for the target and the occupation of a wider and separate area in the SH2 domain could represent the main reasons for the more effective block of the interaction between STAT3 and kinases or other proteins, induced by (**88**), avoiding at the same time and with high efficiency, the phosphorylation of these residues compared to other STAT3 inhibitors [104].

OPB-31121 (**88**) entered Phase I clinical trials as an orally bioavailable STAT3 inhibitor for cancer treatment. The results of the first-in-human phase I study for (**88**), administered once per day for 28 days in patients with advanced solid tumors, provided evidence for the actual possibility of treating patients with STAT3 inhibitors. [107].

Many compounds blocking STAT3 have off-target toxicities, which limit their utilization, whereas (**88**) demonstrated to be relatively safe during the trials performed. However, (**88**) has a unique mechanism of action, which allows to achieve tumor shrinkage, a very important finding for *in vivo* studies, as well as a 19 months progression-free survival achieved by one patient during the trials, demonstrating outstandingly valid antitumor effect [107].

The derivative OPB-51602 (**89**) (structure undisclosed Fig. (**15**)), is a novel inhibitor, that binds with high affinity to the SH2 domain, effectively inhibiting STAT3 phosporylation and cancer cell growth. It is currently in phase I clinical trials in patients with refractory solid tumors as an oral STAT3 inhibitor , demonstrating a promising activity against NSCLC [108, 109].

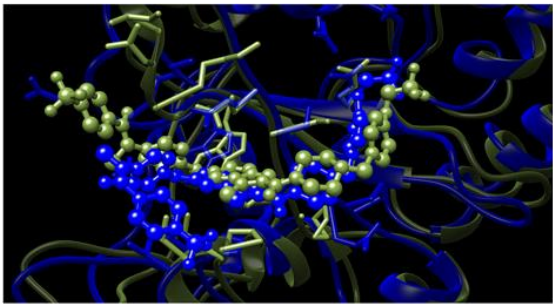

Fig. (15). OPB-51602 (**89**) interaction with STAT3 [108]

2.3.3.3. ***Mixed mechanism inhibitors***

The 2-[(aminocarbonyl)amino]-5-(4-fluorophenyl)-3-thiophenecarboxamide domain (TPCA-1) (**90**) (Fig. (**16**)), previously reported as IkB kinases (IKK) inhibitor, not only inhibited NF-kb signaling but was also found to be able to interact with the SH2 domain as showed by docking studies, exhibiting a direct dual inhibitory activity. [110]

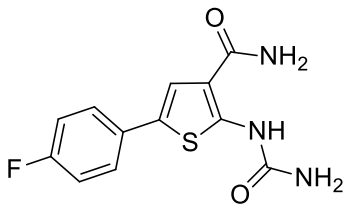

TPCA-1 (**90**)

Fig. (16). Structure of dual inhibitor (**90**) inhibiting STAT3 SH2 domain

The previously mentioned hydroxamic acid and benzoic acid derivatives SH5-07 (**15**) (Fig. (**5**)), and SH4-54 (**16**) (Fig. (**5**)), analogues of BP-1- 102 (**72**), were evaluated through Nuclear Magnetic Resonance, also showing interactions with the SH2 domain of STAT3 [46, 96].

2.3.3.4. Metal complexes

Organometallic derivatives have been recently considered as possible alternatives to organic compounds as targeted agents against protein kinases or as inhibitors of protein-protein interaction.

Platinum-based chemotherapeutic drugs are already extensively used in the treatment of cancer and the covalent binding to DNA is generally regarded as their main mechanism of action. However, only 5–10% of the platinum covalently bound in the cell is actually bound to DNA, whereas the great part of the compound that enters the cell forms protein-platinum complexes, provoking conformational changes and altering the biological function of the targets [111]. Western blot analysis showed that treatment with cisplatin, oxaliplatin and carboplatin induces dephosphorylation of all STATs tyrosine at high concentration. Further analysis on upstream kinases demonstrated that cisplatin had no effect on Akt or ERK phosphorylation, suggesting compound specificity for STAT proteins [111]. Supplementary studies concerning STAT deactivation pathways (like inhibition via PIAS proteins, inactivation by SOCS proteins and dephosphorylation by SHP 1 and 2) demonstrated that cisplatin produces no effect on the expression levels of SOCS, PIAS 1 and 3 nor on STAT phosphorylation, suggesting that STAT dephosphorylation is not caused by activation of STAT inhibitory pathways [111].

Further studies were focused on the platinum compounds ability to bind different proteins, to understand on whether STAT inhibition could be due to a direct binding of cisplatin to STATs. To identify STAT3 inhibitors binding to SH2 domain, platinum-based compounds were analyzed by AlphaScreen-based assay, which measures the binding of STAT proteins to a labeled phosphotyrosine (pTyr) peptide that resembles STAT docking sites. The incubation of STAT1, STAT3, STAT5b and STAT6 with cisplatin resulted in a strong inhibition of pTyr SH2 domain binding in a concentration-dependent manner and independently of the timing of addiction of the p-Tyr. The results showed that platinum compounds target STATs and block SH2 domain interactions, avoiding recruitment of these proteins to the receptor and inhibiting *de novo* phosphorylation and dimerization. Through studies on patients with head and neck squamous cell carcinoma (HNSCC), previously treated with cisplatin-based chemo-radiotherapy or radiotherapy alone, to assess the influence of STAT3 on cisplatin monotherapy efficacy, it was demonstrated that the inhibition of STAT signaling by platinum compounds (cisplatin, carboplatin and oxaliplatin) was provoked by a direct binding of STAT proteins and not only through DNA. Furthermore, recent *in vitro* tests using non-platinum, metal compounds that target STAT3 SH2 domain, confirmed the hypothesis that platinum compounds directly bind to STAT proteins, even though, unfortunately, their exact binding site remains unknown [111].

More recently, new Pt(II) complexes (compounds (**91**)-(**93**), Fig. (**17**)) bearing 1,2,5-oxadiazole ligands have been synthesized starting from a 3-aminomethyl-1,2,5-oxadiaxole scaffold, and evaluated for their ability to disrupt STAT3 dimerization. Ligand (**94**) (Fig. (**17**)) exhibits cytotoxic effects on HCT-116 cells (IC_{50} = 95.2 μM) and a selective ability to interact with STAT3 (IC_{50} = 8.2 μM) vs. STAT1 (IC_{50} > 30 μM). An increased cytotoxicity (IC_{50} = 18.4 μM) and a stronger interaction with STAT3 (IC_{50} = 1.4 μM) were shown by its corresponding platinum complex (**94**), leading to inhibition of its signaling pathway. The cytotoxicity of compound (**93**) was evaluated in cancer cell lines (HCT-116, MCF-7 and DLD-1) and the results show that the compound is significantly active towards the last one cell line, while cisplatin exhibits limited toxicity on all the three cell lines [112]. Moreover, HCT-116 cells were incubated with 25 μM of both ligand (**94**)·HCl and (**93**) for 24 h; resulting in a non-significant alteration of the STAT3 tyrosine phosphorylation state, with a 7.2% and 10.4% inhibition, respectively. A luciferase assay on HeLa cells evidenced that complex (**93**) interferes with STAT3 activity (IC_{50} = 16.7 μM), whereas ligand (**94**)·HCl did not show relevant effects up to 30 μM. Furthermore, an *in vivo* test on mice showed that treatment with complex (**93**) does not provoke significant weight loss, whereas mice treated with ligand (**94**)·HCl and cisplatin experienced a decrease in body weight. The overall results suggest a possible dual targeting mechanism of compound (**93**). Therefore, other biochemical approaches are needed to fully understand the interaction of ligand (**94**)·HCl and complex (**93**) with specific cysteines of STAT3 domain [112].

In the last years, rhodium (III) complexes were analyzed to discover new potent inhibitors of STAT3, binding the SH2 domain. Through a screening of a library of 11 rhodium (III) and iridium (III) complexes, on the bases of their ability to inhibit STAT3 DNA binding activity, compound (**95**) (Fig. (**17**)), exhibited potent anti-tumor activities in an *in vivo* mouse xenograft model of melanoma. During a cytotoxicity evaluation, complex (**95**) showed a potent cytotoxic activity against A375.S2 (IC_{50} = 6.6 ± 3.0 μM) and A2058 human melanoma cells (IC_{50} <1 μM), and it exhibited good cytotoxicity towards A375 human melanoma cells (IC_{50} = 17.2 ± 4.9 μM). Compound (**95**) discriminates between normal and cancer cells, as demonstrated by the low cytotoxicity found against HaCAT human keratinocytes (IC_{50}> 100 μM) and normal human dermal fibroblasts (IC_{50}>100 μM), which are not cancerous. On the contrary, other members of the original library showed a low ability to discriminate between the two cell types [113]. The biological efficacy of complex (**95**) was tested using a mouse xenograft tumor model. A375 cells (human malignant melanoma) were injected subcutaneously in mice that were treated four times a week with 75 mg/Kg of the compound (**95**) or vehicle. At sacrifice (day 35), treated tumors resulted visibly smaller compared to the ones of the vehicle control group and a substantial difference in the estimated volumes of tumors in the two groups was visible starting

from day 16 on. Similarly, tumor weight after sacrifice in the treated group was 60% reduced compared to that of the control group. In addition, treated mice showed no hint of general toxicity or weight loss during the experiment, nor substantial difference between the two groups of mice was found in the weights of the heart, liver, and kidney after sacrifice. Such results demonstrate the ability of the rhodium (III) complex (**95**) to inhibit the growth of skin cancer tissue *in vivo*, without producing excessive toxicity in mice [113]. Compound (**95**) ability to bind STAT3 SH2 domain was discovered during a fluorescence polarization assay, which showed that (**96**) is able to remove the high-affinity peptide 5'-FAM-GpYLPQTV from the SH2 domain of STAT3 in a dose-dependent manner (IC_{50} = 4.8 μM), while, in a cell-free assay, it blocked the DNA-binding activity of STAT3 (IC_{50} = 0.83 ± 0.17 μM). Western blotting analysis revealed that treatment of A375 cells with complex (**95**) provokes a dose-dependent reduction of STAT3 p-Tyr705 while having no effect on total STAT3. Moreover, in EGF-stimulated A375 cells, it suppressed STAT3-directed luciferase reporter activity (IC_{50} = 2.4 ± 0.2 μM). Furthermore, compound (**95**) did not show noticeable effect against Jak2, mTor or TNF-α activity and levels, unlike previously developed iridium(III) and rhodium(III) complexes [113]. In conclusion, new cyclometalated rhodium(III) complex (**95**) represents the first example of organometallic compound belonging to a Group 9, useful as a direct inhibitor of STAT3 or as scaffold for future development of highly potent STAT3 SH2 domain inhibitors [113]. Considering other coordination complexes, functionalized bis dipicolylamine (BDPA) copper (II) derivatives were identified as SH2 domain proteomimetics. In particular complex (**96**) (Fig. (**18**)), characterized by a rigid m-xilyl linkages tested by FP (K_i= 15 ± 9 μM) showed a most potent inhibitory activity respect to the mimetic bearing a more flexible linkage (1,5-propyl analog, K_i= 128 ± 15 μM). The titration (ITC), FP and EMSA assays results suggest that the main inhibition mode is based on mimicry of SH2 domain's pY binding function. Moreover compound (**96**) exhibited a significant antiproliferative activity on DU145, OCI-AML2 and MDA468 cell lines ($IC_{50\ s}$= 11.5 ± 4.2 μM, 11.3 ± 6.3 μM and 5.0 ± 0.5 μM respectively) [114].

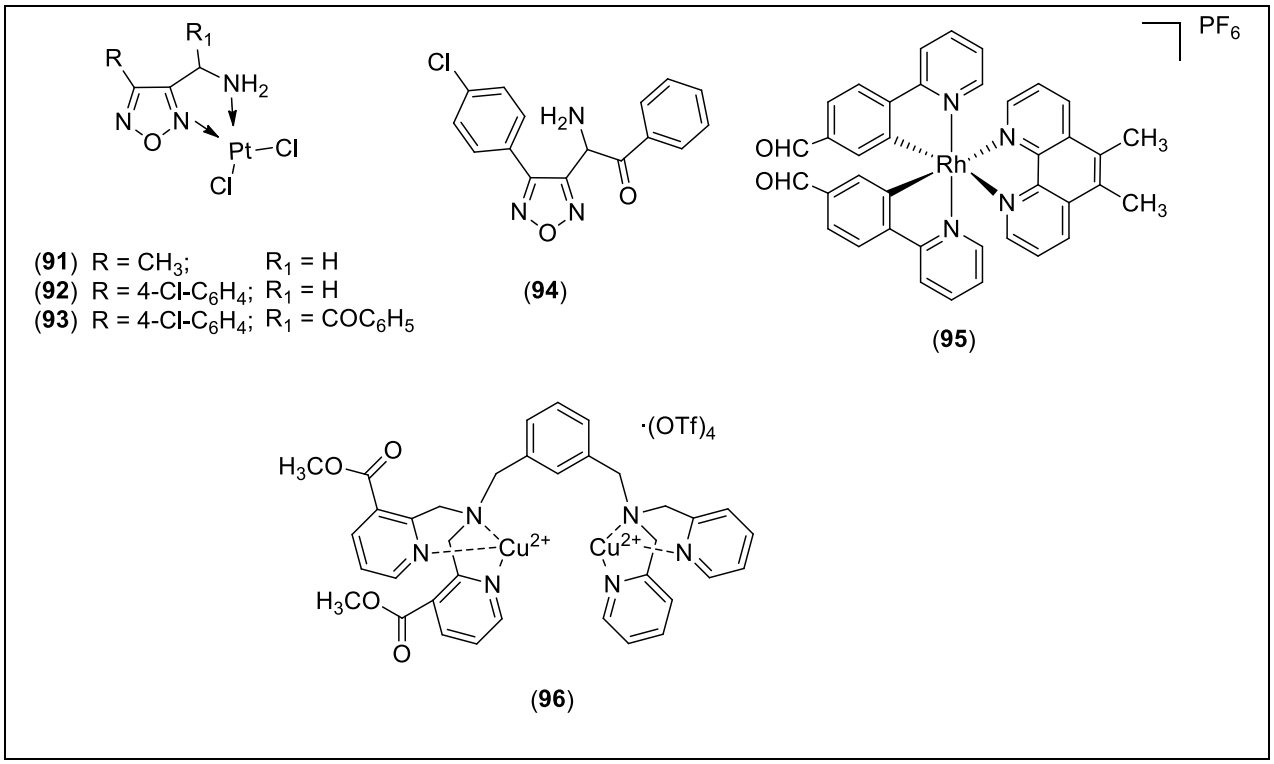

Fig. (17). Structures of ligand and metal complexes inhibiting STAT3 SH2 domain .

2.3.3.5 Patented compounds

A purine derivative (**97**) (Fig. (**18**)) exhibited a good selectivity and affinity for the SH2 domain tested by SPR (K_d= 39 µM) and an interesting antiproliferative activity *versus* NIH3T3/v-Src, DU145, Panc-1, and MDA-MB-231 cell lines ($IC_{50\ s}$= 41.1 µM, 65.3 µM, 77.2 µM and 66.1 µM respectively) [115].

By N-alkylation of compound (**74**) with the (*p*-cyclohexyl)benzyl moiety, the hydrophobic derivative S3I-20-1066 (or SF-1-066) (**98**) (Fig. (**18**)) showed a doubled potency in a test evaluating the SH2 domain-binding affinity through SPR assay (K_d= 2.75 µM). The interesting result was related to the efficacious occupation of the hydrophobic SH2 domain sub-pocket. Moreover, compound (**98**) is able to significantly disrupt the binding of pY-peptide to STAT3 (IC_{50} = 23 µM). It selectively inhibits the proliferation of MDA-MB-231, NIH3T3/v-Src and Panc-1 cell lines (IC_{50} = 37 µM, 35 µM and 48 µM respectively). The activity of compound (**98**) was tested in MDA-MB-231 cells xenograft model, leading to an important reduction of tumor size [116].

Concerning other salicylic acid derivatives, by a structure-based high-throughput virtual screening, compound (**99**) (Fig. (**18**)), related to (**72**) and compound (**100**) (Fig. (**18**)), deriving from (**98**), were

identified [117]. With respect to the parent compounds both are characterized by a trifluorophenyl moiety in substitution of the methyl group linked to sulfonamide group, showing an enhanced activity and a dose-dependent cytotoxicity against RPMI-8226.

Compound (**101**) (Fig. (**18**)) (SH-4-054) presents a benzoic moiety in place of the salicylic group [117] and exhibited the most potent activity (IC_{50} = 66 ± 33 nM in BTSC127EF cell line). It binds to the SH2 domain very strongly (SPR, K_d= 300 ± 27 nM), although it showed off-target effects involving other proteins containing the SH2 and SH3 domains. However, compound (**100**) was able to reduce tumor development in mice affected by BTSC73M brain tumors.

Compound (**102**) (Fig. (**18**)) (S3I-1757) [118] inhibited STAT3 phosphorylation and its dimerization, showing a significant inhibitory activity (FP, IC_{50} = 15 µM). Docking studies suggested its interaction with R609 and K591 present in the SH2 domain although FP results indicated that it binds to the pY705 binding domain.

Among the naphtalenesulfonamide derivatives designed on the basis of a directed fragment-based drug design, compound (**103**) (Fig. (**18**)) [119] was tested against human sarcoma cell lines RH30, RD2 and U2OS, showing IC_{50} values of 0.55, 1.39 and 0.52 µM, respectively. Moreover, (**102**) exhibited a significant inhibitory activity on breast cancer growth in a mouse tumor model.

Among a series of phosphopeptides designed for targeting the SH2 domain, the most interesting compound pCinn-Nle-mPro-Gln-NHBn (**104**) (Fig. (**18**)) [120] showed an $IC_{50=}$ 51 nM .

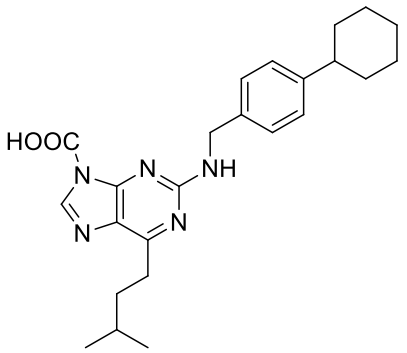

(**97**)

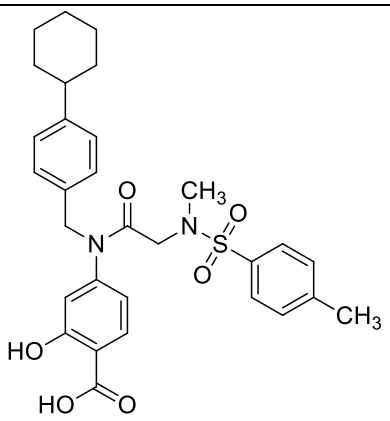

SF-1-066 or S3I-20-1066 (**98**)

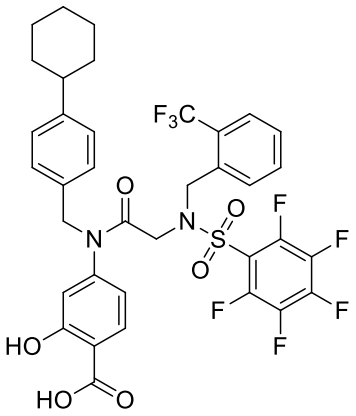

(**99**)

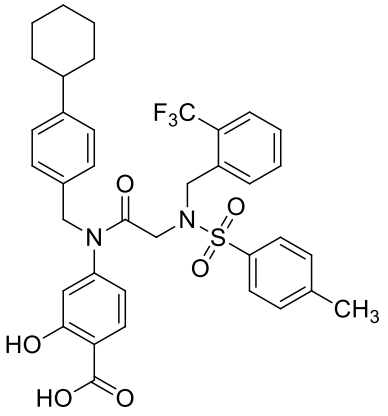

(**100**)

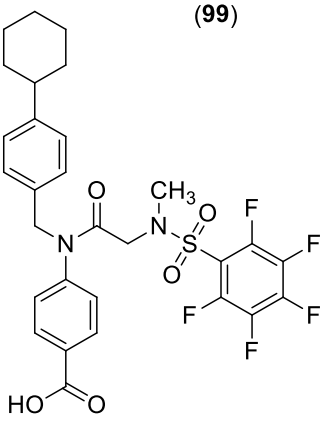

(**101**)

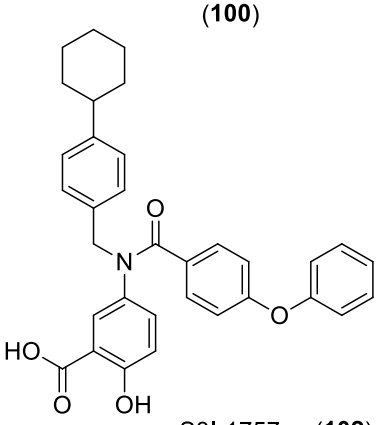

S3I-1757 (**102**)

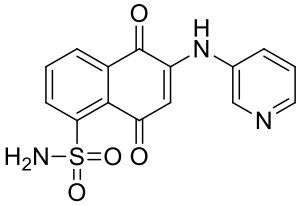

(**103**)

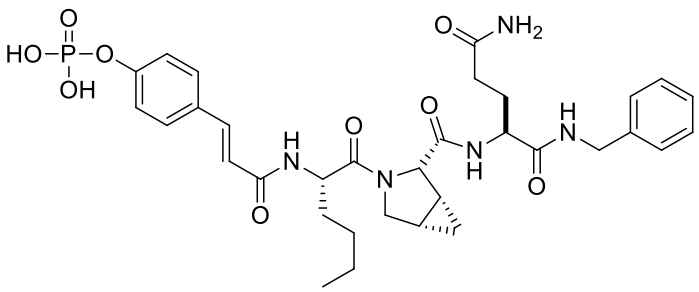

pCinn-Nle-mPro-Gln-NHBn (**104**)

Fig. (18). Patented SH2 domain inhibitors structures

2.4. Targeting amino acids

2.4.1 Cysteine

The alkylation of reactive cysteines has recently emerged as a potential novel strategy to obtain a direct inhibition of STAT3 functions. STAT3 contains twelve cysteine residues (Cys108, 251, 259, 328, 367, 418, 426, 468, 542, 550, 687, and 712), with a different potential reactivity towards electrophiles. Cys108 is probably solvent-exposed, considering it lies in a flexible region near the N-terminus; likewise, Cys259, 418, 426 and 712 face outwards towards the solvent. Cys251, 328 and 550 are likely shielded. Cys468 is solvent-exposed in the absence of a DNA binding partner, whereas Cys367, 542, and 687 are less exposed. Some of these residues play a significant role in preserving STAT3 structure and functions, so they could be conveniently exploited as therapeutic targets [121].

The dimerization of p-STAT3 monomers can be regarded as the triggering event in STAT3-mediated transcription, as it allows the translocation of the activated factor into the cell nucleus, its interaction with specific DNA binding sites and the subsequent regulation of the gene expression. Recently, u-STAT3 has been shown to be able to follow a similar pathway, much like its phosphorylated congener. Its dimerization process is based on the formation of non-covalent bonds between different aminoacidic residues; the dimeric structure is stabilized by two intermolecular S-S bridges, formed between two pairs of cysteines, namely Cys367 - Cys542 and Cys418 - Cys426. The importance of these disulfide bonds in the maintenance of the structural and functional integrity of STAT3 was demonstrated by the fast dissociation of the dimeric form, as a result of the reduction of the S-S-links, obtained with DTT. In particular, the bridge between Cys367 and Cys542 seems to be of pivotal importance in the stabilization of the dimer, since mutations in these residues have been shown to prevent STAT3-DNA interaction, suggesting a possible alteration of the conformation of the dimeric species [122].

Cys468, a residue located in the DNA binding domain of STAT3, and absent in STAT1, was identified as another possible site of alkylation, thanks to the potential selectivity of action that could be achieved [31].

The mechanism of action of some established STAT3 inhibitors, like Galiellalactone (**105**) or Stattic, has yet to be fully understood; some of them share reactive chemical moieties capable of modifying cysteine residues, which might allow them to act as STAT3 cysteine alkylators, thanks to their interaction with different residues, based on their position and reactivity [123].

Furthermore, STAT3 possesses a unique surface cysteine (Cys468) sited in the DNA binding domain. STAT1 equivalent residue is a serine. Alkylation of Cys468 blocks STAT3 DNA binding and induces apoptosis in human tumor cell lines characterized by high levels of p-STAT3 [31].

2.4.1.1 Natural compounds

Among the natural compounds capable of alkylating STAT3 cysteines, Galiellalactone (**105**) (Fig. (**19**)), a known DBD inhibitor, is one of the most important. It is a fungal metabolite that covalently binds to one or more cysteines on STAT3, blocking STAT3-DNA binding and STAT3 signaling, with no effect on upstream tyrosine phosphorylation. This molecule behaves as a Michael acceptor, forming a stable adduct with S-nucleophiles, like cysteines. Therefore, the binding is irreversible, and it lasts even after the removal of the compound, which occurs after a considerable amount of time, considering the relatively long half-life of GL (> 8 hours). GL was shown to bind Cys542 in the LD, and Cys367 and Cys468 in the DBD. These cysteines are not present in STAT1, thus representing a potentially selective target for STAT3 inhibition. Even though Galiellalactone is not specific for STAT3 (considering the high number of Cys-containing proteins inside the cell), it interacts with a surprisingly small number of additional targets, causing minimal cytotoxic consequences in non-STAT3-dependent cells [124].

Galiellalactone can inhibit the growth and induce the apoptosis of p-STAT3-expressing cells *in vitro*, while *in vivo* it delays the development of primary tumors [124]. An MTT assay demonstrated the ability of GL to limit the invasiveness, reduce the viability, and induce the apoptosis of DU145 and DU145-Luc cell lines, in a concentration-dependent manner (range 2.5 – 25 μM). The use of *zVADfmk*, a broad caspase inhibitor, resulted in a partial reduction of cell death, suggesting that GL can induce apoptosis by both a caspase-dependent and a caspase-independent mechanism. *In vivo* studies, performed using an orthotopic mouse model of prostate cancer (PCa), infected with DU145-Luc cells, proved that the use of GL (5 mg/kg) for 7 weeks can slow down tumor growth after 2/3 weeks of treatment. At the end of the study, bioluminescence images of GL-treated animals displayed much smaller tumors compared to the vehicle-treated animals, considering both tumor weight and volume. On the other hand, average animal weight did not change [125].

Eriocalyxin B (**106**) (Figure (**19**)), a traditional Chinese medicinal herb, was identified in a library screening as a specific STAT3 inhibitor [125]. It is isolated from the leaves of *Isodon Eriocalyx laxiflora*, and used for its anti-inflammatory and anti-bacterial activities [123, 126].

Compound (**106**) is a 7,20-epoxy-ent-kaurane-type diterpenoid, containing two α,β-unsaturated carbonyl groups, which are pivotal for the biological activity: one of them, linked to C1, covalently binds a cysteine residue located near the SH2 domain of STAT3 (Cys712) through a Michael addiction reaction, thus preventing STAT3 phosphorylation. 123 126 The other one, located in ring D, forms an H-bond with Asn647. The hydroxyl groups on C6 and C7 contribute to the stabilization of the link through the formation of additional H-bonds, which play an important role in maintaining the cytotoxicity [123].

A luciferase reporter assay was responsible for the identification of (**106**) as an inhibitor of cytokine-induced STAT3 activation; further Western blot studies, performed on different cell lines including lung adenocarcinoma A549 cells and breast cancer cells (MDA-MB-231 and MDA-MB-468), confirmed its ability to impair the activation of both IL-6-induced and constitutive Tyr705 phosphorylation, in a dose- and time-dependent fashion [127].

In vitro assays (Eurofins' KinaseProfiler™) revealed that (**106**) inhibited neither STAT3 upstream kinases (JAK1, JAK2, EGFR, cSrc) nor STAT3-unrelated kinases (MAPK1, PI3K); also, it did not affect the de-phosphorylation of STAT3, induced by the Protein Tyrosine Phosphatases (PTP) 127.

The addition of DTT and GSH to the biological assays abolished the activity of (**106**), proving the essentiality of its interaction with a Cys residue. In an attempt to verify the target of such an interaction, STAT3 Cys residues were mutated: (**106**) proved to be able to inhibit all the mutated forms of STAT3, except for the Cys712-mutant. The comparison of the sequences surrounding Cys712 showed that they were not conserved in other STATs, confirming that (**106**) had no effects on INF-γ-induced STAT1/STAT5 phosphorylation (INF-γ blocks cell growth by activating STAT1), whereas it could only inhibit the phosphorylation of STAT3 [123, 128] LC-MS analyses were also performed by incubating the inhibitor with a synthetic peptide, containing Cys712. Interestingly, the use of a different Cys-containing peptide resulted in a 10-fold decrease in EB activity. This observation confirmed EB selectivity towards STAT3 127.

Cucurbitacins are a family of natural triterpenoids, which have been employed for many years as traditional remedies, because of their strong bioactivities. They can react with cysteine thiols, causing a broad range of modifications, deriving from the inhibition of several protein targets. More recently, their potent cytotoxicity has led to extensive investigations on their potential use as anti-

cancer drugs [129].

In this context, a study identified cucurbitacin Q **(107)** (Fig. (**19**)) as an inhibitor of STAT3 activation, inducing apoptosis and inhibiting human tumor growth in mice. Cuc Q selectively triggers the apoptosis in tumor cells exhibiting high levels of activated STAT3, but is inactive on p-STAT3-independent tumors [129].

The biological activity of (**107**) was assessed on lung adenocarcinoma A549 cells and human breast carcinoma MDA-MB-435 and MDA-MB-468 cells, all expressing very high levels of p-STAT3. The IC_{50} values were determined, showing a good inhibition of STAT3 activation: 3.7 ± 1.7 µM in A549, 0.9 ± 0.6 µM in MDA-MB-435 and 1.4 ± 0.7 µM in MDA-MB-468. Cuc Q proved to be selective for STAT3, displaying IC_{50} values greater than 10 µM *versus* JAK2. Human breast carcinoma MDA-MB-453 cells, which do not present constitutive activation of STAT3, were used to test the response of STAT3-independent tumors to (**107**). After a treatment with 10 µM (**107**) for 24 hours, MDA-MB-453 cells displayed only a negligible increase of the percentage of apoptotic cells (4.7-fold with respect to the control), in strong contrast with the values obtained for STAT3-dependent cell lines, like A549 (27.4-fold) and MDA-MB-435 (25.9-fold) [129].

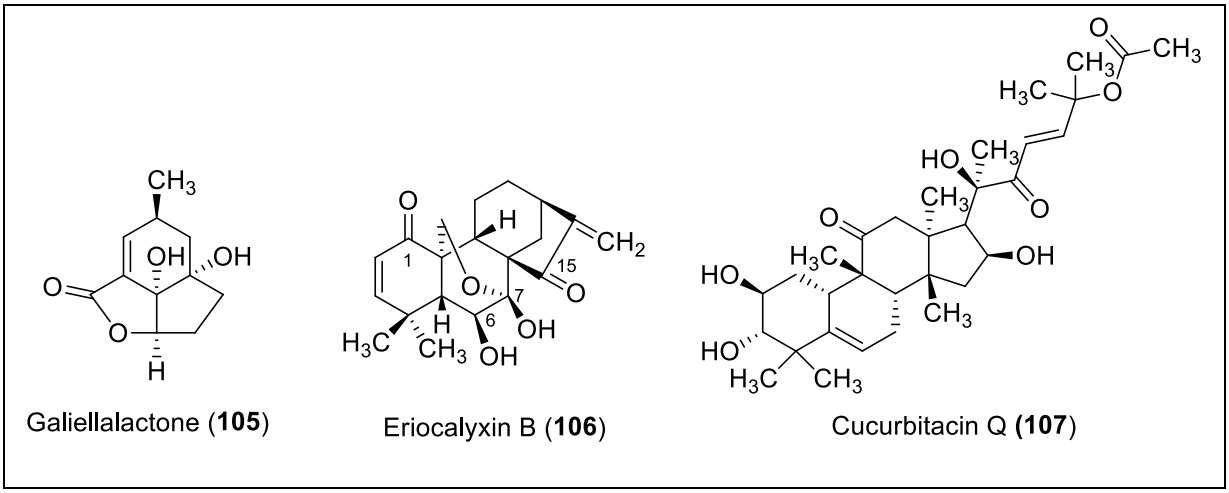

Fig. (19). Natural compounds structures targeting cysteines

2.4.1.2 Semi-synthetic compounds

Despite its significant activity against STAT3-dependent tumors, Galiellalactone is characterized by a very low bioavailability after oral administration, which makes it unsuitable for this preferential route. In an attempt to solve this complication, a prodrug, 3β-(*N*-acetyl-L-cysteinemethylester)-2aβ,3-dihydrogaliellalactone, also known as GPA512 (**108**) (Fig. (**20**)), was synthesized: chemically, it is a stable adduct obtained by conjugating GL with a substituted thiol group [130,

131] While GL only achieved *in vivo* efficacy by intraperitoneal administration, biological tests performed on GPA512 showed it is an orally active STAT3 inhibitor [131].

The rationale behind the design of (**108**) was the hypothesis that the poor oral bioavailability of Galiellalactone (**108**) was to be ascribed to its intestinal metabolism, more than to a permeability issue (relatively quick T_{max} of 30 minutes, after a single oral dose of 10 mg/kg). Quite possibly, GL is metabolized to a glutathionylated derivative in the intestinal membrane and then excreted through efflux pumps. In (**108**), the (**105**) scaffold is pre-conjugated with *N*-acetyl cysteine methyl ester: in this way, it is protected from further conjugation with glutathione and made capable of penetrating the intestinal membrane. Pharmacokinetic data seemed to support this theory: the $AUC_{0-\infty}$ of GL increased from 6 to 120 μg/mL·min after a single oral dose of 10 mg/kg of (**105**) and (**108**), respectively; similarly, the C_{max} raised from 52 to 1893 ng/mL. Data suggest that the *N*-acetyl cysteine methyl ester prodrug is rapidly metabolized by hydrolyzation to the corresponding free carboxylic acid, which is less stable in physiological conditions and releases the active parent drug with a spontaneous reversible Michael addiction reaction [131].

The biological activity of (**108**) was evaluated through a cell proliferation measurement performed on prostate cancer DU145 cells, using the WST-1 assay: the prodrug showed an IC_{50} value of 4.81 μM, which was very similar to that of the parent compound (3.02 μM). *In vivo* activity was assessed on mice, bearing DU145 cells: the animals were treated with the prodrug (40 mg/kg) 5 times a week for 4 weeks. The tumor growth rate was found to be significantly reduced after 26-29 days, compared to the control, without any significant side effect [131].

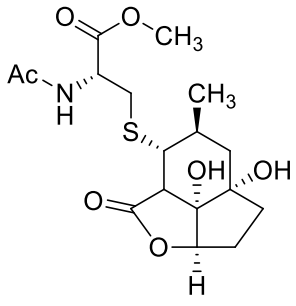

GPA512 (**108**)

Fig. (20). Semi-synthetic compound (**108**) targeting cysteines.

2.4.1.3. Synthetic compounds

A small molecule, C48 or NCS-368262 (**109**) (Fig. (**21**), was identified as a novel STAT3 inhibitor through a computationally-assisted similarity search, performed over a large molecular library, including compounds from the National Cancer Institute (NCI) and a commercial database; the template C36 (**110**) had been previously selected by virtual ligand screening (VLS) and Electrophoretic Mobility Shift Assay (EMSA) as a hit, with an IC_{50} of 30-50 μM. The same test was run on (**109**), revealing its ability to block STAT3-DNA binding with an IC_{50} value of 10-50 μM; only this compound was selected for further development, because, differently from all other analogs, it proved to be stable in aqueous solutions. Additionally, (**109**) interfered with STAT1/STAT3 heterodimers, though at higher concentrations (IC_{50} 50-100 μM), and had no effect on p-STAT1 homodimers (IC_{50} > 500 μM) [31].

Timing seems to be of pivotal importance in the interaction of (**109**) with STAT3: STAT3-DNA binding can be inhibited only before the interaction between STAT3 and the DNA occurs. Conversely, the pre-incubation of STAT3 with DNA, followed by the addition of C48 leads to no consequences on STAT3-DNA binding. This observation implies that C48 binding site can only be accessed before the interaction of STAT3 with the DNA [31].

The activity of (**109**) relies on its reactive benzylic carbon, which is capable of alkylating a specific cysteine residue of STAT3, Cys468: it is located on the DNA binding surface of STAT3 and, if modified, it prevents DNA binding by steric hindrance. Cys468 is typical of STAT3, conferring selectivity over STAT1 and STAT5, in which that position is occupied by a serine residue. To further confirm Cys468 involvement in C48 activity, a STAT3 mutant, bearing a serine residue in place of the natural cysteine, was produced and treated with (**109**), resulting in no evident inhibitory activity [31].

Compound (**109**) induced apoptosis in two breast cancer cell lines bearing constitutive p-STAT3 (MDA-MB-468 and MDA-MB-231), but had no effect on a human prostate cancer cell line (LNCaP), lacking constitutive STAT3-DNA binding activity. The IC_{50} value for the induction of apoptosis in MDA cells was 10-20 μM, after a 48 hours treatment with 1-20 μM C48. Further investigations revealed that the compound does not inhibit upstream kinases (JAK1, JAK2, Src), and, additionally, it facilitates the de-phosphorylation of STAT3 [31].

Compound (**109**) proved to be able to significantly reduce tumor growth *in vivo*, both in a nude mouse model with subcutaneously established MDA-MB-468 human breast tumor xenografts and in a syngeneic mouse model with C3L5 murine breast adenocarcinoma cells, after a treatment with

200 mg/kg C48, daily for 5 days per week. The measurements were taken twice a week, for 8 weeks and 26 days, respectively [31].

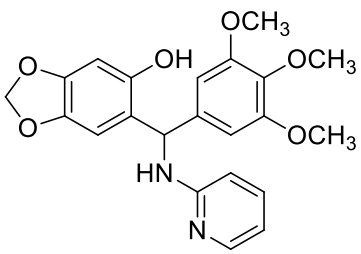

C48 (**109**)

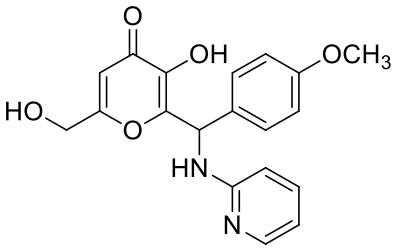

C36 (**110**)

Fig. (21). Synthetic compound (**109**) and (**110**) targeting cysteines.

2.4.1.4. Dual inhibitors

Some STAT3 inhibitors that act by binding to the DBD, the SH2 domain or other targets have also been shown to interact with specific cysteine residues of the primary sequence of STAT3.

2.4.1.4.1. Natural compounds

Withaferin A (**111**) ((Fig. (**22**)), isolated from *Whitania somnifera*, belongs to the withanolide family, a group of more than 600 natural products characterized by a steroidal backbone, bearing a highly oxidized A,B-ring system and a δ-lactone, linked to the D ring. Withaferin A possesses a pleiotropic activity, behaving as an antitumor, anti-inflammatory and antioxidant agent, thanks to its interaction with a considerable number of molecular targets, including STAT3. The mechanism of action seems to rely on the formation of a covalent bond between the C3 of (**111**) and a cysteine residue of the target, probably located in the vicinity of Tyr705 in the SH2 domain: therefore, the 2-en-1-one moiety was identified as the pharmacophore. This compound was found to inhibit both constitutive and IL-6-induced STAT3 phosphorylation in Caki cells and MDA-MB-231 cells, respectively. An increase in the number of apoptotic Caki cells was observed upon treatment with withaferin A; given the low selectivity of this compound, the correlation between STAT3 inhibition and apoptosis was experimentally ascertained by verifying that the overexpression of STAT3 could actually limit withaferin A-induced apoptosis. Additional tests showed that this compound is capable of inhibiting the constitutive phosphorylation of JAK2, while it has no effect on *c*-Src [132, 133].

Analogous results were obtained on HCT116 cells, in which the treatment with (**111**) at

concentrations below 5 μM attained a 69% reduction in cell proliferation after 12 hours. The effect of withaferin-A on the growth of HCT116 cells *in vivo* was evaluated by using a xenograft mouse tumor model: the administration of the inhibitor (2 mg/kg) every 2 days for 32 days led to a significant decrease in the volume of the tumor, as compared to the control, without substantial changes in the body weight of the animal [134].

Similar studies were conducted on multiple myeloma and neuroblastoma cells, with comparable effects [135].

Withacnistin (**112**) (Fig. (**22**)) is a C18-functionalized molecule, very similar to withaferin A, which also inhibits STAT3 phosphorylation. SAR studies revealed that the introduction of an ethanol Michael adduct at C3 of withacnistin abolishes the inhibitory effect on the JAK/STAT pathway, thus confirming the cruciality of the A-ring enone [132, 133].

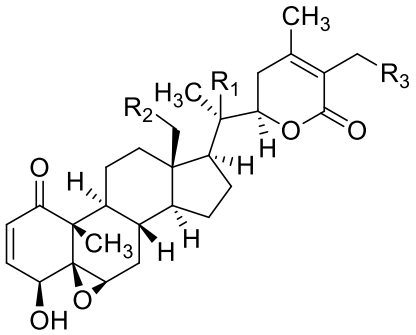

Withaferin A (**111**): R_1 = H, R_2 = H, R_3 = OH

Withacnistin (**112**): R_1 = H, R_2 = OAc, R_3 = H

Fig. (22). Dual inhibitors (**111**) and (**112**) structures.

2.4.1.4.2. Synthetic compounds

Stattic **(52)** ((Fig. (**12**)), is an established STAT3 inhibitor, which acts by binding thiol-containing cysteine residues, located in the SH2 domain; more recently, it has also demonstrated the ability to alkylate four cysteines on u-STAT3 [31 136]. Previous studies had suggested that the mechanism of action of Stattic could depend on the formation of a covalent link with Cys468 of p-STAT3, resulting in a steric hindrance, capable of preventing the dimerization. However, since *in vitro* studies seemed to indicate u-STAT3, more than p-STAT3, as the putative target of Stattic, a MS-based investigation was carried out to identify the Cys residues, modified by the inhibitor on the unphosphorylated form of the protein. Cys251, Cys259, Cys367 and Cys426 were identified as the targets of Stattic on u-

STAT3; as most of them were found to be embedded in the protein structure rather than located on the protein–protein or protein–DNA interfaces, a different mechanism of action was proposed, involving subtle changes in the protein tertiary structure, rather than direct steric hindrance, as possible determinants of the inhibition of the homodimerization process [136].

S3I-201, also known as NSC-74859 (**74**) (Fig. (**13**)), was identified through a structure-based virtual screening of the National Cancer Institute (NCI) chemical library as a potent STAT3 inhibitor targeting the SH2 domain, with an IC_{50} value of 86 μM, as determined by EMSA. From the structural point of view, it is composed of a glycolic acid core; the carboxylic acid forms an amide bond with 4-aminosalicylic acid, while the hydroxyl group is tosylated. Computational studies, performed with GOLD, showed that this compound binds into two of the three sub-pockets of the SH2 domain, namely the hydrophilic cavity bounded by Lys591, Arg609, Ser611, Ser613 (with the salicylic portion), and the hydrophobic pocket delimited by Ile634 and the hydrocarbon portions of the side chains of Lys591 and Arg595 (with the tosyl moiety). According to this model, the salicylic portion acts as a p-Tyr mimetic, interacting with the p-Tyr binding site, thus preventing STAT3 phosphorylation and dimerization [65].

However, the tosylate moiety of (**74**) could also be an excellent leaving group and undergo a nucleophilic attack at the carbon atom to which it is bound. Although there is no decisive proof that S3I-201 also acts as an irreversible inhibitor, the presence of several nucleophilic residues in the SH2 domain, like Cys418 and Cys712, together with the relative lability of the tosyl group, make this hypothesis rather likely. Indeed, the conversion of the *O*-tosyl group to the non-labile *N*-methyl-tosyl group resulted in a drastic decrease in the inhibitory activity of a series of S3I-201 derivatives. Unfortunately, irreversible inhibitors usually display a poor protein selectivity and relatively tight SAR [65].

Bendamustine (**113**) (Fig. (**23**)) is an FDA-approved alkylating agent, which is active against B-cell non-Hodgkin lymphoma, chronic lymphocytic leukemia and multiple myeloma. It is composed of a benzimidazole ring, substituted with a 2-chloroethylamine group, responsible for the alkylating effect, and a butyric acid side chain. Its superior activity, compared to other alkylators, suggested it might possess additional mechanisms of action. An AlphaScreen binding assay was used to test the interaction between (**113**) and the SH2 domain of STAT3: the compound proved to be able to selectively inhibit STAT3-SH2 (IC_{50} = 7.4 μM), over STAT1 (IC_{50} = 60 μM) and Grb2 (IC_{50} > 100 μM). The inhibitory activity was abolished by both the addition of L-cysteine (200 μM) and 2-

mercaptoethanol (200 μM), suggesting an involvement of the Cys residues in the mechanism of action. To verify this hypothesis, STAT3 was incubated with a thiol-reactive probe (Alexa Fluor 488 C5 maleimide): the addition of (**113**) resulted in a reduction of the fluorescence intensity in a dose-dependent fashion. By employing STAT3 mutants, Cys550 and Cys712 were identified by AlphaScreen assays as the targets of (**113**): the alkylation of these residues was shown to prevent the dimerization of STAT3, its binding to the DNA and the expression of STAT3-dependent genes (e.g. c-myc) [137]. Compound (**113**) was found to be active on the p-STAT3-rich cell line MDA-MB-468 in a dose-dependent manner (0.1–100 μM for 48 h), but was ineffective against low p-STAT3 cell lines, like MDA-MB-453 [137]. Bendamustine was also shown to decrease STAT3 phosphorylation at Tyr705; however, it is still unclear whether this effect is due to a direct inhibition or to an impairment of one of the upstream kinases [137].

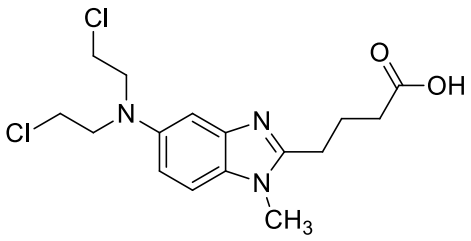

Bendamustine (**113**)

Fig. (23). Structure of synthetic alkylating compound (**113**) targeting cysteines.

2.4.2 Tyrosine

Tyr705, a residue located in the SH2 domain, plays a fundamental role in the STAT3 signaling pathway, since its phosphorylation allows the activation of STAT3 and its subsequent homodimerization. The dimer, formed as a result of the interaction between the p-Tyr motifs of two monomers, translocates into the nucleus and binds to specific DNA sequences, thus affecting cellular functions through the regulation of gene expression.

Piperlongumine (**114**) (Fig. (**24**)), a natural alkyl amide isolated from the fruit of the long pepper (*Piper longum*) and used for centuries in Ayurvedic medicine to cure a wide range of illnesses, was identified by a high-throughput fluorescence microscopy (HTFM) screening of the Prestwick chemical library as an inhibitor of STAT3 nuclear translocation [138].

In order to determine its mechanism of action, a surface plasmon resonance assay was performed, revealing that PL directly and potently inhibits the binding of STAT3 to its phosphotyrosyl peptide ligand (IC_{50} = 1.5 μM), by interacting with Tyr705 [138].

Compound (**114**) was found to inhibit constitutive STAT3 phosphorylation in breast cancer cell lines (MDA-MB-231 and MDA-MB-468), with an IC_{50} value in the range 0.4 – 2.8 μM, attaining a > 70% reduction of p-STAT3 after 1.5 hours of treatment. Kinetic studies were performed by adding PL (30 μM) for 15 min – 24 h to MDA-MB-468 cells: the levels of p-STAT3 were lowered by > 50% within 15 minutes, and maximally reduced within 30 minutes. Similarly, (**114**) was capable of completely inhibiting IL-6-induced STAT3 phosphorylation on a set of breast cancer cell lines (MCF-7, MDA-MB-453 and T47D), with IC_{50} values in the low micromolar range (IC_{50} = 0.9 μM on MCF-7 and MDA-MB-453, 2.7 μM on T47D). Consequently, (**114**) was able to interfere with the expression of several STAT3-regulated genes, including the anti-apoptotic *Bcl-2*, *BcL-xL*, *Survivin*, *XIAP* and *CIAP*, as confirmed by the analysis of the mRNA levels of 51 STAT3-dependent genes by real-time PCR in MDA-MB-468 cells, treated with the inhibitor (30 μM for 6–8 h) [138].

Moreover, a phosphoprotein antibody array analysis revealed that (**114**) (30 μM for 2 hours) does not modulate STAT3 upstream kinases, like Janus, Src or receptor tyrosine kinases, in MDA-MB-468 cells [138].

Although (**113**) proved to be more efficient in p-STAT3-high cell lines (IC_{50}s in the range 2.8 - 12.9 μM within 16 hours) compared to p-STAT3-low cell lines (IC_{50}s in the range 15.5 - 100 μM), the incubation of the latter for a longer period of time (80 hours) resulted in the observation that (**114**) can reduce the amount of total STAT3 in these cells, too. Therefore, (**114**) not only reduced the levels of constitutive and IL-6-induced p-STAT3, but it was also able to interfere with u-STAT3, with a yet-to-be understood mechanism [138].

Compound (**114**) was also active *in vivo*, being capable of inducing the regression of breast cancer cell line xenografts in nude mice, through efficient reduction of p-STAT3; additionally, it proved to be well-tolerated up to a dose of 30 mg/kg/day for 14 days [138].

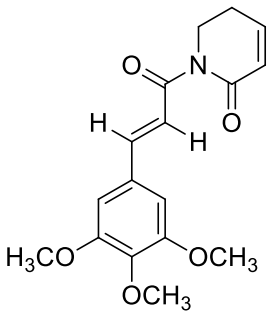

Piperlongumine (**114**)

Fig. (24). Structure of natural compound (**114**) targeting tyrosines.

3. CONCLUSION

The World Health Organization refers to cancer as one of the leading causes of morbidity and mortality worldwide (WHO report 2017). Unfortunately, standard chemotherapy targets cellular structures and mechanisms, which are also present in healthy cells, leading to a great variety of side effects that, could damage the patient. Furthermore, one of the major concerns in chemotherapy is the insurgence of chemo-resistance. This leads to the need of new drugs, selectively acting on tumor targets. Over the last two decades, STAT3 signaling pathway has been confirmed to play a pivotal role in initiating and sustaining pathological processes, and its inhibitors are currently under investigation for the treatment of oncologic, hematologic and chronic inflammatory diseases. Moreover, clinical evidence strongly suggests that this therapeutic approach could also be beneficial for patients with vasculo-proliferative diseases like restenosis, atherosclerosis and pulmonary arterial hypertension [139]. Since STAT3 constitutive activation can be found in up to 70% of tumors, and normal cells are generally able to bypass STAT3 blockage, STAT3 could be considered as a novel and valuable target for anti-cancer therapy, as its inhibition selectively induces the apoptosis of cancerous cells. [29].

There are two different approaches to inhibit STAT3: the direct inhibition, and indirect inhibition, which aims at blocking STAT3-activating upstream proteins. However, the indirect inhibition can provoke serious side effects, because the upstream proteins and kinases that are blocked through this strategy play numerous and different roles inside the cell, leading to the disruption of several signals with many undesired consequences in the human body.

Instead, direct inhibition is surely the best approach because it could allow a high selectivity of the treatment. Briefly, direct inhibitors interact with STAT3 domains in order to block its activity and consequently the transcription of STAT3-regulated genes.

For instance, direct inhibitors could target the DNA binding domain (DBD), preventing the binding of the protein to its correspondent sequences in the DNA.

To this class of inhibitors includes synthetic compounds as well as peptide aptamers, but for the latter there are still some aspects that need to be studied more deeply, like their cell permeation or their conjugation with nanoparticles (i.e. the construction of phosphopeptide conjugates with molecules mediating the cellular uptake gave some interesting results) [49].

Concerning the decoy oligdeoxyonucleotides (ODNs), encouraging results for cancer immunotherapies were reported for effective and safe CpG-STAT3 inhibitors using TLR9-targeted delivery of oligonucleotide therapeutics.
Notably among the antisense oligonucleotides (ASOs), ISIS 481464 (AZD9150) (a synthetic derivative complementary to mRNA for STAT3) was well-tolerated and showed anti-tumor activity in patients with lymphoma, in a first-in-human phase I trial.
However, the most represented are STAT3 direct inhibitors targeting the SH2-domain. This domain allows the p-STAT3 dimerization, which is important for the transfer into the nucleus and then for its transcription activity.
Concerning the SH2 domain, two important issues have to be considered: the great similarity between STAT1 and STAT3 SH2 domain sequences could represent an obstacle for the development of selective inhibitors. Moreover, the design of novel inhibitors could be extremely challenging because the SH2 domain and the phosphopeptide-binding interface are highly unstructured and dynamic regions [61].

Nevertheless, computational and experimental studies led to the discovery of natural, semi-synthetic and synthetic inhibitors (structurally heterogeneous, like phosphopeptide mimics, non-peptide small molecules, natural-product-like and metal-based inhibitors). Notably, among the synthetic SH2 domain inhibitors, compound OPB-51602 is actually in phase I clinical trials.

Furthermore, in the last decade, it has been discovered that some molecules are able to interact directly with different amino acids in STAT3 primary sequence, in particular some cysteines and tyrosine705. Concerning cysteine residues, a few of them are specific to STAT3 with respect to the other isoforms, an example being Cys468.

Finally, during the last years it has been demonstrated that various known direct inhibitors (Stattic, STX-0119 etc.) exhibit their activity through interactions involving different STAT3 domains, thus showing a mixed mechanism of action. Inserire rif.

To date few reported inhibitors succeed in entering clinical trials, although there is no marketed STAT3 inhibitor yet, because of their poor selectivity and undesirable pharmacokinetic/dynamic properties.

STAT3 is overexpressed in a wide range of tumors and its inhibition causes the growth arrest and apoptosis in STAT3-dependent tumor cells selectively; multiple oncogenic pathways converge on it and last but not least it plays a role in tumor immune evasion [140]. Therefore, direct inhibition of STAT3 could represent a promising approach for the discovery of potential anticancer agents,

allowing the selective targeting of pathways, which are vital for cancerous cells, without affecting normal cells.

REFERENCES

[1] Ihle, J.N. The Stat family in cytokine signaling. *Curr. Opin. Cell Biol.*, **2001**, *13*(2), 211-217.

[2] Lai, S.Y.; Johnson, F.M. Defining the role of the JAK–STAT pathway in head and neck and thoracic malignancies: implications for future therapeutic approaches. *Drug Resist. Updat.*, **2010**, *13*(3), 67–78.

[3] Debnath, B.; Xu, S.; Neamati, N. Small molecule inhibitors of signal transducer and activator of transcription 3 (Stat3) protein. *J. Med. Chem.*, **2012**, *55*(15), 6645–6668.

[4] Pellegrini, S.; Dusanter-Fourt, I. The structure, regulation and function of the Janus kinases (JAKs) and the signal transducers and activators of transcription (STATs). *Eur. J. Biochem.*, **1997**, *248*(3), 615-633.

[5] Zhang, X.; Darnell, J.E., Jr. Functional importance of Stat3 tetramerization in activation of the α2-macroglobulin gene. *J. Biol. Chem.*, **2001**, *276*(36), 33576-33581.

[6] Levy, D.E.; Darnell, J.E., Jr. Signalling: STATs: transcriptional control and biological impact. *Nat. Rev. Mol. Cell Biol.*, **2002**, *3*(9), 651-662.

[7] Schindler, C.; Levy, D.E.; Decker, T. JAK–STAT signaling: from interferons to cytokines. *J. Biol. Chem.*, **2007**, *282*(28), 20059-20063.

[8] Bowman, T.; Garcia, R.; Turkson, J.; Jove, R. STATs in oncogenesis. *Oncogene*, **2000**, *19*(21), 2474-2488.

[9] Bromberg, J.F.; Horvath, C.M.; Wen, Z.; Schreiber, R.D.; Darnell, J.E., Jr. Transcriptionally active STAT1 is required for the antiproliferative effects of both interferon alpha and interferon gamma. *Proc. Natl. Acad. Sci. USA.*, **1996**, *93*(15), 7673-7678.

[10] Furtek, S.L.; Matheson, C.J.; Backos, D.S.; Reigan, P. Evaluation of quantitative assays for the identification of direct signal transducer and activator of transcription 3 (STAT3) inhibitors. *Oncotarget*, **2016**, *7*(47), 77998-78008.

[11] Carpenter, R.L.; Lo, H.-W. STAT3 target genes relevant to human cancers. *Cancers*, **2014**, *6*(2), 897-925.

[12] Obana, M.; Maeda, M.; Takeda, K.; Hayama, A.; Mohri, T.; Yamashita, T.; Nakaoka, Y.; Komuro, I.; Takeda, K.; Matsumiya, G.; Azuma, J.; Fujio, Y. Therapeutic activation of signal transducer and activator of transcription 3 by interleukin-11 ameliorates cardiac fibrosis after myocardial infarction. *Circulation*, **2010**, *121*(5), 684−691.

[13] Khan, J.A.; Cao, M.; Kang, B.Y.; Liu, Y.; Mehta, J.L.; Hermonat, P.L. AAV/hSTAT3-gene delivery lowers aortic inflammatory cell infiltration in LDLR KO mice on high cholesterol. *Atherosclerosis*, **2010**, *213*(1), 59−66.

[14] Wang, P.; Yang, F.J.; Du, H.; Guan, Y.F.; Xu, T.Y.; Xu, X.W.; Su, D.F.; Miao, C.Y. Involvement of leptin receptor long isoform (LepRb)-STAT3 signaling pathway in brain fat mass- and obesity-associated (FTO) downregulation during energy restriction. *Mol. Med.*, **2011**, *17*(5-6), 523−532.

[15] Mair, M.; Zollner, G.; Schneller, D.; Musteanu, M.; Fickert, P.; Gumhold, J.; Schuster, C.; Fuchsbichler, A.; Bilban, M.; Tauber, S.; Esterbauer, H.; Kenner, L.; Poli, V.; Blaas, L.; Kornfeld, J.W.; Casanova, E.; Mikulits, W.; Trauner, M.; Eferl, R. Signal transducer and activator of transcription 3 protects from liver injury and fibrosis in a mouse model of sclerosing cholangitis. *Gastroenterology*, **2010**, *138*(7), 2499−2508.

[16] Pang, M.; Ma, L.; Gong, R.; Tolbert, E.; Mao, H.; Ponnusamy, M.; Chin, Y.E.; Yan, H.; Dworkin, L.D.; Zhuang, S. A novel STAT3 inhibitor, S3I-201, attenuates renal interstitial fibroblast activation and interstitial fibrosis in obstructive nephropathy. *Kidney Int.*, **2010**, *78*(3), 257−268.

[17] Gao, H.; Ward, P.A. STAT3 and suppressor of cytokine signaling 3: potential targets in lung inflammatory responses. *Expert Opin. Ther. Targets*, **2007**, *11*(7), 869−880.

[18] Yu, H.; Lee, H.; Herrmann, A.; Buettner, R.; Jove, R. Revisiting STAT3 signalling in cancer: new and unexpected biological functions. *Nat. Rev. Cancer*, **2014**, *14*(11), 736-746.

[19] Darnell, J.E., Jr. Validating Stat3 in cancer therapy. *Nat. Med.*, **2005**, *11*(6), 595-596.

[20] Masciocchi, D.; Gelain, A.; Villa, S.; Meneghetti, F.; Barlocco, D. Signal transducer and activator of transcription 3 (STAT3): a promising target for anticancer therapy. *Future Med. Chem.*, **2011**, *3*(5), 567–597.

[21] Masciocchi, D.; Gelain, A.; Porta, F.; Meneghetti, F.; Pedretti, A.; Celentano, G.; Barlocco, D.; Legnani, L.; Toma, L.; Kwon, B.-M.; Asai, A.; Villa, S. Synthesis, structure-activity relationships and stereochemical investigations of new tricyclic pyridazinone derivatives as potential STAT3 inhibitors. *Med. Chem. Commun.*, **2013**, *4*(8), 1181-1188.

[22] LaPorte, M.G.; Wang, Z.; Colombo, R.; Garzan, A.; Peshkov, V.A.; Liang, M.; Johnston, P.A.; Schurdak, M.E.; Sen, M.; Camarco, D.P.; Hua, Y.; Pollock, N.I.; Lazo, J.S.; Grandis, J.R.; Wipf, P.; Huryn, D.M. Optimization of pyrazole-containing 1,2,4,triazolo-[3,4-b] thiadiazines, a new class of STAT3 pathway inhibitors. *Bioorg. Med. Chem. Lett.*, **2016**, *26*(15), 3581-3585.

[23] Matsumoto, S.; Takuwa, T.; Kondo, N.; Hasegawa, S. Influence of a STAT3 inhibitor on tumor infiltrating lymphocytes in malignant pleural mesothelioma. *J. Clin. Oncol.*, **2017**, *35*(15), e23078.

[24] Zhang, W.; Ma, T.; Li, S.; Yang, Y.; Guo, J.; Yu, W.; Kong, L. Antagonizing STAT3 activation with benzo[*b*]thiophene 1,1-dioxide based small molecules. *Eur. J. Med. Chem.*, **2017**, *125*, 538-550.

[25] Park, J.H.; Hong, S.Y.; Kim, J.; Lee, H.J.; Lee, H.H.; Kim, K.Y.; Lee, S.W.; Oh, H.-M.; Rho, M.-C.; Lee, B.-G.; Song, Y.-H. Convenient synthesis of novel phenylpyrimido[1,2-c]thienopyrimidinones as IL-6/STAT3 inhibitors. *Heterocycles*, **2015**, *91*(4), 835-848.

[26] Timofeeva, O.A.; Gaponenko, V.; Lockett, S.J.; Tarasov, S.G.; Jiang, S.; Michejda, C.J.; Perantoni, A.O.; Tarasova, N.I. Rationally designed inhibitors identify STAT3 N-domain as a promising anticancer drug target. *ACS Chem. Biol.*, **2007**, *2*(12), 799-809.

[27] Mäe, M.; Langel, U. Cell-penetrating peptides as vectors for peptide, protein and oligonucleotide delivery. *Curr. Opin. Pharmacol.*, **2006**, *6*(5), 509-514.

[28] Timofeeva, O.A.; Tarasova, N.I.; Zhang, X.; Chasovskikh, S.; Cheema, A.K.; Wang, H.; Brown, M.L.; Dritschilo, A. STAT3 suppresses transcription of proapoptotic genes in cancer cells with the involvement of its N-terminal. *Proc. Natl. Acad. Sci. USA*, **2013**, *110*(4), 1267–1272.

[29] Fagard, R.; Metelev, V.; Souissi, I.; Baran-Marszak, F. STAT3 inhibitors for cancer therapy: Have all roads been explored? *JAKSTAT*, **2013**, *2*(1), e22882.

[30] Ginter, T.; Fahrer, J.; Kröhnert, U.; Fetz, V.; Garrone, A.; Stauber, R.H.; Reichardt, W.; Müller-Newen, G.; Kosan, C.; Heinzel, T.; Krämer, O.H. Arginine residues within the DNA binding domain of STAT3 promote intracellular shuttling and phosphorylation of STAT3. *Cell. Signal.*, **2014**, *26*(8), 1698-1706.

[31] Buettner, R.; Corzano, R.; Rashid, R.; Lin, J.; Senthil, M.; Hedvat, M.; Schroeder, A.; Mao, A.; Hermann, A.; Yim, J.; Li, H.; Yuan, Y.C.; Yakushijin, K.; Yakushijin, F.; Vaidehi, N.; Moore, R.; Gugiu, G.; Lee, T.D.; Yip, R.; Chen, Y.; Jove, R.; Horne, D.; Williams, J.C. Alkylation of cysteine 468 in Stat3 defines a novel site for therapeutic development. *ACS Chem. Biol.*, **2011**, *6*(5), 432-443.

[32] Zhang, J.-T.; Liu, J.-Y. Drugging the “undruggable” DNA-binding domain of STAT3. *Oncotarget*, **2016**, *7*(41), 66324-66325.

[33] Lee, D.Y.; Hwang, C.J.; Choi, J.Y.; Park, M.H.; Song, M.J.; Oh, K.W.; Son, D.J.; Lee, S.H.; Han, S.B.; Hong, J.T. Inhibitory effect of carnosol on phthalic anhydride-induced atopic dermatitis via inhibition of STAT3. *Biomol. Ther.*, **2017**, *25*(5), 535-544.

[34] Rocha, J.; Eduardo-Figueira, M.; Barateiro, A.; Fernandes, A.; Brites, D.; Bronze, R.; Duarte, C.M.; Serra, A.T.; Pinto, R.; Freitas, M.; Fernandes, E.; Silva-Lima, B.; Mota-Filipe, H.; Sepodes, B. Anti-inflammatory effect of rosmarinic acid and an extract of *Rosmarinus officinalis* in rat models of local and systemic inflammation. *Basic Clin. Pharmacol. Toxicol.*, **2015**, *116*(5), 398-413.

[35] de A.R. Oliveira, G.; de Oliveira, A.E.; da Conceicao, E.C.; Leles, M.I. Multiresponse optimization of an extraction procedure of carnosol and rosmarinic and carnosic acids from rosemary. *Food Chem.*, **2016**, *211*, 465-473.

[36] Park, K.-W.; Kundu, J.; Chae, I.-G.; Kim, D.-H.; Yu, M.-H.; Kundu, J.K.; Chun, K.-S. Carnosol induces apoptosis through generation of ROS and inactivation of STAT3 signaling in human colon cancer HCT116 cells. *Int. J. Oncol.*, **2014**, *44*(4), 1309-1315.

[37] Kashyap, D.; Kumar, G.; Sharma, A.; Sak, K.; Tuli, H.S.; Mukherjee, T.K. Mechanistic insight into carnosol-mediated pharmacological effects: recent trends and advancements. *Life Sci.*, **2017**, *169*, 27-36.

[38] Fossey, S.L.; Bear, M.D.; Lin, J.; Li, C.; Schwartz, E.B.; Li, P.K.; Fuchs, J.R.; Fenger, J.; Kisseberth, W.C.; London, C.A. The novel curcumin analog FLLL32 decreases STAT3 DNA binding activity and expression, and induces apoptosis in osteosarcoma cell lines. *BMC Cancer*, **2011**, *11*, 112.

[39] Rath, K.S.; Naidu, S.K.; Lata, P.; Bid, H.K.; Rivera, B.K.; McCann, G.A.; Tierney, B.J.; Elnaggar, A.C.; Bravo, V.; Leone, G.; Houghton, P.; Hideg, K.; Kuppusamy, P.; Cohn, D.E.; Selvendiran, K. HO-3867, a safe STAT3 inhibitor, is selectively cytotoxic to ovarian cancer. *Cancer Res.*, **2014**, *74*(8), 2316-2327.

[40] Shi, L.; Zheng, H.; Hu, W.; Zhou, B.; Dai, X.; Zhang, Y.; Liu, Z.; Wu, X.; Zhao, C.; Liang, G. Niclosamide inhibition of STAT3 synergizes with erlotinib in human colon cancer. *OncoTargets Ther.*, **2017**, *10*, 1767-1776.

[41] Huang, W.; Dong, Z.; Wang, F.; Peng, H.; Liu, J.-Y.; Zhang, J.-T. A small molecule compound targeting STAT3 DNA-binding domain inhibits cancer cell proliferation, migration and invasion. *ACS Chem. Biol.*, **2014**, *9*(5), 1188-1196.

[42] Huang, W.; Dong, Z.; Chen, Y.; Wang, F.; Wang, C.J.; Peng, H.; He, Y.; Hangoc, G.; Pollok, K.; Sandusky, G.; Fu, X.-Y.; Broxmeyer, H.E.; Zhang, Z.-Y.; Liu, J.-Y.; Zhang, J.-T. Small-molecule inhibitors targeting the DNA-binding domain of STAT3 suppress tumor growth, metastasis and STAT3 target gene expression in vivo. *Oncogene*, **2016**, *35*(6), 783-792.

[43] Sun, S.; Yue, P.; He, M.; Zhang, X.; Paladino, D.; Al-Abed, Y.; Turkson, J.; Buolamwini, J.K. An integrated computational and experimental binding study identifies the DNA binding domain as the putative binding site of novel pyrimidinetrione signal transducer and activator of transcription 3 (STAT3) inhibitors. *Drug Des.*, **2017**, *6*(1), 1000142.

[44] Assi, H.H.; Paran, C.; VanderVeen, N.; Savakus, J.; Doherty, R.; Petruzzella, E.; Hoeschele, J.D.; Appelman, H.; Raptis, L.; Mikkelsen, T.; Lowenstein, P.R.; Castro, M.G. Preclinical characterization of signal transducer and activator of transcription 3 small molecule inhibitors for primary and metastatic brain cancer therapy. *J. Pharmacol. Exp. Ther.*, **2014**, *349*(3), 458-469.

[45] Ashizawa, T.; Miyata, H.; Iizuka, A.; Komiyama, M.; Oshita, C.; Kume, A.; Nogami, M.; Yagoto, M.; Ito, I.; Oishi, T.; Watanabe, R.; Mitsuya, K.; Matsuno, K.; Furuya, T.; Okawara, T.; Otsuka, M.; Ogo, N.; Asai, A.; Nakasu, Y.; Yamaguchi, K.; Akiyama, Y. Effect of the STAT3 inhibitor STX-0119 on the proliferation of cancer stem-like cells derived from recurrent glioblastoma. *Int. J. Oncol.*, **2013**, *43*(1), 219-227.

[46] Yue, P.; Lopez-Tapia, F.; Paladino, D.; Li, Y.; Chen, C.H.; Namanja, A.T.; Hilliard, T.; Chen, Y.; Tius, M.A.; Turkson, J. Hydroxamic acid and benzoic acid-based STAT3 inhibitors suppress human glioma and breast cancer phenotypes in vitro and in vivo. *Cancer Res.*, **2016**, *76*(3), 652-663.

[47] Szelag, M.; Wesoly, J.; Bluyssen, H.A. Advances in peptidic and peptidomimetic-based approaches to inhibit STAT signaling in human diseases. *Curr. Protein Pept. Sci.*, **2016**, *17*(2), 135-146.

[48] Teng, P.; Zhang, X.; Wu, H.; Qiao, Q.; Sebti, S.M.; Cai, J. Identification of novel inhibitors that disrupt STAT3–DNA interaction from a γ-AApeptide OBOC combinatorial library. *Chem. Commun.*, **2014**, *50*(63), 8739-8742.

[49] Niu, Y.; Hu, Y.; Li, X.; Chen, J.; Cai, J. γ-AApeptides: design, synthesis and evaluation. *New J. Chem.*, **2011**, *35*(3), 542-545.

[50] Liu, K.; Lin, B.; Lan, X. Aptamers: a promising tool for cancer imaging, diagnosis, and therapy. *J. Cell. Biochem.*, **2013**, *114*(2), 250-255.

[51] Farokhzad, O.C.; Jon, S.; Khademhosseini, A.; Tran, T.N.; Lavan, D.A.; Langer, R. Nanoparticle-aptamer bioconjugates: a new approach for targeting prostate cancer cells. *Cancer Res.*, **2004**, *64*(21), 7668-7672.

[52] Nagel-Wolfrum, K.; Buerger, C.; Wittig, I.; Butz, K.; Hoppe-Seyler, F.; Groner, B. The interaction of specific peptide aptamers with the DNA binding domain and the dimerization domain of the transcription factor Stat3 inhibits transactivation and induces apoptosis in tumor cells. *Mol. Cancer Res.*, **2004**, *2*(3), 170-182.

[53] Zhang, X.; Zhang, J.; Wang, L.; Wei, H.; Tian, Z. Therapeutic effects of STAT3 decoy oligodeoxynucleotide on human lung cancer in xenograft mice. *BMC Cancer*, **2007**, *7*, 149.

[54] Leong, P.L.; Andrews, G.A.; Johnson, D.E.; Dyer, K.F.; Xi, S.; Mai, J.C.; Robbins, P.D.; Gadiparthi, S.; Burke, N.A.; Watkins, S.F.; Grandis, J.R. Targeted inhibition of Stat3 with a decoy oligonucleotide abrogates head and neck cancer cell growth. *Proc. Natl. Acad. Sci. USA*, **2003**, *100*(7), 4138-4143.

[55] Souissi, I.; Ladam, P.; Cognet, J.A.; Le Coquil, S.; Varin-Blank, N.; Baran-Marszak, F.; Metelev, V.; Fagard, R. A STAT3-inhibitory hairpin decoy oligodeoxynucleotide discriminates between STAT1 and STAT3 and induces death in a human colon carcinoma cell line. *Mol. Cancer*, **2012**, *11*, 12.

[56] Souissi, I.; Najjar, I.; Ah-Koon, L.; Schischmanoff, P.O.; Lesage, D.; Le Coquil, S.; Roger, C.; Dusanter-Fourt, I.; Varin-Blank, N.; Cao, A.; Metelev, V.; Baran-Marszak, F.; Fagard, R. A STAT3-decoy oligonucleotide induces cell death in a human colorectal carcinoma cell line by blocking nuclear transfer of STAT3 and STAT3-bound NF-κB. *BMC Cell. Biol.*, **2011**, *12*, 14.

[57] Sen, M.; Thomas, S.M.; Kim, S.; Yeh, J.I.; Ferris, R.L.; Johnson, J.T.; Duvvuri, U.; Lee, J.; Sahu, N.; Joyce, S.; Freilino, M.L.; Shi, H.; Li, C.; Ly, D.; Rapireddy, S.; Etter, J.P.; Li, P.-K.; Wang, L.; Chiosea, S.; Seethala, R.R.; Gooding, W.E.; Chen, X.; Kaminski, N.; Pandit, K.; Johnoson, D.E.; Grandis, J.R. First-in-human trial of a STAT3 decoy oligonucleotide in head and neck tumors: implications for cancer therapy. *Cancer Discov.*, **2012**, *2*(8), 694-705.

[58] Zhang, Q.; Hossain, D.M.S.; Duttagupta, P.; Moreira, D.; Zhao, X.; Won, H.; Buettner, R.; Nechaev, S.; Majka, M.; Zhang, B.; Cai, Q.; Swiderski, P.; Kuo, Y.-H.; Forman, S.; Marcucci, G.; Kortylewski, M. Serum-resistant CpG-STAT3 decoy for targeting survival and immune checkpoint singaling in acute myeloid leukemia. *Blood*, **2016**, *127*(13), 1687-1700.

[59] Kortylewski, M.; Moreira, D. Myeloid cells as a target for oligonucleotide therapeutics: turning obstacles into opportunities. *Cancer Immunol. Immunother.*, **2017**, *66*(8), 979-988.

[60] Njatcha, C.; Farooqui, M.; Grandis, J.R.; Siegfried, J.M. Targeting the EGFR/STAT3 axis in NSCLC with resistance to EGFR tyrosine kinase inhibitors using an oligonucleotide-based decoy. *Cancer Res.*, **2017**, *77*(13), 4101.

[61] Resetca, D.; Haftchenary, S.; Gunning, P.T.; Wilson, D.J. Changes in signal transducer and activator of transcription 3 (STAT3) dynamics induced by complexation with pharmacological inhibitors of Src homology 2 (SH2) domain dimerization. *J. Biol. Chem.*, **2014**, *289*(47), 32538-32547.

[62] Shin, D.-S.; Kim, H.-N.; Shin, K.D.; Yoon, Y.J.; Kim, S.-J.; Han, D.C.; Kwon, B.-M. Cryptotanshinone inhibits constitutive signal transducer and activator of transcription 3 function through blocking the dimerization in DU145 prostate cancer cells. *Cancer Research*, **2009**, *69*(1), 193-202.

[63] Park, I.H.; Li, C. Characterization of molecular recognition of STAT3 SH2 domain inhibitors through molecular simulation. *J. Mol. Recognit.*, **2011**, 24(2), 254-265.

[64] Yesylevskyy, S.O.; Ramseyer, C.; Pudlo, M.; Pallandre, J.R.; Borg, C. Selective inhibition of STAT3 with respect to STAT1: insights from molecular dynamics and ensemble docking simulations. *J. Chem. Inf. Model.*, **2016**, *56*(8), 1588-1596.

[65] Fletcher, S.; Page, B.D.G.; Zhang, X.; Yue, P.; Li, Z.H.; Sharmeen, S.; Singh, J.; Zhao, W.; Schimmer, A.D.; Trudel, S.; Turkson, J.; Gunning, P.T. Antagonism of the Stat3–Stat3 protein dimer with salicylic acid based small molecules. *ChemMedChem*, **2011**, *6*(8), 1459-1470.

[66] Zhang, X.; Yue, P.; Page, B.D.; Li, T.; Zhao, W.; Namanja, A.T.; Paladino, D.; Zhao, J.; Chen, Y.; Gunning, P.T.; Turkson, J. Orally bioavailable small-molecule inhibitor of transcription factor Stat3 regresses human breast and lung cancer xenografts. *Proc. Natl. Acad. Sci. USA*, **2012**, *109*(24), 9623-9628.

[67] Namanja, A.T.; Wang, J.; Buettner, R.; Colson, L.; Chen, Y. Allosteric communication across STAT3 domains associated with STAT3 function and disease-causing mutation. *J. Mol. Biol.*, **2016**, *428*(3), 579-589.

[68] Li, W.; Saud, S.M.; Young, M.R.; Colburn, N.H.; Hua, B. Cryptotanshinone, a Stat3 inhibitor, suppresses colorectal cancer proliferation and growth in vitro. *Mol. Cell. Biochem.*, **2015**, *406*(1-2), 63-73.

[69] Tang, Z.; Tang, Y.; Fu, L. Growth inhibition and apoptosis induction in human hepatoma cells by tanshinone II A. *J. Huazhong Univ. Sci. Technolog. Med. Sci.*, **2003**, *23*(2), 166-168.

[70] Yuan, S.L.; Wei, Y.Q.; Wang, X.J.; Xiao, F.; Li, S.F.; Zhang, J. Growth inhibition and apoptosis induction of tanshinone II-A on human hepatocellular carcinoma cells. *World J. Gastroenterol.*, **2004**, *10*(14), 2024-2028.

[71] Su, C.-C.; Chen, G.-W.; Kang, J.-C.; Chan, M.-H. Growth inhibition and apoptosis induction by tanshinone IIA in human colon adenocarcinoma cells. *Planta Med.*, **2008**, *74*(11), 1357-1362.

[72] Jin, D.-Z.; Yin, L.-L.; Ji, X.-Q.; Zhu, X.-Z. Cryptotanshinone inhibits cyclooxygenase-2 enzyme activity but not its expression. *Eur. J. Pharmacol.*, **2006**, *549*(1-3), 166-172.

[73] Dell'Orto, S.; Masciocchi, D.; Villa, S.; Meneghetti, F.; Celentano, G.; Barlocco, D.; Colombo, D.; Legnani, L.; Toma, L.; Jeon, Y.J.; Kwon, B.-M.; Asai, A.; Gelain, A. Modeling, synthesis and NMR characterization of novel chimera compounds targeting STAT3. *Med. Chem. Commun.*, **2014**, *5*, 1651-1657.

[74] Kim, J.-K.; Kim, J.-Y.; Kim, H.-J.; Park, K.-G.; Harris, R.A.; Cho, W.-J.; Lee, J.-T.; Lee, I.-K. Scoparone exerts anti-tumor activity against DU145 prostate cancer cells via inhibition of STAT3 activity. *PloS One*, **2013**, *8*(11), e80391.

[75] Sethi, G.; Chatterjee, S.; Rajendran, P.; Li, F.; Shanmugam, M.K.; Wong, K.F.; Kumar, A.P.; Senapati, P.; Behera, A.K.; Hui, K.M.; Basha, J.; Natesh, N.; Luk, J.M.; Kundu, T.K. Inhibition of STAT3 dimerization and acetylation by garcinol suppresses the growth of human hepatocellular carcinoma in vitro and in vivo. *Mol. Cancer*, **2014**, *13*, 66.

[76] Wang, Y.; Ren, X.; Deng, C.; Yang, L.; Yan, E.; Guo, T.; Li, Y.; Xu, M.X. Mechanism of the inhibition of the STAT3 signaling pathway by EGCG. *Oncol. Rep.*, **2013**, *30*(6), 2691-2696.

[77] Mantaj, J.; Rahman, S.M.A.; Bokshi, B.; Hasan, C.M.; Jackson, P.J.M.; Parsons, R.B.; Rahman, K.M. Crispene E, a *cis*-clerodane diterpene inhibitsSTAT3 dimerization in breast cancer cells. *Org. Biomol. Chem.*, **2015**, *13*(13), 3882-3886.

[78] Bill, M.A.; Nicholas, C.; Mace, T.A.; Etter, J.P.; Li, C.; Schwartz, E.B.; Fuchs, J.R.; Young, G.S.; Lin, L.; Lin, J.; He, L.; Phelps, M.; Li, P.-K.; Lesinski, G.B. Structurally modified curcumin analogs inhibit STAT3 phosphorylation and promote apoptosis of human renal cell carcinoma and melanoma cell lines. *PloS One*, **2012**, *7*(8), e40724.

[79] Jordan, B.C.; Kumar, B.; Thilagavathi, R.; Yadhav, A.; Kumar, P.; Selvam, C. Synthesis, evaluation of cytotoxic properties of promising curcumin analogues and investigation of possible molecular mechanisms. *Chem. Biol. Drug Des.*, **2018**, *91*(1), 332–337.

[80] Liu, L.-J.; Leung, K.-H.; Chan, D.-S.; Wang, Y.-T.; Ma, D.-L.; Leung, C.-H. Identification of a natural product-like STAT3 dimerization inhibitor by structure-based virtual screening. *Cell Death Dis.*, **2014**, *5*, e1293.

[81] Liu, L.; Wu, Y.; Cao, K.; Xu, Y.-Y.; Gao, X.-H.; Chen, H.-D.; Geng, L. Shikonin inhibits IFN-γ-induced K17 over-expression of HaCaT cells by interfering with STAT3 signaling. *Int. J. Clin. Exp. Pathol.*, **2015**, *8*(8), 9202-9207.

[82] Qiu, H.-Y.; Zhu, X.; Luo, Y.-L.; Lin, H.-Y.; Tang, C.-Y.; Qi, J.-L.; Pang, Y.-L.; Yang, R.-W.; Lu, G.-H.; Wang, X.-M.; Yang, Y.-H. Identification of new shikonin derivatives as antitumor agents targeting STAT3 SH2 domain. *Sci. Rep.*, **2017**, *7*(1), 2863.

[83] Yan, W.; Tu, B.; Liu, Y.-Y.; Wang, T.-Y.; Qiao, H.; Zhai, Z.-J.; Li, H.-W.; Tang, T.-T. Suppressive effects of plumbagin on invasion and migration of breast cancer cells via the inhibition of STAT3 signaling and down-regulation of inflammatory cytokine expression. *Bone Res.*, **2013**, *4*, 362-370.

[84] Lin, L.; Liu, A.; Peng, Z.; Lin, H.-J.; Li, P.-K.; Li, C.; Lin, J. STAT3 is necessary for proliferation and survival in colon cancer-initiating cells. *Cancer Res.*, **2011**, *71*(23), 7226-7237.

[85] Bhasin, D.; Cisek, K.; Pandharkar, T.; Regan, N.; Li, C.; Pandit, B.; Lin, J.; Li, P.-K. Design, synthesis, and studies of small molecule STAT3 inhibitors. *Bioorg. Med. Chem. Lett.*, **2008**, *18*(1), 391-395.

[86] Dhanik, A.; McMurray, J.S.; Kavraki, L.E. Binding modes of peptidomimetics designed to inhibit STAT3. *PLoS One*, **2012**, *7*(12), e51603.

[87] Schust, J.; Sperl, B.; Hollis, A.; Mayer, T.U.; Berg, T. Stattic: a small-molecule inhibitor of STAT3 activation and dimerization. *Chem. Biol.*, **2006**, *13*(11), 1235-1242.

[88] Matsuno, K.; Masuda, Y.; Uehara, Y.; Sato, H.; Muroya, A.; Takahashi, O.; Yokotagawa, T.; Furuya, T.; Okawara, T.; Otsuka, M.; Ogo, N.; Ashizawa, T.; Oshita, C.; Tai, S.; Ishii, H.; Akiyama, Y.; Asai, A. Identification of a new series of STAT3 inhibitors by virtual screening. *ACS Med. Chem. Lett.*, **2010**, *1*(8), 371-375.

[89] Asai, A.; Matsuno, K.; Ogo, N.; Yokotagawa, T.; Takahashi, O.; Akiyama, Y.; Ashizawa, T.; Okawara, T. Preparation of quinolinecarboxamide derivatives as STAT3 inhibitors. WO 2010004761 A1, January 14, 2010.

[90] Akiyama, Y.; Nonomura, C.; Ashizawa, T.; Iizuka, A.; Kondou, R.; Miyata, H.; Sugino, T.; Mitsuya, K.; Hayashi, N.; Nakasu, Y.; Asai, A.; Ito, M.; Kiyohara, Y.; Yamaguchi, K. The anti-tumor activity of the STAT3 inhibitor STX-0119 occurs via promotion of tumor-infiltrating lymphocyte accumulation in temozolomide-resistant glioblastoma cell line. *Immunol. Lett.*, **2017**,*190*, 20-25.

[91] Botta, A.; Sirignano, E.; Popolo, A.; Saturnino, C.; Terracciano, S.; Foglia, A.; Sinicropi, M.S.; Longo, P.; Di Micco, S. Identification of lead compound as inhibitors of STAT3: design, synthesis and bioactivity. *Mol. Inform.*, **2015**, *34*(10), 689-697.

[92] Pallandre, J.R.; Borg, C.; Rognan, D.; Boibessot, T.; Luzet, V.; Yesylevskyy, S.; Ramseyer, C.; Pudlo, M. Novel aminotetrazole derivatives as selective STAT3 non-peptide inhibitors. *Eur. J. Med. Chem.*, **2015**, *103*, 163-174.

[93] Ji, P.; Xu, X.; Ma, S.; Fan, J.; Zhou, Q.; Mao, X.; Qiao, C. Novel 2-carbonylbenzo[b]thiophene 1,1-dioxide derivatives as potent inhibitors of STAT3 signaling pathway. *ACS Med. Chem. Lett.*, **2015**, *6*(9), 1010-1014.

[94] Gao, D.; Xiao, Q.; Zhang, M.; Li, Y. Design, synthesis and biological evaluation of benzyloxyphenyl-methylaminophenol derivatives as STAT3 signaling pathway inhibitors. *Bioorg. Med. Chem.*, **2016**, *24*(11), 2549-2558.

[95] Ji, P.; Yuan, C.; Ma, S.; Fan, J.; Fu, W.; Qiao, C. 4-carbonyl-2,6-dibenzylidenecyclohexanone derivatives as small molecule inhibitors of STAT3 signaling pathway. *Bioorg. Med. Chem.*, **2016**, *24*(23), 6174-6182.

[96] Leung, K.-H.; Liu, L.-J.; Lin, S.; Lu, L.; Zhong, H.-J.; Susanti, D.; Rao, W.; Wang, M.; Che, W.I.; Chan, D.S.-H.; Leung, C.-H.; Chan, P.W.H.; Ma, D.-L. Discovery of a small-molecule inhibitor of STAT3 by ligand-based pharmacophore screening. *Methods*, **2015**, *71*, 38-43.

[97] Daka, P.; Liu, A.; Karunaratne, C.; Csatary, A.; Williams, C.; Xiao, H.; Lin, J.; Xu, Z.; Page, R.C.; Wang, H. Design, synthesis and evaluation of XZH-5 analogues as STAT3 inhibitors. *Bioorg. Med. Chem.*, **2015**, *23*(6), 1348-1355.

[98] Xiao, H.; Bid, H.K.; Jou, D.; Wu, X.; Yu, W.; Li, C.; Houghton, P.J.; Lin, J. A novel small molecular STAT3 inhibitor, LY5, inhibits cell viability, cell migration and angiogenesis in medulloblastoma cells. *J. Biol. Chem.*, **2015**, *290*(6), 3418-3429.

[99] Yu, W.; Xiao, H.; Lin, J.; Li, C. Discovery of novel STAT3 small molecule inhibitors via in silico site-directed fragment-based drug design. *J. Med. Chem.*, **2013**, *56*(11), 4402-4412.

[100] Yu, P.Y.; Gardner, H.L.; Roberts, R.; Cam, H.; Hariharan, S.; Ren, L.; Le Blanc, A.K.; Xiao, H.; Lin, J.; Guttridge, D.C.; Mo, X.; Bennett, C.E.; Coss, C.C.; Ling, Y.; Phelps, M.A.; Houghton, P.; London, C.A. Target specific, in vivo pharmacokinetics, and efficacy of the putative STAT3 inhibitor LY5 in osteosarcoma, Ewing's sarcoma and rhabdomyosarcoma. *PloS One*, **2017**, *12*(7), e0181885.

[101] Gabriele, E.; Ricci, C.; Meneghetti, F.; Ferri, N.; Asai, A.; Sparatore, A. Methanethiosulfonate derivatives as ligands of the STAT3-SH2 domain. *J. Enz. Inhib. Med. Chem.*, **2017**, *32*(1), 337–344.

[102] Gabriele, E.; Porta, F.; Facchetti, G.; Galli, C.; Gelain, A.; Meneghetti, F.; Rimoldi, I.; Romeo, S.; Villa, S.; Ricci, C.; Ferri, N.; Asai, A.; Barlocco, D.; Sparatore, A. Synthesis of new dithiolethione and methanethiosulfonate systems endowed with pharmaceutical interest. *Arkivoc*, **2017**, 235-250.

[103] Huang, M.; Chen, Z.; Zhang, L.; Huang, Z.; Chen, Y.; Xu, J.; Zhang, J.; Shu, X. Screening and biological evaluation of a novel STAT3 signaling pathway inhibitor against cancer. *Bioorg. Med. Chem. Lett.*, **2016**, *26*(21), 5172-5176.

[104] Brambilla, L.; Genini, D.; Laurini, E.; Merulla, J.; Perez, L.; Fermeglia, M.; Carbone, G.M.; Pricl, S.; Catapano, C.V. Hitting the right spot: mechanism of action of OPB-31121, a novel and potent inhibitor of the signal transducer and activator of transcription 3 (STAT3). *Mol. Oncol.*, **2015**, *9*(6), 1194-1206.

[105] Kim, M.J.; Nam, H.J.; Kim, H.P.; Han, S.W.; Im, S.A.; Kim, T.Y.; Oh, D.Y.; Bang, Y.J. OPB-31121, a novel small molecular inhibitor, disrupts the JAK2/STAT3 pathway and exhibits an antitumor activity in gastric cancer cells. *Cancer Lett.*, **2013**, *335*(1), 145-152.

[106] Hayakawa, F.; Sugimoto, K.; Harada, Y.; Hashimoto, N.; Ohi, N.; Kurahashi, S.; Naoe, T. A novel STAT inhibitor, OPB-31121, has a significant antitumor effect on leukemia with STAT-addictive oncokinases. *Blood Cancer J.*, **2013**, *3*, e166.

[107] Oh, D.-Y.; Lee, S.-H.; Han, S.-W.; Kim, M.-J.; Kim, T.-M.; Kim, T.-Y.; Heo, D.S.; Yuasa, M.; Yanagihara, Y.; Bang, Y.-J. Phase I study of OPB-31121, an oral STAT3 inhibitor, in patients with advanced solid tumors. *Cancer Res. Treat.*, **2015**, *47*(4), 607-615.

[108] Genini, D.; Brambilla, L.; Laurini, E.; Merulla, J.; Civenni, G.; Pandit, S.; D'Antuono, R.; Perez, L.; Levy, D.E.; Pricl, S.; Carbone, G.M.; Catapano, C.V. Mitochondrial dysfunction induced by a SH2 domain-targeting STAT3 inhibitor leads to metabolic synthetic lethality in cancer cells. *Proc. Natl. Acad. Sci. USA*, **2017**, *114*(25), E4924-E4933.

[109] Wong, A.L.; Soo, R.A.; Tan, D.S.; Lee, S.C.; Lim, J.S.; Marban, P.C.; Kong, L.R.; Lee, Y.J.; Wang, L.Z.; Thuya, W.L.; Soong, R.; Yee, M.Q.; Chin, T.M.; Cordero, M.T.; Asuncion, B.R.; Pang, B.; Pervaiz, S.; Hirpara, J.L.; Sinha, A.; Xu, W.W.; Yuasa, M.; Tsunoda, T.; Motoyama, M.; Yamauchi, T.; Goh, B.C. Phase I and biomarker study of OPB-51602, a novel signal transducer and activator of transcription (STAT) 3 inhibitor, in patient with refractory solid malignancies. *Ann. Oncol.*, **2015**, *26*(5), 998-1005.

[110] Nan, J.; Du, Y.; Chen, X.; Bai, Q.; Wang, Y.; Zhang, X.; Zhu, N.; Zhang, J.; Hou, J.; Wang, Q.; Yang, J. TPCA-1 is a direct dual inhibitor of STAT3 and NF-kB and regresses mutant EGFR-associated human non-small cell lung cancers. *Mol. Cancer Ther.*, **2014**, *13*(3), 617-629.

[111] Hato, S.V.; Figdor, C.G.; Takahashi, S.; Pen, A.E.; Halilovic, A.; Bol, K.F.; Vasaturo, A.; Inoue, Y.; de Haas, N.; Verweij, D.; Van Herpen, C.M.L.; Kaanders, J.H.; van Krieken, J.H.J.M.; Van Laarhoven, H.W.M.; Hooijer, G.K.J.; Punt, C.J.A.; Asai, A.; de Vries, I.J.M.; Lesterhuis, W.J. Direct inhibition of STAT signaling by platinum drugs contributes to their anti-cancer activity. *Oncotarget*, **2017**, *8*(33), 54434-54443.

[112] Porta, F.; Facchetti, G.; Ferri, N.; Gelain, A.; Meneghetti, F.; Villa, S.; Barlocco, D.; Masciocchi, D.; Asai, A.; Miyoshi, N.; Marchianò, S.; Kwon, B.-M.; Jin, Y.; Gandin, V.; Marzano, C.; Rimoldi, I. An in vivo active 1,2,5-oxadiazole Pt(II) complex: a promising anticancer agent endowed with STAT3 inhibitory properties. *Eur. J. Med. Chem.*, **2017**, *131*, 196-206.

[113] Ma, D.-L.; Liu, L.-J.; Leung, K.-H.; Chen, Y.-T.; Zhong, H.-J.; Chan, D.S.-H.; Wang, H.-M.D.; Leung, C.-H. Antagonizing STAT3 dimerization with a rhodium(III) complex. *Angew. Chem. Int. Ed. Engl.*, **2014**, *53*(35), 9178-9182.

[114] Drewry, J.A.; Fletcher, S.; Yue, P.; Marushchak, D.; Zhao, W.; Sharmeen, S.; Zhang, X.; Schimmer, A.D.; Gradinaru, C.; Turkson, J.; Gunning, P.T. Coordination complex SH2 proteomimetics: an alternative approach to disrupting oncogenic protein-protein interactions. *Chem. Commun.*, **2010**, *46*(6), 892-894.

[115] Turkson, J.; Gunning, P. Substituted 2-(9H-purin-9-yl)acetic acid analogs as inhibitors of STAT3. WO 2011163424 A2, December 29, 2011.

[116] Turkson, J.; Gunning, P. Compounds that suppress cancer cells and exhibit antitumor activity. WO 2010117438 A2, October 14, 2010.

[117] Fishel, M.L.; Gunning, P.T.; Haftchenary, S.; Page, B.D.G.; Weiss, S.; Luchman, H.A. Preparation of new salicylic acid derivatives for inhibiting STAT3 and/or STAT5 activity. WO 2013177534 A2, November 28, 2013.

[118] Sebti, S.M.; Lawrence, N.J.; Lawrence, H.R. Preparation of STAT3 dimerization inhibitors. WO 2014070859 A1, May 8, 2014.

[119] Li, C.; Yu, W.; Lin, J. Preparation of naphthalenesulfonamides, naphtho[1,8-cd]isothiazolones, and related compounds as STAT3 inhibitors and their use for treating cancer and other cell proliferation disorders. WO 2014028909 A1, February 20, 2014.

[120] McMurray, J.S.; Mandal, P.K.; Liao, W.S.; Ren, Z.; Chen, X.; Rajaopal, R.; Robertson, F. Preparation of phosphopeptide inhibitors of STAT3. WO 2010118309 A2, October 14, 2010.

[121] Ball, D.P.; Lewis, A.M.; Williams, D.; Resetca, D.; Wilson, D.J.; Gunning, P.T. Signal transducer and activator of transcription 3 (STAT3) inhibitor, S3I-201, acts as a potent and non-selective alkylating agent. *Oncotarget*, **2016**, *7*(15), 20669-20679.

[122] Butturini, E.; Gotte, G.; Dell'Orco, D.; Chiavegato, G.; Marino, V.; Canetti, D.; Cozzolino, F.; Monti, M.; Pucci, P.; Mariotto, S. Intermolecular disulfide bond influences unphosphorylated STAT3 dimerization and function. *Biochem. J.*, **2016**, *473*(19), 3205-3219.

[123] Zhao, Y.; Niu, X.-M.; Quian, L.-P.; Liu, Z.-Y.; Zhao, Q.-S.; Sun, H.-D. Synthesis and cytotoxicity of some new eriocalyxin B derivatives. *Eur. J. Med. Chem.*, **2007**, *42*(4), 494-502.

[124] Don-Doncow, N.; Escobar, Z.; Johansson, M.; Kjellström, S.; Garcia, V.; Munoz, E.; Sterner, O.; Bjartell, A.; Hellsten, R. Galiellalactone is a direct inhibitor of the transcription factor STAT3 in prostate cancer cells. *J. Biol. Chem.*, **2014**, *289*(23), 15969-15978.

[125] Canesin, G.; Evans-Axelsson, S.; Hellsten, R.; Sterner, O.; Krzyzanowska, A.; Andersson, T.; Bjartell, A. The STAT3 inhibitor galiellalactone effectively reduces tumor growth and metastatic spread in an orthotopic xenograft mouse model of prostate cancer. *Eur. Urol.*, **2016**, *69*(3), 400-404.

[126] Sun, H.-D.; Lin, Z.-W.; Niu, F.-D.; Shen, P.-Q.; Pan, L.-T.; Lin, L.-Z.; Cordell, G.A. Diterpenoids from *Isodon eriocalyx* var. *Iaxiflora*. *Phytochemistry*, **1995**, *38*(6), 1451-1455.

[127] Yu, X.; He, L.; Cao, P.; Yu, Q. Eriocalyxin B inhibits STAT3 signaling by covalently targeting STAT3 and blocking phosphorylation and activation of STAT3. *PloS One*, **2015**, *10*(5), e0128406.

[128] Quing, Y.; Stark, G.R. Alternative activation of STAT1 and STAT3 in response to interferon-gamma. *J. Biol. Chem.*, **2004**, *279*(40), 41679-41685.

[129] Sun, J.; Blaskovich, M.A.; Jove, R.; Livingston, S.K.; Coppola, D.; Sebti, S.M. Cucurbitacin Q: a selective STAT3 activation inhibitor with potent antitumor activity. *Oncogene*, **2005**, *24*(20), 3236-3245.

[130] Johansson, M.; Sterner, O. Preparation of tricyclic prodrugs of Galiellalactone. WO 2015132396 A1, September 11, 2015.

[131] Escobar, Z.; Bjartell, A.; Canesin, G.; Evans-Axelsson, S.; Sterner, O.; Hellsten, R.; Johansson, M.H. Preclinical characterization of 3β-(*N*-acetyl-L-cysteine methyl ester)-2aβ,3-dihydrogaliellalactone (GPA512), a prodrug of a direct STAT3 inhibitor for the treatment of prostate cancer. *J. Med. Chem.*, **2016**, *59*(10), 4551-4562.

[132] Tahara, T.; Streit, U.; Pelish, H.E.; Shair, M.D. STAT3 inhibitory activity of structurally simplified withaferin A analogues. *Org. Lett.*, **2017**, *19*(7), 1538-1541.

[133] Um, H.J.; Min, K.-J.; Kim, D.E.; Kwon, T.K. Withaferin A inhibits JAK/STAT3 signaling and induces apoptosis of human renal carcinoma Caki cells. *Biochem. Biophys. Res. Commun.*, **2012**, *427*(1), 24-29.

[134] Choi, B.Y.; Kim, B.-W. Withaferin-A inhibits colon cancer cell growth by blocking STAT3 transcriptional activity. *J. Cancer Prev.*, **2015**, *20*(3), 185-192.

[135] Yco, L.P.; Mocz, G.; Opoku-Ansah, J.; Bachmann, A.S. Withaferin A inhibits STAT3 and induces tumor cell death in neuroblastoma and multiple myeloma. *Biochem Insights*, **2014**, *7*, 1-13.

[136] Heidelberger, S.; Zinzalla, G.; Antonow, D.; Essex, S.; Basu, B.P.; Palmer, J.; Husby, J.; Jackson, P.J.M.; Rahman, K.M.; Wilderspin, A.F.; Zloh, M.; Thurston, D.E. Investigation of the protein alkylation sites of the STAT3:STAT3 inhibitor Stattic by mass spectrometry. *Bioorg. Med. Chem. Lett.*, **2013**, *23*(16), 4719-4722.

[137] Iwamoto, K.; Uehara, Y.; Inoue, Y.; Taguchi, K.; Muraoka, D.; Ogo, N.; Matsuno, K.; Asai, A. Inhibition of STAT3 by anticancer drug bendamustine. *PLoS One*, **2017**, *12*(1), e0170709.

[138] Bharadwaj, U.; Eckols, T.K.; Kolosov, M.; Kasembeli, M.M.; Adam, A.; Torres, D.; Zhang, X.; Dobrolecki, L.E.; Wei, W.; Lewis, M.T.; Dave, B.; Chang, J.C.; Landis, M.D.; Creighton, C.J.; Mancini, M.A.; Tweardy, D.J. Drug-repositioning screening identified piperlongumine as a direct STAT3 inhibitor with potent activity against breast cancer. *Oncogene*, **2015**, *34*(11), 1341-1353.

[139] Dutzmann, J.; Daniel, J.M.; Bauersachs, J.; Hilfiker-Kleiner, D.; Sedding, D.G. Emerging translational approaches to target STAT3 signalling and its impact on vascular disease. *Cardiovasc. Res.*, **2015**, *106*(3), 365-374.

[140] Yang, H; Yamazaki, T.; Pietrocola, F.; Zhou, H.; Zitvogel, L.; Ma, Y.; Kroemer, G. Improvement of immunogenic chemotherapy by STAT3 inhibition. *Oncoimmunology*, **2016**, *5*(2), e1078061.